

**Characterization of an olfactory
receptor mediating aversive behaviour
to a death-associated odour**

Inaugural-Dissertation

zur

Erlangung des Doktorgrades

der Mathematisch-Naturwissenschaftlichen Fakultät

der Universität zu Köln

vorgelegt von

Venkatesh Krishna Subramanian

aus Modinagar, Indien

Köln 2017

Berichterstatter: Prof. Dr. Sigrun I. Korsching

PD Dr. Joachim Schmidt

Prüfungsvorsitzender: Prof. Dr. Peter Kloppenburg

Tag der mündlichen Prüfung: April 2016

TABLE OF CONTENTS

ACKNOWLEDGEMENT.....	1
ZUSAMMENFASSUNG.....	3
ABSTRACT	5
ABBREVIATIONS	7
List of Figures.....	9
Introduction	11
The biology of olfaction.....	11
The Olfactory System.....	12
Signal transduction events mediating olfaction	13
Olfactory sensory neurons.....	14
Olfactory receptor gene family	16
Amines as ligands.....	18
Trace Amine-Associated Receptor Subfamily 13.....	20
TALEN and CRISPR: recent improvements for knockout in zebrafish.....	22
Zinc-finger nucleases	23
The Talen approach to genetic engineering	24
Clustered regularly interspaced short palindromic repeats/CRISPR-associated 9:	25
AIM OF THIS STUDY	27
Results	28
2.1 Preparation, Purification and characterisation of TAAR13c antibody .	28

2.2 The purified antibody labels a sparse population of cells in the olfactory epithelium.....	30
2.3 Co-labelling with acetylated Tubulin and G _{olf} shows expression of TAAR13c in ciliated neurons	31
2.4 Suitability of several neuronal activity markers to show activation of TAAR13c with cadaverine.....	36
2.5 Egr1 as immediate early gene neuronal activity marker, Whole mount in situ on Zebrafish larvae.....	37
2.6 pERK as a neuronal activity marker for TAAR13c activation due to cadaverine.....	38
2.7 Diamine assay using pERK as neuronal activity marker.....	40
2.8 Search for the TAAR glomerulus with the TAAR13c antibody	42
2.8.1 Olfactory Bulb stained with glomerular marker SV2 and co-labelled with TAAR13c antibody.....	42
2.8.2 Attempts to increase sensitivity of the immunological detection of TAAR13c via cadaverine stimulation and different fixation techniques	44
2.9 Ontogenetic onset of avoidance behaviour towards cadaverine.....	45
2.9.1 Observation of behaviour upon sequential increase of cadaverine concentration from 0 mM as control until 300mm threshold.....	48
2.9.2 Method development and optimization for behaviour experiments	49
2.11 Attempted knockout of TAAR13c gene using the CRISPR/Cas method.....	53
2.11.1 Generation of CRISPR gRNAs and CAS9 capped mRNA.....	53
2.11.2 Sequencing revealed high number of background SNP's resulting from the amplification of different TAAR13 subfamily genes	54
2.11.3 Initiation of TAAR13 gene family cluster knock out.....	61
DISCUSSION	63

Molecular characterization of TAAR13c as an olfactory receptor	63
Ontogenetic onset of avoidance behaviour towards cadaverine	69
Mutagenesis of TAAR13c using CRISPR-CAS9	71
Key Findings and conclusions.....	74
Materials and Methods	76
Animal Strains, Breeding and Maintenance	76
Plastic ware.....	76
Chemicals, Enzymes, oligos and Kits	77
Reagents and Solutions	77
Laboratory equipment	78
Bacterial Strains	78
Dissection	78
Tissue Lysis and protein estimation.....	79
Western Blotting.....	79
Signal detection	80
Immunohistochemistry	80
Preparation of the whole mount zebrafish larvae for in-situ hybridization	81
Genome editing using TALEN	82
mRNA transcription in vitro	83
Genome editing using CRISP-CAS9	83
Vectors	83
Production of Cas9 mRNA	83
Production of TAAR13c specific guide RNA	84
Microinjection of CRISPR/Cas9 vectors and screening for genomic alterations	86

T7 Endonuclease I assay	86
Subcloning and Sequencing of T7 Endonuclease I assay-samples	87
Primers and target sites used in TALEN and Crispr-Cas mediated mutations	87
REFERENCES	90
APPENDIX	104
ERKLÄRUNG	105
Lebenslauf	107

ACKNOWLEDGEMENT

It gives me great pleasure to acknowledge and thank the people who were part of my Ph.D journey which I started in 2012. Firstly I would like to thank **Prof.Dr. Sigrun Korsching** who gave me the opportunity to pursue my Ph.D in her Neurobiology lab of at the Institute for Genetics, University of Cologne, Germany. Her mentorship, guidance and criticism helped me develop my scientific acumen. Working under her was a learning experience in scientific writing, presentation and communication, the three most important things I needed improvement upon. I would like to thank her especially for not giving up on me during a tumultuous phase of my Ph.D.

I extend my sincere gratitude to **PD Dr. Joachim Schmidt** for accepting to be my second referee. I thank **Prof.Dr. Peter Kloppenburg** for accepting to chair my defense.

I would like to thank **AG Hammerschmidt** for sharing the LoligoTrack software and valuable inputs in Zebrafish behaviour tracking. I would like to thank **Dr. Hans-Martin Pogoda** for his inputs and suggestions regarding TALEN and Immunostaining experiments.

I extend my gratitude to **Kathy Joergens** from the graduate school for biological sciences for her cooperation in visa and contract related issues. I also thank **Dr. Isabell Witt** for her timely help and facilitating my move from contract to the graduate school for biological sciences.

My parents Mr.K.Subramanian and Mrs.Parvathi Manian are the most important people in my life to whom any amount of gratitude would be insufficient. I thank them for being the moral and motivational support throughout my life. I am greatly indebted to my brother Dr.Santosh Krishna for being a pillar of strength and bearing my worst outbursts at times of stress. His constant guidance and constructive criticism shaped my Ph.D and taught me several aspects of research life. I also extend my heartfelt gratitude

to my Bhabi Mrs.Kavita Kawathekar Krishna for her constant support and motivation during times of stress and sharing many moments of joy. I also thank my sweet niece Swara Krishna for her love towards her Chachu, Her chachu will always love her evermore.

I extend my heartfelt gratitude to Hemal Bhasin for her support and belief in me. She was an amazing friend who stood by me in times of stress and motivated me.

I would like to thank my close friends Vimal Rawat, Deepak Bhandari, Daniel Kowatschew, Aathmaja Rengarajan, Rohan Raut and many other friends for interesting conversations and fun moments spent with them.

I thank my international labmates Ivan Ivandic, Milan Dieris, Vladimir Shiryagin Gaurav Ahuja Adnan Syed Kanika Sharma Shahrzad Bozorgnia for being nice colleagues. Their cultural diversity and unique personalities gave me a wonderful learning experience.

I thank our lab manager Mr. Mehmet Saltuerk for taking good care of the zebrafish and help in some experiments and for the wonderful conversations on diverse topics.

Last but not the least I thank the people of Cologne for their warm and gracious hospitality.

ZUSAMMENFASSUNG

Der Riechsinn beeinflusst das Verhalten in der gesamten Tierwelt und ist oftmals ein unverzichtbarer Sinn der für Organismen, falls nicht vorhanden, auch lebensbedrohlich sein kann. Geruchsstoffe werden im Nasenepithel von Riechepithelzellen, den sogenannten Rezeptor Neuronen erkannt. Diese Rezeptorneuronen exprimieren G-Protein gekoppelte Rezeptoren, zu welchem auch die TAARs (Trace Amine Associated Receptors) gehören. TAARs sind oftmals in der Regulierung und Steuerung von Sozialverhalten involviert. Die vorliegende Arbeit handelt über die molekulare Charakterisierung von TAAR13c, einem Mitglied der TAAR Familie. Kadaverin ist chemisch gesehen ein di-Amin und entsteht bei der bakteriellen dekarboxylierung von Lysin, meist in verrottendem Gewebe. Es ist bekannt das Kadaverin der Primärligand für den TAAR13c Rezeptor ist und Verhaltensversuche im Zebrafisch haben gezeigt, dass es wenn vorhanden zum Aversen Verhalten führt. In der vorliegenden Arbeit wurde herausgefunden, dass TAAR13c im Nasenepithel des Zebrafisches von zilierten Rezeptorneuronen exprimiert wird. Doppelmarkierungs-Experimente mit einem neuronalen Aktivitätsmarker (cFos) haben gezeigt, dass Kadaverin nach Applikation, eine Vielzahl von Neuronen aktiviert, mitunter auch TAAR13 positive Neuronen. Ein anderer Aktivitätsmarker, Egr1 stellte sich auch als nicht selektiv heraus. Histologische Färbungen mit einem dritten Neuronalen Aktivitätsmarker namens pERK, der nicht von der Genexpression abhängt sondern über Phosphorylierung reguliert wird und somit viel schneller ist, zeigte spärliche neuronale Aktivität nach der Stimulation mit Kadaverin und anderen di-Aminen. Doppelmarkierungsexperimente mit einem TAAR13c Antikörper und pERK nach einer Kadaverinstimulation zeigte eine Kollokalisierung auf zellulärer Ebene. Der ontogenetische Beginn von aversivem Verhalten des larvalen Zebrafisches wurde anhand eines Präferenz-Apparats getestet und es wurde

ein Trend zum Aversen Verhalten im larvalen Zebrafisch festgestellt. Es wurden Versuche unternommen mit der TALEN und der CRISPR/Cas9 Methode das TAAR13c Gen auszuschalten, leider führte dies nicht zum Erfolg aufgrund von fehlenden Überprüfungsmethoden. Die sehr große Sequenzhomologie zwischen den Subtypen der TAAR Gene und eine sehr große A-T region machten es unmöglich eine spezifische Überprüfungsmethode zu etablieren. Durch eine Optimierung der Überprüfungsmethode wurden schliesslich zwei putative TAAR13c Mutanten hergestellt. Letzendlich sollten neue Mutagenese Konstrukte gegen die TAAR sub- Familie es ermöglichen eine funktionierende TAAR Mutante im Zebrafisch zu erstellen.

ABSTRACT

Olfaction or the sense of smell is a strong driver of behavior in many animals and is important for their survival. Odors are perceived through a complex molecular recognition process which involves detection of odorants by odorant receptors in olfactory sensory neurons located in the nasal olfactory epithelium. The odorant receptors belong to the G protein–coupled receptors (GPCRs) class of proteins, which includes the trace amine–associated receptors (TAARs), a class of GPCRs associated with the detection of social cues. The present study focused on molecular characterization of a TAAR receptor, TAAR13c, in zebrafish. Cadaverine, a diamine produced by bacterial decarboxylation of lysine, and thus associated with odor emanating from decaying flesh was reported to be the primary ligand for TAAR13c. Aversion to cadaverine was observed in adult Zebrafish by behavior experiments.

Here, the cell type expressing TAAR13c receptors was identified as ciliated OSNs. Double-labeling of TAAR13c-expressing neurons with cFos as neuronal activity marker after stimulation with cadaverine showed widespread expression of cFos in many cells, a few of which were also TAAR13c-positive. Another activity marker tested, Egr1, was also found to be nonselective. However, pERK, an activity marker, which does not rely on gene expression, but on phosphorylation and is therefore much faster, showed sparse cells activated after stimulation with cadaverine and a series of other diamines with different chain length. Double-labeling with pERK antibody and TAAR13c antibody showed cellular co-localization of pERK and TAAR13c signals upon cadaverine stimulus.

Ontogenetic onset of avoidance behavior was studied using a two channel choice apparatus in Zebrafish larvae. A trend towards avoidance of cadaverine was observed from the larval behavior experiments.

Knockout of TAAR13c was attempted using TALEN and Crispr-Cas9 mediated mutagenesis. Unfortunately it was not possible to design completely specific screening strategies due to high sequence identity within the five members of the TAAR13 subfamily and the AT-rich coding region of TAAR13c. Two putative knockout mutations were obtained with optimized screening methods. Finally, the design of new constructs for a TAAR13 subfamily knockout may provide a useful tool in the future for creating a functional Taar13 knockout in zebrafish.

ABBREVIATIONS

CRISPR	Clustered Regularly Interspaced Short Palindromic Repeats
DAPI	4',6-diamidino-2-phenylindole
dpf	days post fertilization
GPCRs	G-protein coupled receptors
gRNA	single guide RNA
IEG	Immediate early gene
IHC	Immunohistochemistry
OE	Olfactory epithelium
OR	Olfactory receptors
OSN	Olfactory sensory neurons
pERK	phosphorylated Extracellular Signal-Regulated Protein Kinase
SV2	synaptic vesicle glycoprotein 2
TAARs	Trace Amine-Associated Receptors
TALEN	Transcription activator-like effector nuclease
TCA	Trichloroaceticacid
V1Rs	Vomeronasal Receptors Family Type1
V2Rs	Vomeronasal Receptors Family Type2

LIST OF FIGURES

Figure 1. The olfactory system.....	13
Figure 2.The Schematic representation of cAMP second messenger cascade of olfactory sensory neurons.	14
Figure 3. A summary of TAAR ligands, their expression patterns, and behavioral roles	20
Figure 4. The positions of five TAAR13 genes as it appears in ENSEMBL browser	21
Figure 5. Schematic representation of various genome-editing platforms	26
Figure 6. Purification and characterization of TAAR13c antibody	29
Figure 7. Immunohistochemical detection of TAAR13c in ciliated neurons of the olfactory epithelium of adult zebrafish	31
Figure 8. Double Immunohistochemistry on Olfactory Epithelium of Adult Zebrafish.....	32
Figure 9. G _{olf} labelling of adult zebrafish olfactory epithelium	33
Figure 10. TAAR13c Inhibitor peptide assay at 0.5 molar peptide excess & co-labeling with microvillous neuron marker Calretinin as control	35
Figure 11. c-Fos and TAAR13c Co-localization experiment	37
Figure 12. Wholemout in situ on zebrafish larvae using the Egr1 probe.....	38
Figure 13. The neuronal activity marker pERK labels TAAR13c-expressing cells in adult zebrafish OE.....	40
Figure 14. Diamines elicit pERK increase in olfactory sensory neurons	42
Figure 15. Whole mount IHC with TAAR13c antibody on Adult Zebrafish Olfactory Bulb	44
Figure 16. Whole mount Immunohistochemistry on Zebrafish larvae	46
Figure 17. The zebrafish larval behavior apparatus	47
Figure 18.Larval behavior dose response with increasing concentration of Cadaverine stimulus	50

Figure 19. Screening of putative mutant larvae at 24hpf after TALEN injections in fertilized oocytes.....	52
Figure 20. Initial Screening for putative mutants using Surveyor assay	54
Figure 21. The high sequence identity within TAAR13 gene family	55
Figure 22. Alignment of sequenced amplicons with TAAR13 subfamily	56
Figure 23. Screening for putative mutants using the most specific TAAR13c primers possible that also enclose the target site	57
Figure 24. Sequence analysis of putative knock outs	59
Figure 25. Amino acid sequences of putative knock out within TAAR13 subfamily	60
Figure 26. Strategy for creating a TAAR13 subfamily knockout.....	62
Figure 27. In situ hybridisation and TAAR13c IHC (Right)	64
Figure 28. CRISPR-CAS cloning strategy.....	85

INTRODUCTION

The biology of olfaction

Olfaction, the sense of smell is one of the primary senses in humans and in other animals. Olfactory sense is pivotal in communicating with our surrounding and provides vertebrates and arthropods with the ability to sense food, evade predators, localise prey, recognize kin (Gerlach et al., 2008), select mates and reproduce, detect changes in habitat and environment and overall is an essential feature of life. Olfactory sense is also a defence and offense mechanism seen in many animals. Animals such as skunks emit repugnant odours in order to evoke avoidance response in their predators (Ferrero and Liberles, 2010).

Olfaction is also tightly linked to emotional states, and certain odours trigger a variety of emotions and behavioural responses. Odours are associated with memory, pleasure, disgust, fear, desire and these emotional states can help the animal find prey or food, evade a predator, find a mate or trigger unique behavioural responses. In many vertebrate species, e.g. rodents, olfaction plays a much larger role than in humans and is central to their survival. The relative prominence of brain centers dedicated to olfactory signal processing is correspondingly larger in such species. From an evolutionary perspective, olfaction is one of the most primitive senses with astounding complexity during the evolution of vertebrates.

Odorants are detected upon interaction with olfactory receptors (ORs) in the nose. Molecular biology of olfaction has seen tremendous progress since the discovery of the vertebrate olfactory receptor family in rat by scientists Linda Buck and Richard Axel (Buck and Axel, 1991), who later won the Nobel Prize for their discovery. The first olfactory receptors which were cloned as a part of this monumental study were rodent G-protein coupled receptors (GPCRs). With further advances in genome sequencing and availability of

whole genomes sequences of various other organisms, the characterisation of olfactory receptor repertoires has expanded massively. As a result a comprehensive insight into the olfactory system in early diverging vertebrates such as fish came to light which was previously unknown. Zebrafish provides an attractive model system in developmental biology to study the molecular and functional mechanisms underlying the olfactory-driven behaviours (Fishman, 2001). There have been massive advances in elucidating the genetics, developmental processes, neurophysiology, behavioural patterns and structures underlying the zebrafish olfactory system (Braubach et al., 2009; Korsching et al., 1997; Miyasaka et al., 2013).

The Olfactory System

The Olfactory system consists of the olfactory epithelium in the nose, the olfactory bulb as first projection area, and the olfactory cortex (Figure 1). Furthermore these regions have manifold connections to several other brain regions such as habenula, and amygdala. Olfactory perception is initiated by highly specialized olfactory sensory neurons (OSNs) which house the olfactory receptors (Fleischer et al., 2009; Gaillard et al., 2004). The olfactory receptors are integral membrane proteins. Some olfactory receptors bind odorants with high specificity; others have broad ligands or targets. These olfactory receptors are present on ciliary structures present on the apex of the neurons and these ciliary structures are exposed to the environment, enabling them to capture and bind the odorant. There exists a family of olfactory binding proteins to which the odorant molecule binds, and which are believed to assist in transport of the odorants. At the base of the neuronal cell body an axon extends toward the olfactory bulb. Within the olfactory bulb, olfactory neurons express a particular receptor bundle and converge to form synapses with post synaptic cells (Figure 1). The junctions form a spherical unit called a glomerulus and eventually a complex network of glomerulus, the glomeruli (Fleischer et al., 2009; Kermen et al., 2013).

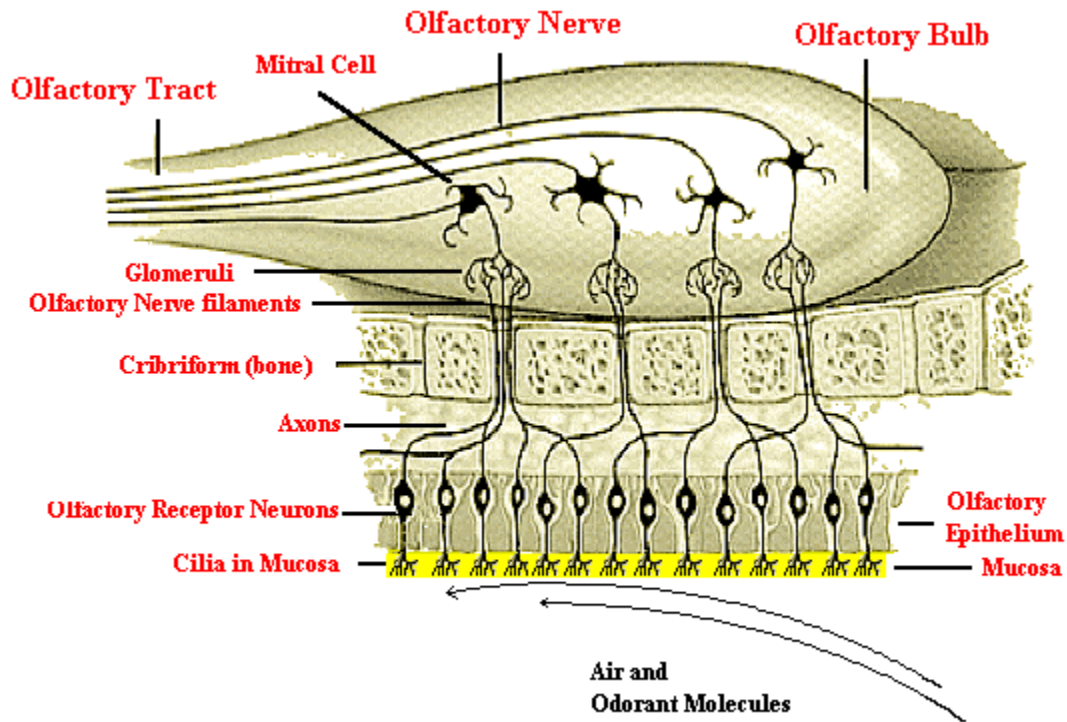


Figure 1. The olfactory system

(Adapted from a paper that appears at <http://www.leffingwell.com/olfaction.htm>).

The scientific advancements in the last few decades, facilitated by improved genetic and molecular tools have identified many multigene families encoding olfactory receptors. Such a diverse array of olfactory receptors accounts for the ability of the olfactory system to detect and distinguish a diverse range of chemical odorants.

Signal transduction events mediating olfaction

Soon after ligand binding, the GPCRs undergo a conformational change and initiate an intra-cellular signaling via a G-protein with which it associates (Figure 2). G-protein is a molecular switch, which can be activated to bind GTP (guanosine triphosphate) or deactivated to bind GDP. When the olfactory receptor couples to the G-protein, the GDP in the alpha subunit of the corresponding G-protein is replaced by GTP. This GTP-bound G-protein activates the enzyme adenylyl cyclase, which catalyzes the conversion of

ATP to cAMP (cyclic adenosine monophosphate) which acts as secondary messenger. An elevation of cAMP leads to the opening of cyclic nucleotide gated (CNG) ion channels, allowing Na^+ and Ca^{2+} ions into the cell. This results in membrane depolarization. The action potentials in axons of the OSN transmits the chemosensory information to the olfactory bulb (Hayden and Teeling, 2014; Munger et al., 2009).

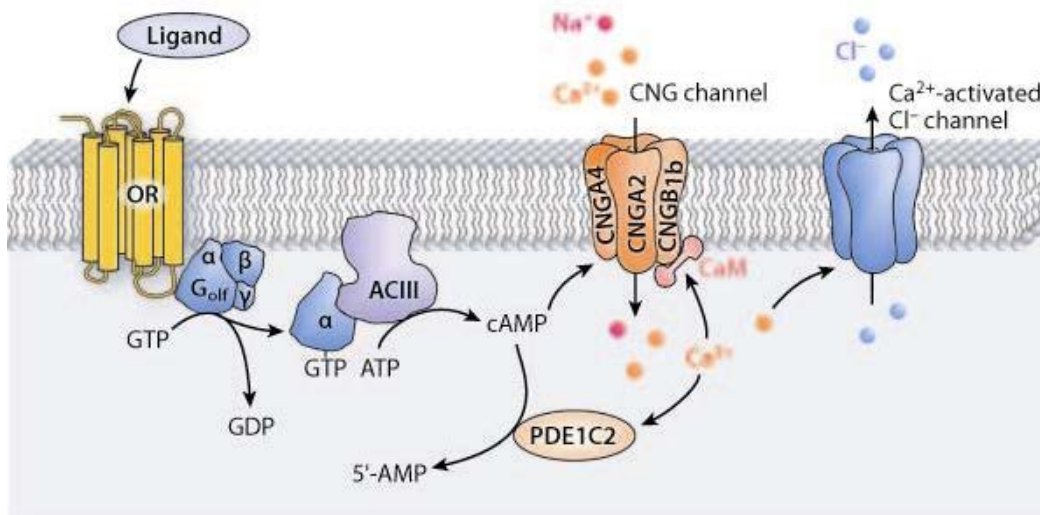


Figure 2. The Schematic representation of cAMP second messenger cascade of olfactory sensory neurons.

Binding of an odorant to its cognate OR results in the activation of heterotrimeric G protein. Activated G protein in turn activates type III adenylyl cyclase (AC3), leading to the production of cyclic AMP (cAMP) from ATP. High cAMP leads to opening of the cyclic nucleotide-gated (CNG) ion channel, leading to the influx of Na^+ and Ca^{2+} and subsequent depolarization of the cell. Figure from (Munger et al., 2009).

Olfactory sensory neurons

The model organism of this study is Zebrafish (*Danio rerio*), in which the olfactory system is highly conserved. Zebrafish Olfactory Sensory Neurons (OSNs) are comprised of three morphologically distinct types of cells: Ciliated, microvillous and Crypt. While ciliated and microvillous cells are present in higher vertebrates, crypt cells have only been found in fish

(Kermen et al., 2013). Most OSNs express only one type of receptor (Sato et al., 2007). Ciliated OSNs express $G\alpha_{olf}$ while Microvillous OSNs are heterogeneous, with many expressing $G\alpha_{q/11}$, whereas crypt OSNs express $G\alpha_o$ (Hansen et al., 2003).

Ciliated neurons: Ciliated neurons have long dendrites and few cilia and are located in deep layer of Olfactory epithelium (OE) (Hansen and Zielinski, 2005; Kermen et al., 2013). Ciliated neurons express OR family of olfactory receptors and mainly project to the dorsal and medial olfactory bulb (Yoshihara, 2009). Subsets of zebrafish olfactory sensory neurons express members of the Trace Amine-Associated Receptor (TAAR) gene family (Hussain et al., 2009; Kermen et al., 2013). The signal transduction of ciliated OSN uses cyclic nucleotide-gated channel A2 subunit, and olfactory marker protein (OMP) (Sato et al., 2005; Sato et al., 2007). Ciliated cells respond to amino acids, urine extracts with bile acids and have been proposed to be involved in alarm substance detection (Sato and Suzuki, 2001).

Microvillous neurons: Microvillous neurons have shorter dendrites and microvilli and are located in the intermediate layer of OE (Hansen and Zielinski, 2005; Kermen et al., 2013). Microvillous cells express Vomeronasal receptor (VR) family of olfactory receptors and transient receptor potential channel C2 (TRPC2) (Sato et al., 2005; Yoshihara, 2009). They have been shown to project to the lateral olfactory bulb. Microvillous cells have been shown to respond to amino acids and nucleotides (Hansen et al., 2003).

Crypt neurons: Crypt neurons are pear shaped cells with a crypt-like apical invagination. These are specific to fish and contain microvilli and few cilia (Hansen and Zielinski, 2005; Hansen et al., 1999). Crypt cells project to the ventral olfactory bulb in carp and to the dorsomedial olfactory bulb in zebrafish (Gayoso et al., 2012). Crypt cells have been shown to express a member of the Vomeronasal receptor (VR) family in zebrafish (Oka et al.,

2012). Molecular markers characterizing crypt neurons are TrkA- and S100-like immunoreactivity (TrkA-ir, S100-ir) (Catania et al., 2003; Germana et al., 2004). Crypt cells have been proposed to participate in reproductive pheromone detection (Bazaes et al., 2013).

Kappe neurons: Kappe neurons are a recently identified fourth population of olfactory sensory neurons in zebrafish (Ahuja et al., 2014). This novel neuronal population identified by G_o-ir does not express established markers of ciliated, microvillous and crypt neurons, but appears to have microvilli. Furthermore, they have a unique cell shape and spatial position which is significantly different from either crypt, ciliated or microvillous neurons.

Olfactory receptor gene family

Four olfactory receptor gene families have been characterized to date in teleost, all of which belong to families of GPCRs which contain seven hydrophobic membrane spanning domains (Korsching, 2009). These include Odorant receptors (ORs), Vomeronasal Receptors Family Type1 (V1Rs), Vomeronasal Receptors Family Type2 (V2Rs) and Trace Amine-Associated Receptor Family (TAARs). The mammals contain an additional fifth family called formyl peptide receptor (FPRs). Around 300 genes in zebrafish encode potential olfactory receptors. The four classes of zebrafish olfactory receptors are described below in detail:

Odorant receptors (ORs): ORs belong to the rhodopsin class of GPCRs with a seven-membrane domain topology (Mombaerts, 2004). OR gene family in zebrafish contains about 140 genes as compared to up to two thousand genes in mammals (Fleischer et al., 2009; Korsching, 2009; Miyasaka et al., 2013; Venkatesh et al., 2014). ORs are intron less and are expressed in ciliated neurons. The ORs have a hypervariable region in their transmembrane domain which is the presumed site of ligand binding enabling them to detect a wide range of chemical odours in their environment

(DeMaria and Ngai, 2010). Olfactory receptors are expressed according to the “one neuron, one receptor” rule, in which each olfactory neuron expresses a singular odorant receptor (Chess et al., 1994; Serizawa et al., 2003).

Vomeronasal Receptors Family Type1&2 (V1Rs and V2Rs):

Vomeronasal receptor family is expressed in the accessory olfactory organs named Vomeronasal organ (VNO). There are two types of Vomeronasal receptors: V1Rs, which are located in the apical compartment and V2Rs which are located in the basal compartment of the VNO (Dulac, 2000). The vomeronasal receptors too belong to GPCRs and are implicated in detection of pheromones. Unlike the terrestrial vertebrates, teleost fishes do not have a VNO and their V1Rs and V2Rs are expressed in the main olfactory epithelium.

The teleost odorant receptors A (ORA) family is related to mammalian V1Rs and are related to the class A GPCRs (Behrens et al., 2014; Pfister et al., 2007; Pfister and Rodriguez, 2005; Saraiva and Korsching, 2007). ORA receptors exhibit high sequence diversity. The teleost ORA receptor gene family is relatively small with typically 6 members only, compared to over 100 genes in the corresponding rodent V1R gene family. Moreover there are very few gene birth and death events in the ORA family, compared to the rapidly evolving V1R family (Zapilko and Korsching, 2016).

The teleost OlfC is related to Mammalian V2Rs and belongs to class C GPCRs. They have a large (70 kDa) N-terminal extracellular domain (Pin et al., 2003). About 50 V2R genes are present in the zebrafish genome while no intact V2R genes are present in humans (Shi and Zhang, 2009). Fish V2Rs have been proposed to recognize mainly amino acids (Luu et al., 2004). Mammalian V2Rs may also recognize small peptides that serve as ligands for major histocompatibility complex (MHC) molecules (Leinders-Zufall et al., 2004; Leinders-Zufall et al., 2014).

Trace Amine-Associated Receptor Family (TAARs):

TAARs belong to the class A (rhodopsin-like) GPCRs. The fish TAAR gene repertoire appears to be much larger than the mammalian repertoire with 112 TAARs in zebrafish and only 15 characterized TAARs in mice (Hussain et al., 2009). TAAR genes segregate into 3 classes, with the third and youngest class emerging in teleost fish (Hussain et al., 2009). This third class is actually the largest clade in teleost fish TAARs (Hussain et al., 2009; Liberles, 2015). TAARs share homology with biogenic amine receptors such as serotonin and dopamine receptors which recognize amines through a key salt bridge involving three conserved transmembrane aspartic acid residues (Shi and Javitch, 2002). All TAARs except TAAR1 function as olfactory receptors, based on studies in rodent, primate, and fish where they are involved primarily in detecting social or alarm cues using volatile amines as ligands (Hussain et al., 2009; Liberles, 2015; Pacifico et al., 2012). OSNs expressing TAARs co-express Golf, the G protein to which odorant receptors couple (Liberles and Buck, 2006). TAAR repertoire has undergone expansion, contraction, and mutations across the phylogeny allowing recognition of diverse amines (Hussain et al., 2009; Liberles, 2015).

Amines as ligands

Biogenic amines are an important class of chemical messengers which regulate a range of behavioral and emotional states. They include neurotransmitters like dopamine and serotonin and several hormones, many of them interacting with GPCRs. They are synthesized from aromatic amino acids and their synthetic pathways include a decarboxylation step that is catalyzed by one of several aromatic amino acid decarboxylases (Zucchi et al., 2006). The biogenic amines that are present in the central nervous system at very low concentrations in the order of 0.1-10nM are referred to as trace amines. These trace amines were eponymous for the dedicated class of receptors for amine odors/ligands in the OE called TAARs (Ferrero and

Liberles, 2010; Liberles and Buck, 2006). Ligands have been identified for TAAR1, TAAR3, TAAR4, TAAR5, TAAR7s, TAAR8s, TAAR9, and TAAR13c using high through-put chemical screens and medicinal chemistry approaches (Borowsky et al., 2001; Bunzow et al., 2001; Ferrero et al., 2012; Liberles and Buck, 2006; Scanlan et al., 2004). Each of these TAARs detects amines. TAAR1, which is not expressed in OE detects various biogenic amines and other TAARs which are expressed in OE detects volatile odors, some also natural products (Figure 3). TAARs have been implicated in mediating both aversion and attraction behavior (Hussain et al., 2013; Liberles, 2015). Recently, high throughput chemical screens were performed which reports recognition of ligands for 11 TAARs from zebrafish (Li et al., 2015).

A special class of amines is diamines, which possess two amine groups. Physiologically relevant diamines are cadaverine and putrescine, which arise from bacterial decarboxylation of the amino acids lysine and arginine, respectively. Cadaverine is a strongly repulsive odour for zebrafish and humans, whereas it has been reported to be feeding attractants for rats as well as goldfish (Heale et al., 1996; Rolen et al., 2003).

TAAR	Species	Expression	Ligand (EC ₅₀)	Odor source	Behavior
1	h, m, r, z	non-olfactory	trace amines, other		
2	h, m, r	OE (m: dorsal)			
3	m, r	OE (m: dorsal)	isopentylamine A (10 μM)		Aversion (m)
4	m, r	OE (m: dorsal)	2-phenylethylamine B (3 μM)	carnivore urine	Aversion (m*, r)
5	h, m, r	OE (m: dorsal)	trimethylamine C (300 nM)	male mouse urine	Attraction (m*) Aversion (r, h)
6	h, m, r	OE (m: ventral)			
7s	m (5), r (7)	OE (m: both)	N,N-dimethylalkylamines D (1-30 μM)		
8s	h, m (3), r (3)	OE (m: dorsal)	N-methylpiperidine E (100 nM)		
9	h, m, r	OE (m: dorsal)	N-methylpiperidine E (20 μM)		Aversion (m)
13c	z	OE	cadaverine F (20 μM)	decomposing tissue	Aversion (z, m)

Figure 3. A summary of TAAR ligands, their expression patterns, and behavioral roles

Table modified from (Liberles, 2015) Human (h), mouse (m), rat (r), and/or zebrafish (z) genomes contain genes from indicated TAAR subfamilies. Mice and rats have multiple TAAR7s and TAAR8s, as indicated in parenthesis. All TAARs except TAAR1 are expressed in olfactory epithelium (OE). The identities, ecological sources, and evoked behavioral responses of TAAR ligands are shown.

Trace Amine-Associated Receptor Subfamily 13

This study is focused on characterization of an olfactory receptor, TAAR13c in zebrafish. The TAAR13 sub family belongs to class II TAAR olfactory receptors, which also have mammalian representatives. There are five genes within this subfamily, which are clustered side by side on the same chromosome in the order: TAAR13E, TAAR13A, TAAR13B, TAAR13D, TAAR13c (Figure 4). The five genes share about 90% identity at the nucleotide level. Cadaverine has been reported to be a *bonafide* ligand for TAAR13c (Hussain 2010; Hussain et al., 2013). Mice lack a TAAR13c

ortholog, yet a role for other TAARs in diamine recognition is supported by the finding that mice lacking all olfactory TAARs fail to avoid cadaverine odor (Dewan et al., 2013; Li et al., 2015; Liberles, 2015). High affinity ligands for other TAAR13 genes have also been reported recently (Li et al., 2015). TAAR13A recognizes histamine, TAAR13D recognizes putrescine, while TAAR13E detects agmatine with highest affinity (Li et al., 2015).

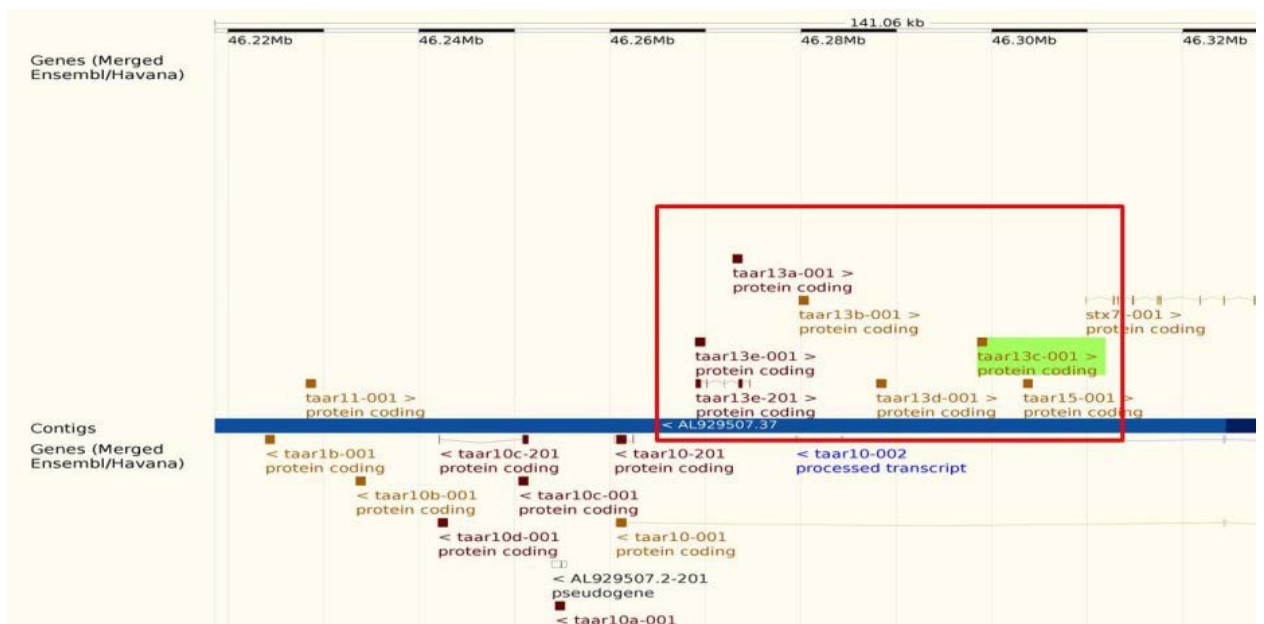


Figure 4. The positions of five TAAR13 genes as it appears in ENSEMBL browser

TALEN and CRISPR: recent improvements for knockout in zebrafish

Ever since the discovery of DNA double helix and genome sequencing, there has been a quest to study the biological function of these sequences and their transcripts. This has been aided by several breakthroughs in the field of genetics. While forward genetics relies on identification of a phenotype followed by isolation of the gene responsible for the phenotype; reverse genetics relies on mutating a particular gene with targeted mutagenesis and then identify the novel function associated with the gene. With the advent of recombinant DNA technology in 1970's, manipulation of genomic sequences became possible aiding the further advancement in the field of reverse genetics. The initial developments made use of homologous recombination for targeted gene mutation, which is an endogenous repair mechanism operating in organisms to deal with DNA damage where two similar DNA strands exchange nucleotide information (Carroll, 2014; Gaj et al., 2013; Smithies et al., 1985). However, this approach was hampered by low frequency of homologous recombination in higher organisms. In mouse, this has been overcome by selection in embryonic stem cells (Mansour et al., 1988), but this approach has not been transferable to most other species.

In zebrafish, before the availability of genome editing techniques, disruption of gene function was mostly achieved by targeted knockdown using anti-sense morpholinos (MO) (Eisen and Smith, 2008). But these knockdowns were temporary, raising the need for a means to generate stable, directed mutations.

The development of targetable nucleases led to the beginning of a new era of genome engineering where virtually any gene could be mutated or deleted. These nucleases can generate double strand breaks in the DNA, which are repaired in the cells by two mechanisms: Homologous recombination (HR) and Non-homologous end joining (NHEJ) (Carroll, 2014; Wyman and

Kanaar, 2006). Homologous recombination along with site specific nucleases can be used to create precise mutations in the target by using a homology-containing donor template. On the other hand, NHEJ does not require a homologous template and re-ligates the broken ends without regard for homology leading to introduction of small insertions and deletions that alter the genome sequence and can thus lead to a knockout of the affected gene (Carroll, 2014; Gaj et al., 2013).

Three major kinds of nucleases are in use for genome editing at present: ZFN's (Zinc-finger nucleases); TALEN's (transcription activator-like effector nucleases) and RNA-guided engineered nucleases (RGENs) derived from the bacterial clustered regularly interspaced short palindromic repeat (CRISPR)–Cas (CRISPR-associated) system. They are briefly discussed in the following sections.

Zinc-finger nucleases

Zinc-finger nucleases (ZFNs) consist of DNA-binding domains derived from natural transcription factors (TFs) that are linked to the nuclease domain of the Type IIS restriction enzyme, FokI. Chandrasekaran and colleagues examined FokI, a Type IIS enzyme, and found that it has physically separable cleavage and binding domains (Carroll, 2011; Li et al., 1992). In addition, the cleavage activity is non-specific and can be re-directed to alternate sites by substituting the natural DNA recognition domains with alternative specific DNA binding domains. In ZFN's the DNA binding domain consists of a series of different C₂H₂ zinc-fingers, which are the most common DNA-binding motif found in higher eukaryotes (Figure 5A). Each zinc-finger recognizes a nucleotide triplet sequence, and 3–6 zinc-fingers are used to generate a single ZFN subunit that binds to DNA sequences of 9–18 bp. Two ZFN monomers are required to dimerize for the nuclease activity to occur. Each monomer binds to their target half site separated by a linker of 5-7 bp.

This requirement for dimerization greatly increases the specificity of target site recognition (Carroll, 2011; Carroll, 2014; Gaj et al., 2013).

As compared to other nucleases, ZFN's have several limitations. In addition to the laborious designing, not all newly assembled ZFN's have high activity and cannot cleave DNA efficiently. They also have high off-target effects and suffer from low target density (Ramirez et al., 2008; Schmid and Haass, 2013).

The Talen approach to genetic engineering

Talens are yet another tool which has emerged in recent years with a potential to modify genomes in a regulated manner (Hubbard et al., 2015). The general composition of TALEN's is similar to that of ZFN's. They too use the same FokI endonuclease domain for cleavage. However, they have a different DNA binding domain called transcription activator-like effectors (TALEs), which are derived from the plant pathogenic Bacterium *Xanthomonas spp* (Carroll, 2014; Kim and Kim, 2014; Schmid and Haass, 2013). The bacterium uses these proteins to import them into host nucleus and regulate host genes to promote infection. TALE's are composed of nearly identical 33–35 amino acids-long repeats each of which recognizes a single base pair in the major groove (Figure 5B). The repeats possess two hypervariable amino acids called repeat-variable di-residues (RVDs) each at positions 12 and 13. The RVDs govern the binding specificity of each repeat to a single nucleotide in the DNA target sequence. Four different RVD modules — namely Asn-Asn, Asn-Ile, His-Asp and Asn-Gly — are most widely used to recognize guanine, adenine, cytosine and thymine, respectively. Each TALEN is composed of transcription activator-like effectors (TALEs) at the amino terminus and the FokI nuclease domain at the carboxyl terminus. Target sequences of TALEN pairs are typically 30–40 bp in length, excluding spacers. TALEN's have a simpler design strategy as compared to ZFN's and also have considerably lower off-target effects. In

addition, their binding affinities are predictable after the code of TALE DNA binding domain was elucidated (Campbell et al., 2013; Carroll, 2014).

Clustered regularly interspaced short palindromic repeats/CRISPR-associated 9:

CRISPR-CAS9 system has emerged as one of the most powerful and a preferential genome editing tool due to its simplicity, efficacy and specificity. CRISPR-CAS9 idea is based on an adaptive immune system widespread among bacteria and archaea. The CRISPR-associated protein Cas9 is an endonuclease that uses a guide sequence within an RNA duplex, tracrRNA:crRNA, to form base pairs with DNA target sequences, enabling Cas9 to introduce a site-specific double-strand break in the DNA (Doudna and Charpentier, 2014). A single guide RNA (sgRNA or gRNA) can be constructed by fusing a crRNA containing the targeting guide sequence to a tracrRNA that facilitates DNA cleavage by Cas9 in vitro (Cong et al., 2013; Jinek et al., 2012) . The gRNA contains a nucleotide sequence at the 5' end that determines the DNA target site by Watson-Crick base pairing and a duplex RNA structure at the 3' side that binds Cas9 (Doudna and Charpentier, 2014; Yang, 2015). The gRNA target site must contain a three nucleotide NGG motif called the protospacer adjacent motif (PAM) downstream of the recognition site for cleavage by Cas9 to occur (Figure 5C). For targeted mutagenesis in zebrafish, the gRNA can be transcribed from a plasmid or from an oligo and co-injected with Cas9 mRNA to induce the mutations at the target site (Schmid and Haass, 2013). CRISPR-CAS9 system has become a preferred genome editing method over TALEN and ZFN's due to its simple and inexpensive design, high efficiency, and ease of multiplexed target recognition.

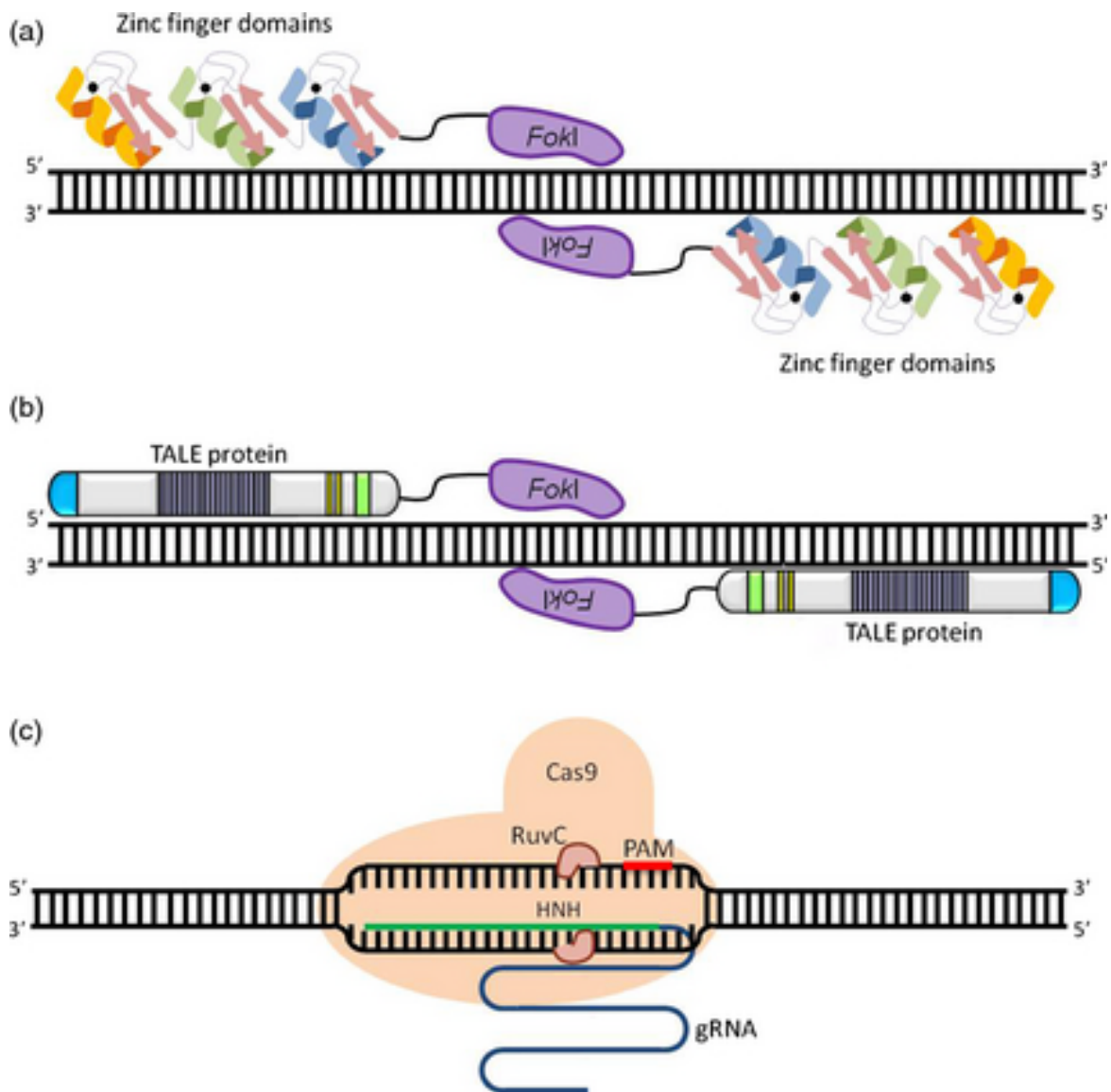


Figure 5. Schematic representation of various genome-editing platforms

Figure taken from (Mahfouz et al., 2014) (a) Zinc finger nucleases (ZFNs) are composed of DNA recognition domains and FokI nuclease catalytic domain fusions. Each zinc finger in the DNA recognition domains binds three nucleotides. On average three to four zinc fingers are fused to recognize 9–12 nucleotides. Two ZFNs are required to produce double-strand breaks (DSB) as the FokI domain requires dimerization to be catalytically active. (b) Transcription activator-like effector nucleases (TALENs) are composed of TAL central DNA-binding repeat domain and FokI catalytic domain fusions. DNA-binding specificity is determined by the 12th and 13th hypervariable residues of each repeat [repeat variable diresidue (RVD)]. Similarly, two TALENs heterodimer binding in a tail-to-tail orientation with proper spacer length to allow dimerization of the FokI domains are required for activity and DSB formation. (c) Clustered regularly interspaced short palindromic repeats (CRISPR)/Cas9 mediates DSBs formation. Cas9 is guided to the 20 nt DNA target by a synthetic single guide RNA (gRNA) molecule composed of crRNA and tracrRNA. Cas9 recognizes a specific protospacer associated motif (PAM) sequence on the DNA (NGG—marked in red) and performs a complete cut with the two active nuclease domains RuvC and HNH (Mahfouz et al., 2014).

AIM OF THIS STUDY

This study focuses on molecular characterization of TAAR13c, an olfactory receptor from the TAAR family. TAAR13c possesses a high affinity ligand, cadaverine, and also is activated by other diamines (Hussain 2010). Cadaverine is a foul-smelling compound emanating from decaying flesh and occurs naturally as a bacterial decarboxylation product of the amino acid lysine. Adult zebrafish was shown to have an aversive behaviour to cadaverine (Hussain 2010), which may be mediated by TAAR13c. My study focuses on further characterization of TAAR13c receptor using a combination of cell biological, animal behavioural experimentation and genetic approaches. The aims of my study are:

1. Molecular characterization of an olfactory receptor TAAR13c and characterization of the neurons which express TAAR13c
2. To establish a functional knockout of TAAR13c in zebrafish
3. To test the onset of aversive behaviour in zebrafish larvae in response to cadaverine as prerequisite for testing a potential loss of aversion towards cadaverine in larval fishes lacking TAAR13c.

RESULTS

2.1 Preparation, Purification and characterisation of TAAR13c antibody

Since there is no commercially available antibody for TAAR13c a highly specific antibody against a specific Zebrafish (*Danio rerio*) TAAR13c peptide was synthesized and purified. The peptide corresponding to the 16 amino acids from the TAAR13c protein sequence from amino acid 234 to 250 was used to immunize rabbits. This peptide is 62-81% identical to other members of the TAAR13 subfamily. This represented a compromise between maximal divergence in this highly similar family and at the same time good antigenicity (Van Regenmortel, 2001). The peptide and the polyclonal antibody was generated by a company, Innovagen. The rabbit polyclonal antibody provided as sera by the company was further purified by affinity purification using the TAAR13c peptide columns procured also from Innovagen (see Materials and Methods for details). The affinity purified antibody with a typical yield of 600- 700 ng/ul was further characterised by western blotting including a peptide competition assay to confirm specificity.

Protein extracts from 4 organs and 3 dpf embryo was prepared in RIPA buffer. The immunizing peptide which binds to the epitope recognized by the antibody was used in 10 fold excess to neutralize the antibody from binding to the TAAR13c antigen present in the protein extracts. Western blot was performed using the purified antibody with all lysates with and without TAAR13c peptide.

Olfactory epithelium contained a major band at 55Kda, which would fit to a glycosylated TAAR13c (protein molecular weight 42 kDa). This band was absent in the peptide-neutralised sample of the same lysate (Figure 6), suggesting the purified antibody to be highly specific for TAAR13c. This band was absent from gills and heart, consistent with the expected tissue

specificity of an olfactory receptor. Heart showed a strongly reacting high molecular weight band, which was not competed by TAAR13c peptide and thus might be due to some cross-reactivity. The aliquots of this antibody were stored at 4°C and used in subsequent experiments.

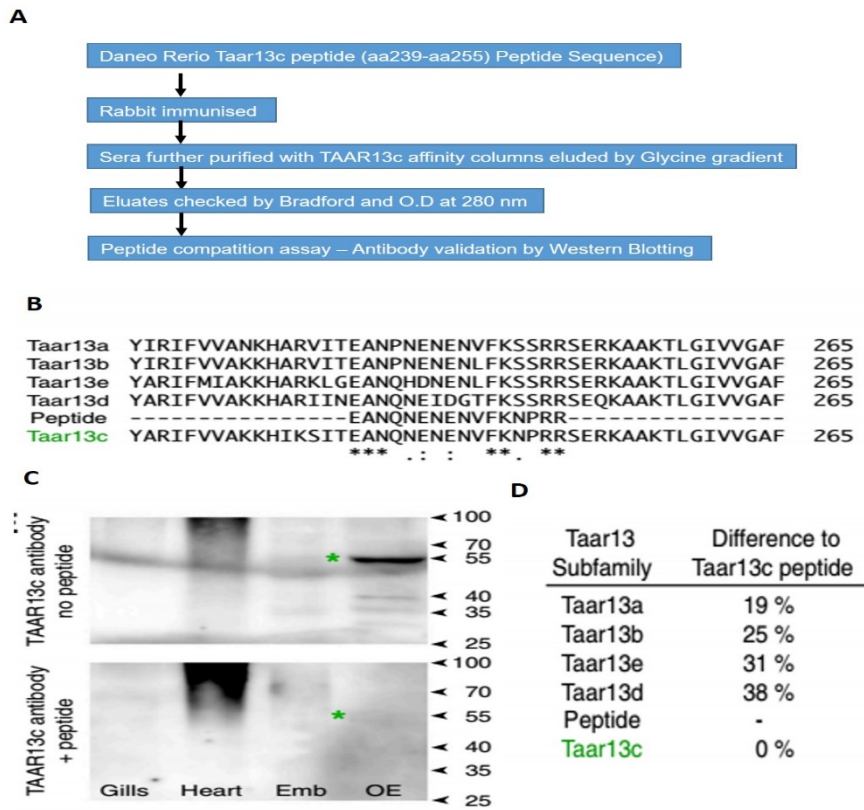


Figure 6. Purification and characterization of TAAR13c antibody

(A) Immunization with TAAR13c peptide and affinity column purification of the resulting antisera. (B) Peptide sequence comparison between TAAR13c immunizing peptide and other members of the TAAR13 subfamily shows specificity of the peptide. The peptide sequence used for immunization is between amino acid positions 234 to 250. (C) Antibody validation by Western blot, using comparison between different organs of zebrafish and peptide competition. A band at 55 kDa in OE and (weakly) in whole embryo (Emb) represents most likely the glycosylated form of TAAR13c (42kDa without glycosylation). The corresponding band is absent in the same organ lysates with the peptide neutralized antibody (green asterisks). The high molecular weight band seen in the heart is unaffected by competition with peptide and thus most likely represents a cross-reacting antigen. (D) Percentage difference of sequence similarity amongst the TAAR13 subfamily members for the immunizing peptide.

2.2 The purified antibody labels a sparse population of cells in the olfactory epithelium

In order to allow a specific labelling of TAAR13c-expressing neurons at the protein level, the affinity purified antibody was used to stain the zebrafish olfactory epithelium. Similar to the western blot the corresponding immunogenic peptide was used to neutralise the antibody in control experiments (refer protocol in materials and methods). The blocking peptide was used in 0.5, 1 and 10 fold molar excess to that of the antibody concentration.

A sparse population of labelled neurons about 2-5 per lamella was seen in the sensory region of the Olfactory Epithelium. The expression pattern is seen as neurons distributed in the inner two thirds of the lamella as a ring around the Central raphe. An IHC was performed on the OE of adult Zebrafish with the Rabbit Taar 13c antibody at a concentration of 5 ug/mL and imaged under a fluorescent microscope. A single neuron labelled with the TAAR13c has been shown (Figure 7A). The cellular morphology strongly suggests a ciliated neuron and the higher magnification (Figure 7C&D) shows a tuft of cilia extending from the apical section of the epithelial lamella. The position of the neurons and pattern of expression was similar to that of expression of TAAR13c RNA in similar cell population as assessed by *in situ* hybridization (Hussain et al., 2009). However, TAAR13c *in situ* probe labels several fold more cells than the antibody (Hussain et al., 2013) suggesting that the antibody is specific for TAAR13c, in contrast to the TAAR13c probe, which may recognize several members of the subfamily.

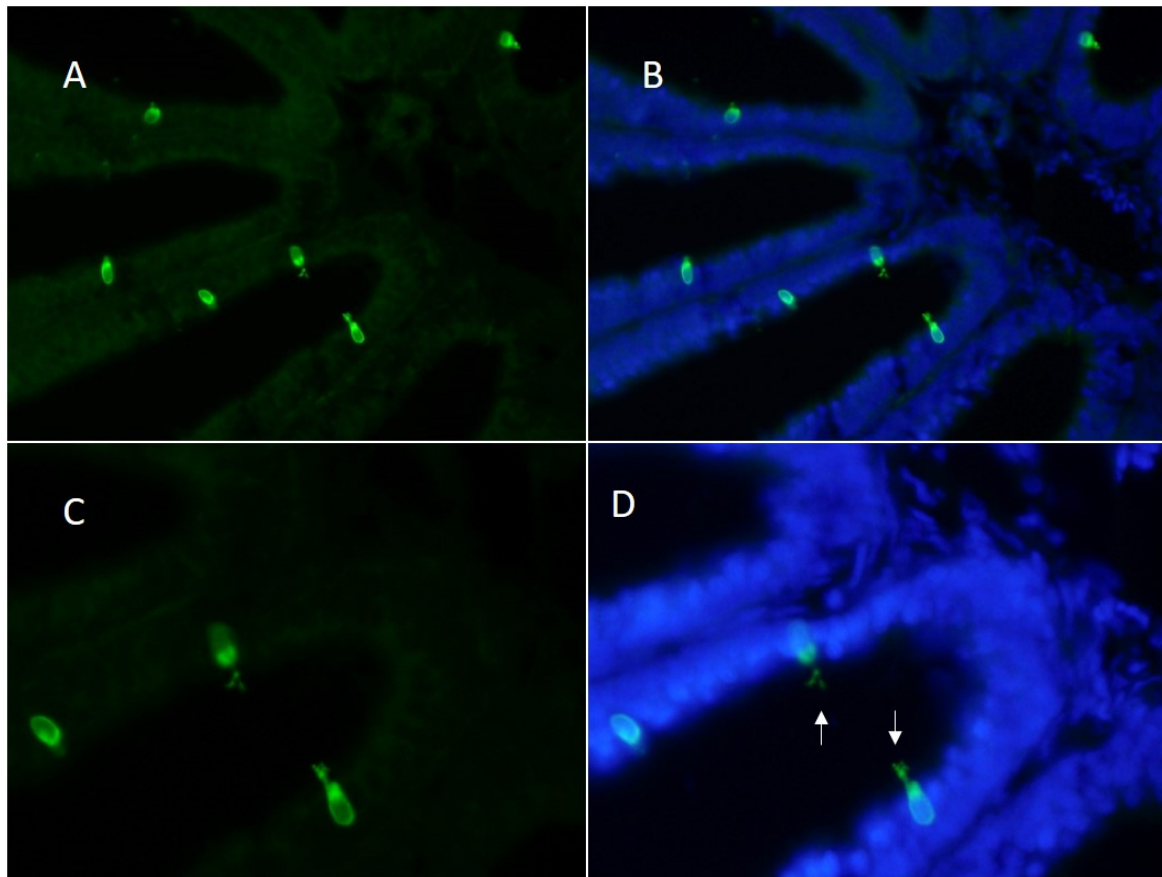


Figure 7. Immunohistochemical detection of TAAR13c in ciliated neurons of the olfactory epithelium of adult zebrafish

(A) TAAR13c-expressing neurons are seen labelled with green fluorescence of the secondary antibody. (B) Merged image of TAAR13c-expressing neurons with DAPI used as nuclear counterstain. Panels C and D show a higher magnification (60X). Long protrusions (arrow) at the apical end of a slender cell body constitute the typical morphology of ciliated neurons. Figure modified from (Hussain et al., 2013).

2.3 Co-labelling with acetylated Tubulin and G_{olf} shows expression of TAAR13c in ciliated neurons

Tubulin is a major component of Cilia and it is present in ciliated neurons in the apical layer of the cilia. This was a major difference from the other cell types because tubulin is present in the acetylated microtubules of cilia and Microvilli and crypt neuron are tubulin negative and actin positive. In Figure 8, we observe a co-label between tubulin and TAAR13c at the apical spot

where the cilia is. This suggests that TAAR13c is expressed exclusively in ciliated neurons.

Another approach to categorize the olfactory receptor neurons is by their expression of G alpha proteins. In the zebrafish olfactory epithelium G_{olf} , G_{01} , G_{02} and G_i have been shown to be present (Oka and Korsching, 2011). G_{olf} has been associated with ciliated neurons, whereas G_{01} and G_{02} are associated with microvillous receptor neurons and G_i with crypt neurons (Ahuja et al., 2013; Oka and Korsching, 2011).

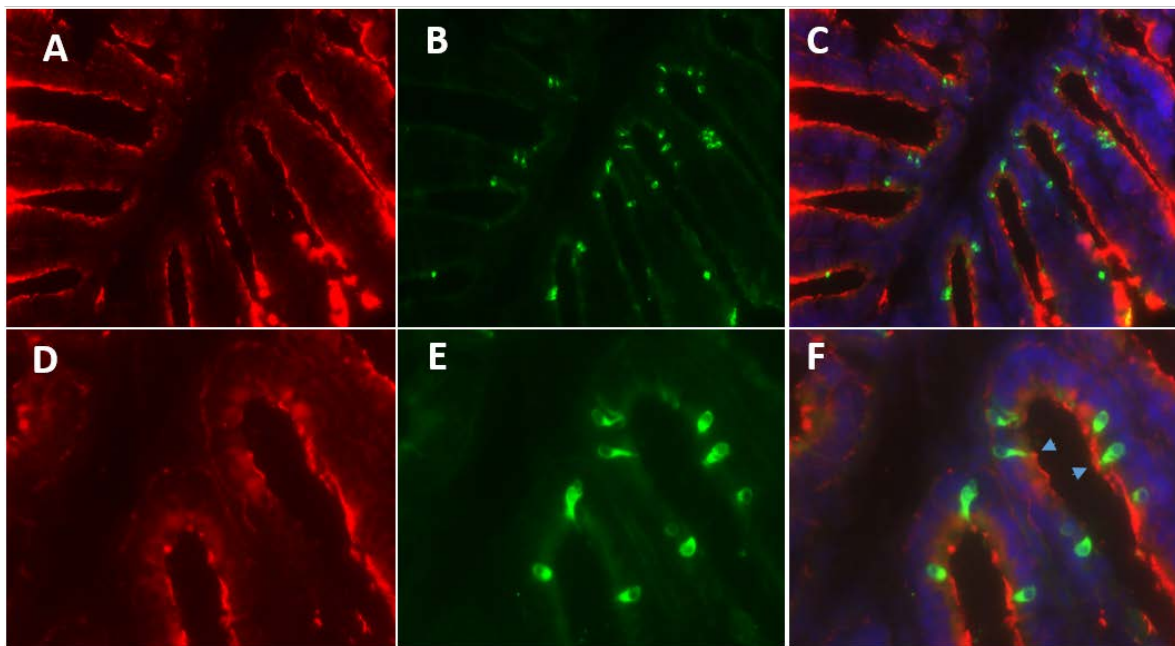


Figure 8. Double Immunohistochemistry on Olfactory Epithelium of Adult Zebrafish

(A) Anti-acetylated tubulin (red fluorescence) labels apical structures. Tubulin is a component of microtubuli present in dendrites, dendritic knob and cilia. (B) TAAR13c labelled neurons (green fluorescence) with protruding cilia. (C) Merged Image with blue DAPI nuclear counterstain. (D) (E) and F show higher magnification, 80x, of panels A, B, and C, respectively. (F) Tubulin dots co-localize with the apical tips of TAAR13c-expressing neurons, arrowheads, confirming TAAR13c-expressing cells as ciliated neurons.

Figure 9 shows a Double IHC between an anti- G_{olf} antibody and TAAR13c. G_{olf} is seen to label all the cilia in each lamella and also demarcates the

sensory and non-sensory cells of the OE. Here we observe co-labelling between G_{olf} positive cells and TAAR13c expressing ciliated neurons indicating that TAAR13c expressing neurons use G-protein G_{olf} for signal transduction. This has been observed in ciliated neurons thereby indicating that TAAR13c is expressed in ciliated neurons.

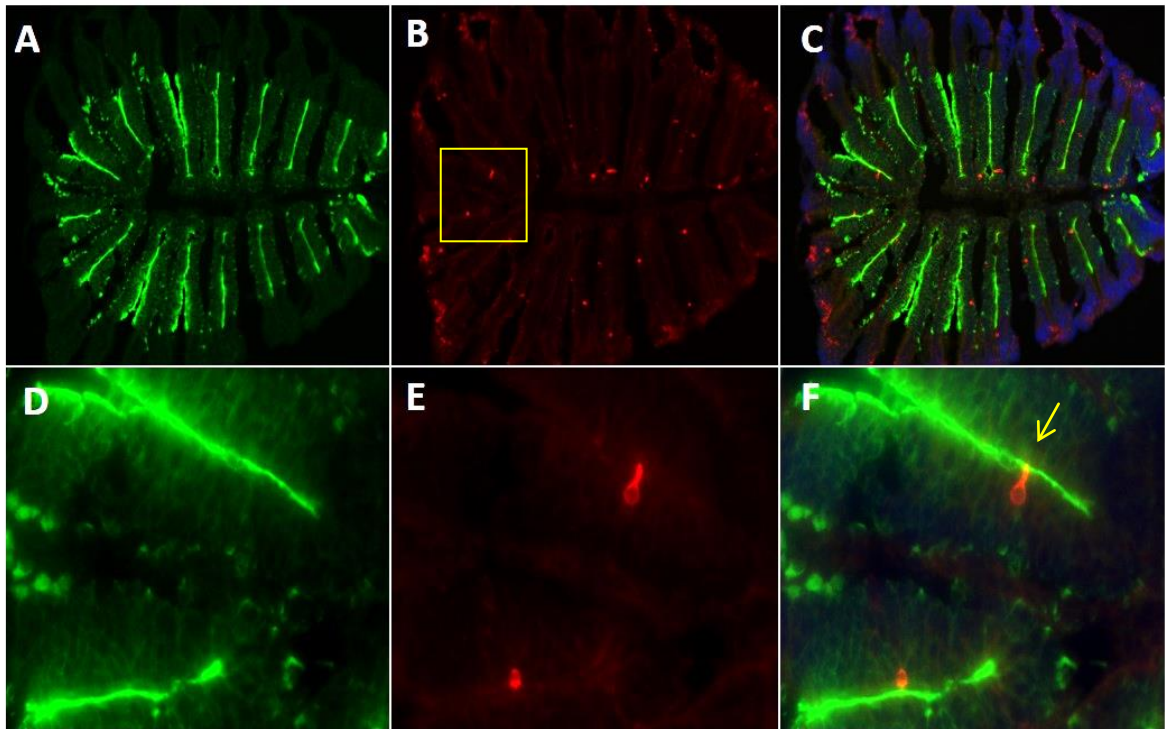


Figure 9. G_{olf} labelling of adult zebrafish olfactory epithelium

(A) Shows the expression pattern of G_{olf} E-7 antibody (green fluorescence). G_{olf} expression is clearly limited to the sensory region of the OE (inner region). (B) Expression pattern of TAAR13c labelled sensory neurons (red fluorescence) (C) Merged Image with DAPI(blue) nuclear counterstain. (D), (E) and (F) Higher magnification at 80X (D) weak TAAR13c labelling is also seen in basal cell bodies, mostly outside the sensory region. (E) Ciliated morphology of a TAAR13c-expressing neuron (red) is seen clearly with the merged image showing co-localization with G_{olf} (see arrow).

The next step was to elucidate the presence of TAAR13c exclusively in the ciliated Olfactory Sensory neurons and also to distinguish the other olfactory sensory neurons from the ciliated ones. Co-labelling of TAAR13c with

Calretinin as a microvillous cell marker was performed to investigate whether TAAR13c is expressed in ciliated or microvillous neurons. The labelling of the TAAR13c expressing cells was somewhat inhibited by the lowest concentration of the blocking peptide (Figure 10), and below detection at both higher concentrations. There was no influence of the peptide on Calretinin staining and moreover none of the Calretinin labelled microvillous neurons showed expression of TAAR13c, suggesting that TAAR13c is expressed in ciliated neurons, but not in microvillus neurons. TAAR13c expression in Crypt neurons was ruled out after V1R related ORA gene ORA4 was shown as being the only receptor expressed in crypt neurons (Oka et al., 2012).

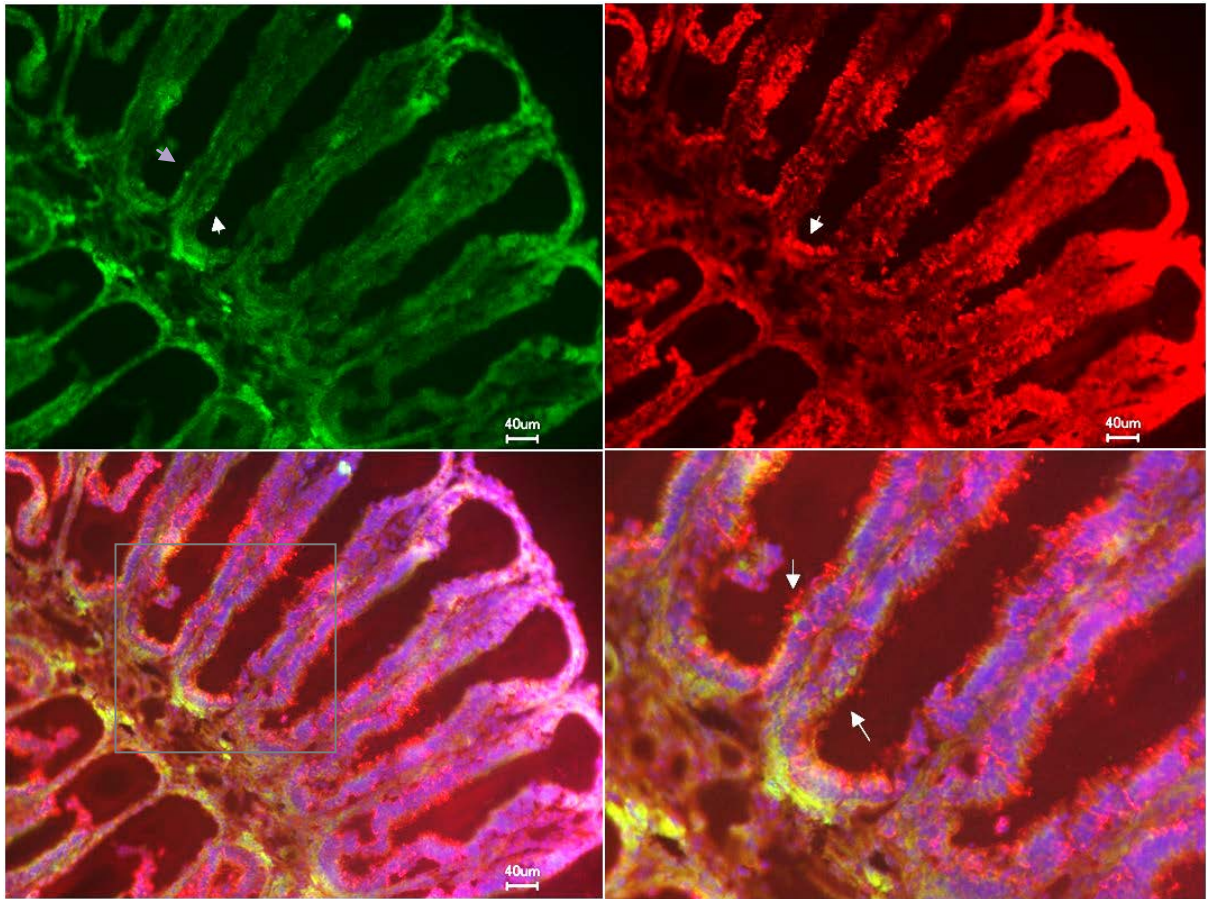


Figure 10. TAAR13c Inhibitor peptide assay at 0.5 molar peptide excess & co-labeling with microvillous neuron marker Calretinin as control

(A) No strongly labeled cells are seen in TAAR13c IHC with 0.5 molar excess of inhibitor peptide, but some faintly labelled cells (arrowheads) are visible, possibly due to incomplete competition. (B) Calretinin IHC labels microvillous neurons (arrow). (C) Merged image with DAPI nuclear counterstain (blue) (D) Higher magnification reveals no co-localization (arrows) between TAAR13c-labelled cells and Calretinin-labelled microvillous neurons.

Taken together, both the co-localisation with ciliated neuron markers such as tubulin and Golf, and the absence of co-localisation with markers for microvillous and crypt neurons shows that TAAR13c is expressed in ciliated receptor neurons.

2.4 Suitability of several neuronal activity markers to show activation of TAAR13c with cadaverine

Immediate early genes are good indicators of neuronal activity in response to an external stimulus, metabolic stress and changes to the physiological state of the organism. c-Fos is a member of the IEG family of transcription factors and a useful indicator of neuronal activity against specific ligands. Cadaverine has been shown in heterologous expression system to activate TAAR13c therefore c-Fos was used in an attempt to localise neuronal activity in TAAR13c expressing neurons after a cadaverine stimulus at 0.1mM. Adult Zebrafish was stimulated with 0.1mM cadaverine for 1 hr, the time taken for c-Fos to accumulate in sufficient quantity after its translation in the cellular nucleus. IHC was performed to label c-Fos and TAAR13c expressing neurons. In Figure 11 we see c-Fos expression is widespread in the lamellae and far exceeds the number of TAAR13c expressing cells. Co-localisation with TAAR13c expressing neurons occur as one among the several c-Fos expressing cells indicating that neuronal activity was not exclusive to the cadaverine stimulus. c-Fos expression indicates that apart from cadaverine stimulus there are other factors which contribute towards overall stress which trigger neuronal activation. Hence c-Fos was not an ideal neuronal activity marker to ascertain cadaverine's link to TAAR13c as its specific ligand. This was unexpected, since c-Fos single labelling had been used successfully for stimulation with cadaverine (Hussain et al., 2013). However, the antibody used in those experiments by Ashiq Hussain had been discontinued, so I had to scout for another c-Fos antibody which is not of rabbit origin since the TAAR13c antibody was synthesised in rabbit. The E-8 mouse anti-c-Fos antibody I selected recognised a different epitope than the K-25 rabbit anti-c-Fos antibody used by Ashiq Hussain.

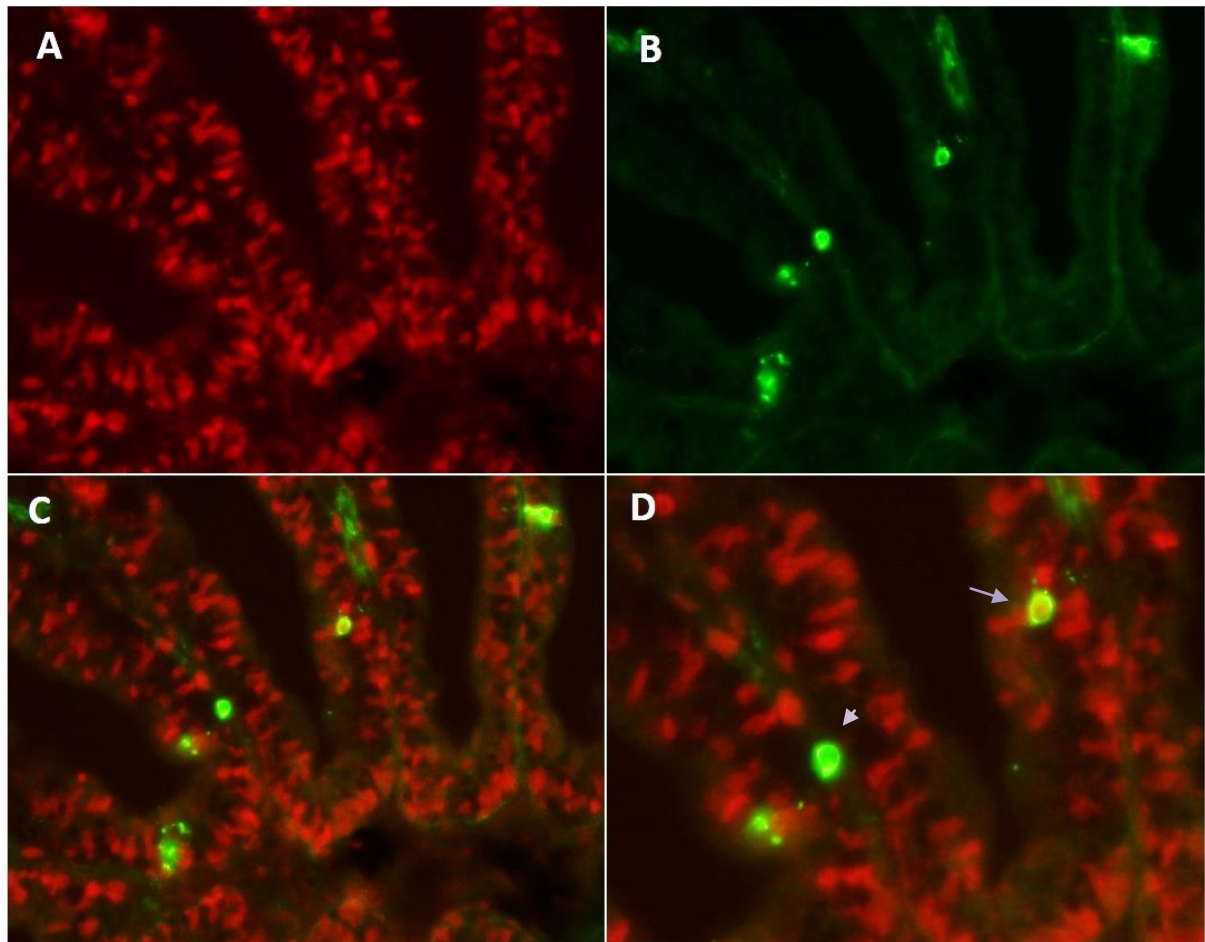


Figure 11. c-Fos and TAAR13c Co-localization experiment

(A) c-Fos E-8 antibody labelling is seen widespread in Adult Zebrafish OE upon a 0.1mM cadaverine stimulus for 1 hour. (B) TAAR13c labelled neurons (green fluorescence) constitutes a sparse population. (C) Merged image of red and green channels shows some TAAR13c cells also are co-labelled with c-Fos-staining. However, no specificity of c-Fos label for TAAR13c cells is seen. (D) Upon higher magnification, some TAAR13c cells are seen co-localizing with c-Fos (arrow), whereas others are negative for c-Fos (arrowhead).

2.5 Egr1 as immediate early gene neuronal activity marker, Whole mount in situ on Zebrafish larvae

Egr1 has been widely used as an immediate early gene for mapping specific neuronal populations and it is a regulatory transcription factor (Kress and Wullimann, 2012). Hence it was also chosen as a candidate to study the neuronal activity response to Cadaverine at 0.1mM. An Egr1 probe was made

(see materials and methods and appendix) to perform whole mount in situ analysis on Zebrafish larvae. Food and water were used as positive and negative controls respectively. It was seen that both cadaverine and food elicits a strong neuronal activity with expression seen widespread in the olfactory epithelium and mouth regions and other areas like the lateral line and tail (Figure 12). Water did not elicit a response in the nose and mouth region however expression was seen in the lateral line.

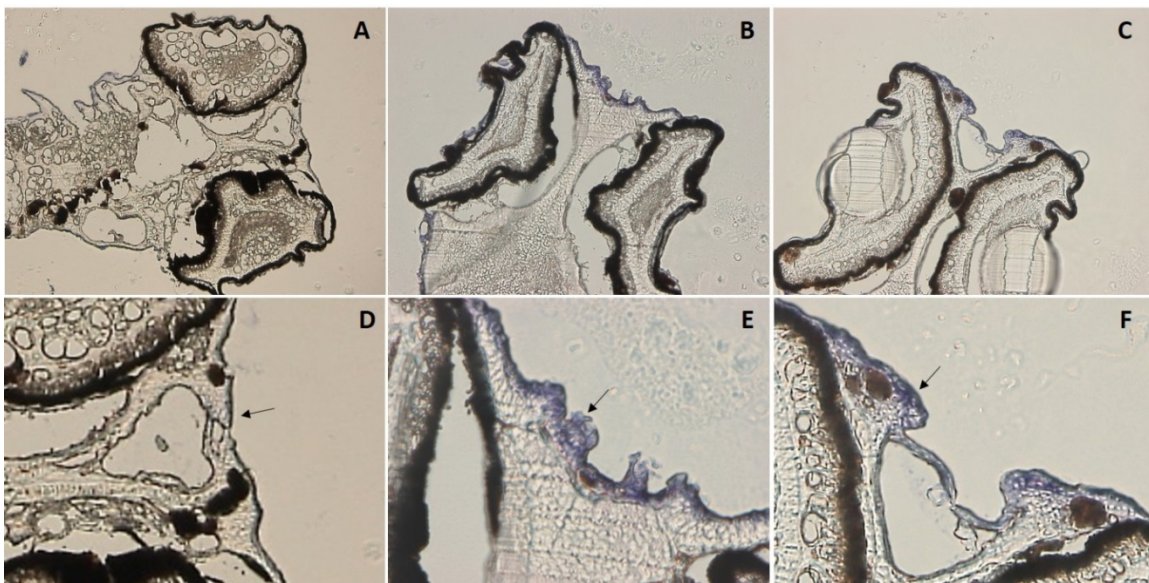


Figure 12. Wholemount in situ on zebrafish larvae using the Egr1 probe

(A) Egr1 staining on Water control revealed no staining on the mouth and nose region. (B) Egr1 stains the nose and mouth region upon stimulating with 0.1mM cadaverine for 1 hour. (C) Food stimulus for 1 hour also stains the mouth and nose region in a pattern similar to cadaverine stimulation. Egr1 staining pattern is seen clearly upon higher magnification (80X) of (A), (B) and (C) in panels (D), (E) and (F). Nose region (arrows) shows similar egr1 staining in cadaverine (E) and food stimulated (F) larvae which is absent in the water control (D)

2.6 pERK as a neuronal activity marker for TAAR13c activation due to cadaverine.

Phosphorylation of ERK protein is one of the first cellular activities which occurs upon an external stimulus. ERK is one of the penultimate kinases of the MAP-Kinase pathway leading to the activation of the downstream target genes such as c-Fos and c-Jun. The activation of the pathway is marked by a

rapid phosphorylation of ERK which serves as a marker of neuronal activation. The robustness of ERK phosphorylation as a readout of neuronal response to a stimulus in comparison to using expression analysis of immediate early gene transcription factors like c-Fos and c-Jun (which takes up to 1 hour for sufficient expression thereby exposing the fish to several stress inducing factors). Three different anti-phospho ERK antibodies were tested and the one with reproducible labelling across experiments was chosen. Co-labelling experiments with anti-TAAR13c and anti-phospho-ERK antibodies after stimulation of fish with cadaverine showed several distinct TAAR13c and pERK labelled neurons (Figure 13). The method of cadaverine stimulus was optimised for maximum pERK detection and co-labelling of pERK and TAAR13c was observed in one of many experiments (Figure 13). Later in a set of parallel experiments it was shown that at 10 μ M cadaverine concentration most pERK expressing neurons also expressed TAAR13c (Hussain et al., 2013). Hence it was postulated that at low cadaverine concentration the receptor-ligand specificity could be shown.

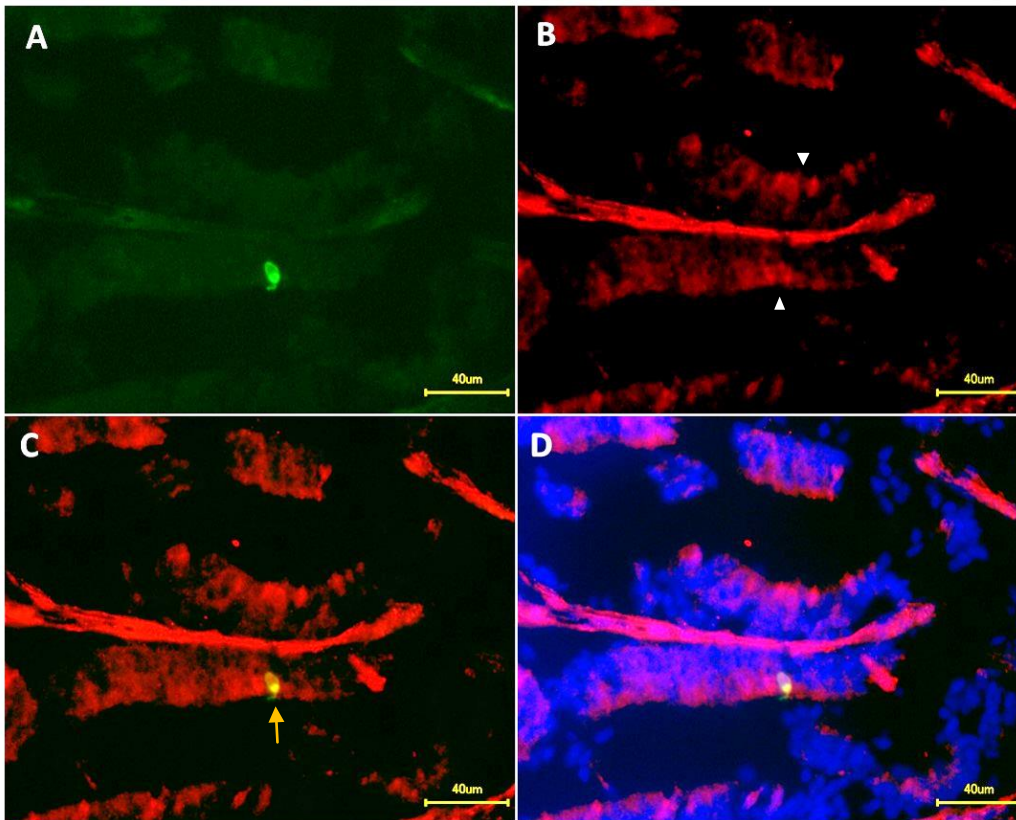


Figure 13. The neuronal activity marker pERK labels TAAR13c-expressing cells in adult zebrafish OE

A) TAAR13c-labelled ciliated neuron (green fluorescence) (B) Several cells are stained by pERK antibody after 0.1mM cadaverine stimulation for 5 minute (arrowheads). (C) The TAAR13c-labelled neuron is also stained by pERK (arrow). (D) Merged channels with DAPI (blue) nuclear counter stain.

2.7 Diamine assay using pERK as neuronal activity marker

Next, other diamines were used as stimulus, and phosphorylation of ERK was analysed, again as a neuronal activity marker. A similar experiment was earlier performed by another graduate student using cFos as the neuronal marker. However, in those experiments cFos showed high background, and so it was advantageous to repeat these experiments using pERK as a marker for neuronal activity. Olfactory tissue was obtained from zebrafish exposed to diamines or water control stimuli and stained using standard immunohistochemical (IHC) techniques. Perk expression was induced by food odor, cadaverine, and other diamines (approx. 6.0 cells per lamella) but

not tank water alone (<0.5 cells per lamella). The background levels in tank water are low, and likely result from residual odors in tank water. Low concentrations of cadaverine and putrescine resulted in very low frequencies of pERK-labeled cells (Figure 14F), consistent with detection by a single olfactory receptor (Hussain et al., 2013). The range of diamine chain lengths (C3 to C10) that stimulate either c-Fos expression or ERK phosphorylation in olfactory tissue includes all diamines that promote aversive behavior (C4 to C8), consistent with this behaviour being mediated by olfaction.

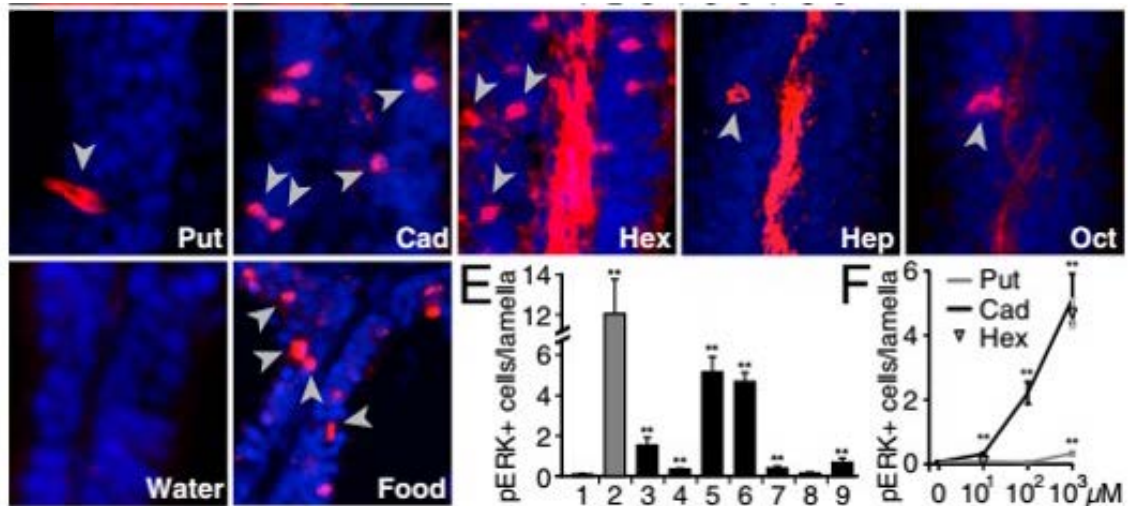


Figure 14. Diamines elicit pERK increase in olfactory sensory neurons

Zebrafish ($n = 14$) were exposed to stimuli indicated (1 mM). Some pERK-labeled cells (red) are emphasized by gray arrowheads; nuclear counterstain (DAPI, blue). Red central stripes in some panels, unspecific label in the basal lamina outside the sensory region. (E and F) Quantification of pERK+ cells/lamella as function of chain length (E) or concentration (F). Values given represent mean \pm SEM. Significance in comparison with water was evaluated by Student t test, $**P < 0.01$. (E) Results from two experiments are shown; 1, water; 2, food extract; 3–8, numbers reflect carbon chain length of diamines; 9, daminododecane. (F) Evaluation was partly on randomized data, no difference was seen between randomized and nonrandomized evaluation (Hussain et al., 2013).

2.8 Search for the TAAR glomerulus with the TAAR13c antibody

2.8.1 Olfactory Bulb stained with glomerular marker SV2 and co-labelled with TAAR13c antibody

The first step in identifying the neuronal circuit activated by cadaverine would be the identification of the target area of TAAR13c-expressing neurons. Due to axonal convergence of same receptor-expressing OSNs (Bozza et al., 2002; Bozza and Kauer, 1998), the target of TAAR13c-expressing neurons is expected to be a single glomerulus. Since TAAR13c is

expressed in ciliated OSNs (see above), its target glomerulus is expected among lateral glomeruli and dorso lateral glomeruli, which constitute the target regions of ciliated neurons (Braubach et al., 2012; Braubach et al., 2013).

In the mammalian system axonal transport of olfactory receptor protein into the target glomerulus has been shown (Wensley 1995). Therefore it was attempted to stain the TAAR13c target glomerulus using the highly specific TAAR13c antibody. Whole mount immunohistochemistry was performed on olfactory bulbs dissected from adult zebrafish. SV2 (synaptic vesicle glycoprotein 2), a known marker of glomeruli (DeMaria et al., 2013; Koide et al., 2009) was used as the counter stain to label all the glomeruli of the bulb and TAAR13c antibody was used in an attempt to label the specific glomerulus. However, the only staining seen was weak homogenous background staining and some blood vessel staining, no glomerular staining could be detected (Figure 15). Most probably the levels of TAAR13c were not high enough to visualize a distinct glomerulus, both in the expected regions and elsewhere, even though a high concentration of the TAAR13c antibody was used (1:50 dilution). This concentration of the antibody is already 5 times higher than the concentration resulting in intensely stained neurons in the olfactory epithelium. In contrast, many glomeruli were visible in the Sv2 labelling, indicating that the immunohistochemical detection *per se* worked well in this experiment.

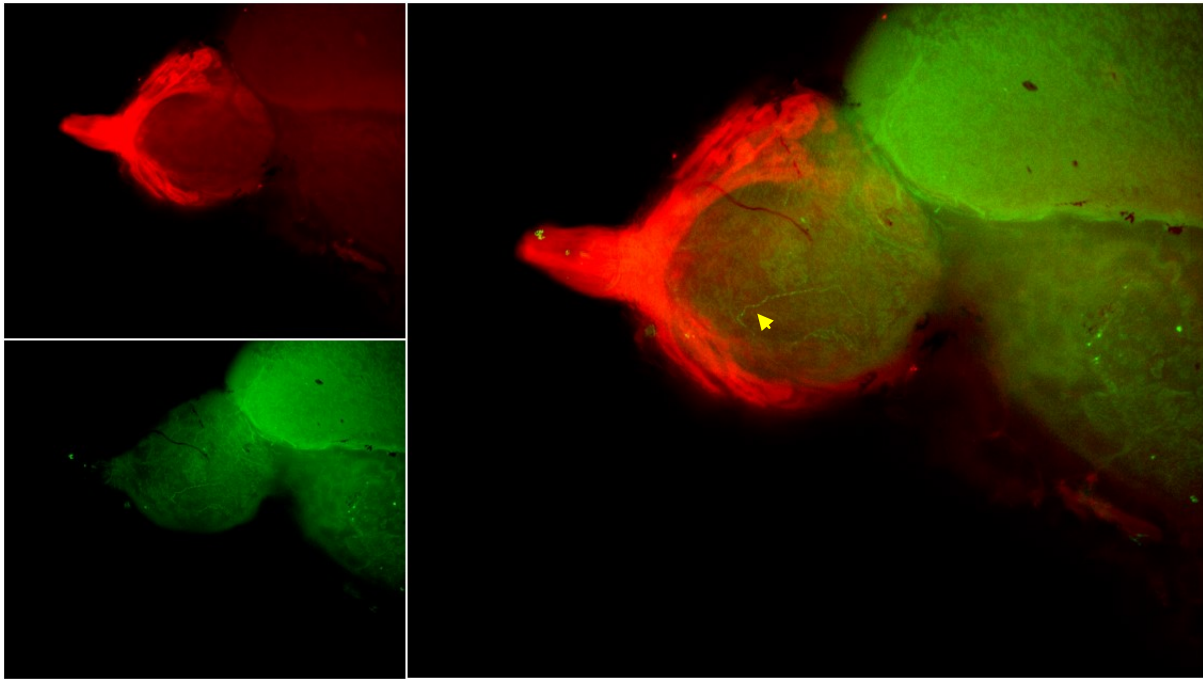


Figure 15. Whole mount IHC with TAAR13c antibody on Adult Zebrafish Olfactory Bulb

(A) Anti SV2 antibody directed against a synaptic vesicle antigen labels glomeruli in the Olfactory bulb (red fluorescence), the nerve endings of the olfactory tract are also seen stained as SV2 is a major component of the synaptic vesicle in neurons. (B) Whole mount labelling with the TAAR13c antibody did not stain any visible fibre bundles or glomerular structures (green fluorescence) (C) The Merged image shows no glomerular co-localization between the SV2 and TAAR13c staining. Some background staining is visible in both the red and green channels, including on blood vessels (yellow arrowhead).

2.8.2 Attempts to increase sensitivity of the immunological detection of TAAR13c via cadaverine stimulation and different fixation techniques

Since it was not possible to detect TAAR13c antibody staining in the olfactory bulb, attempts were made to increase the levels of TAAR13c in the bulb, which would increase the signal from TAAR13c antibody and possibly enable a clear labelling of the glomerulus. Firstly, zebrafish were exposed to 100 μ M cadaverine for one hour before sacrificing them and performing whole mount IHC on the OB of adult zebrafish. The rationale for this experiment was that exposure to ligand is able to upregulate the neuronal activity of responsive neurons (Sullivan and Leon, 1986; Wang et al., 1993;

Youngentob and Kent, 1995) . possibly via an upregulation of the olfactory receptor levels within these neurons. However, cadaverine exposure also did not result in TAAR13c-labeled glomeruli (data not shown).

Next, the fixative was exchanged to 0.2M trichloroacetic acid instead of 4% paraformaldehyde. TCA fixation was shown to increase sensitivity in whole mount OB and OE staining because of its coagulant properties (Ramos-Vara and Miller, 2013). Coagulant fixatives precipitate proteins on the surface and make them more accessible to the antibody. OB were fixed in TCA for 2 hours before staining with SV2 and TAAR13c antibodies. Still, no labeled glomeruli were detectable. It is possible that zebrafish OSNs may transport less receptor to their axons compared to mammalian OSNs.

2.9 Ontogenetic onset of avoidance behaviour towards cadaverine

Adult Zebrafish show aversive behaviour towards cadaverine and TAAR13c has been shown as a receptor for binding cadaverine as a ligand (Hussain 2010; Hussain et al., 2013). Immediate early genes like c-fos and Erk Phosphorylation in TAAR13c expressing neurons have been shown as suitable neuronal activity markers for cadaverine-induced responses in *taaar13c*-expressing OSNs (Isogai et al., 2011; Mirich et al., 2004). TAAR13c expression is seen in zebrafish larvae as young as 5dpf (Figure 16), and it was interesting to see, whether the innate avoidance behaviour to cadaverine and other diamines would already be present at this early developmental stage. If so, this behavior could be used to test potential loss of behaviour after the knockout of TAAR13c, which was being attempted in parallel. In order to determine the onset of cadaverine-elicited behaviour, Zebrafish larval behaviour apparatus was used. This apparatus was modified from (Gerlach et al., 2008). The apparatus is designed to allow the larvae to choose between channels of water and cadaverine from a mixing area of the two channels. Figure 17 illustrates the design of the apparatus where the larva

is introduced in the mixing zone and allowed to acclimatize to the flow conditions before the experiment is started. The larva is observed for swimming behaviour in three phases of the experiment; prephase, test phase, and postphase (see materials and methods for details). Zebrafish have been observed to start swimming at 5 dpf but in this experiment the 7 dpf larvae were observed to stop swimming, even at the minimal rate of flow necessary to minimize mixing between the two channels of water and cadaverine. Thus, this set of experiments could not be evaluated. Next older and stronger larvae at 15-19 dpf were used, which showed consistent swimming behaviour in the flow. It is possible that the generally reduced viability of the fish in the tanks at the time of these experiments contributed to the deficits in the swimming behaviour compared to literature values (Gerlach et al., 2008).

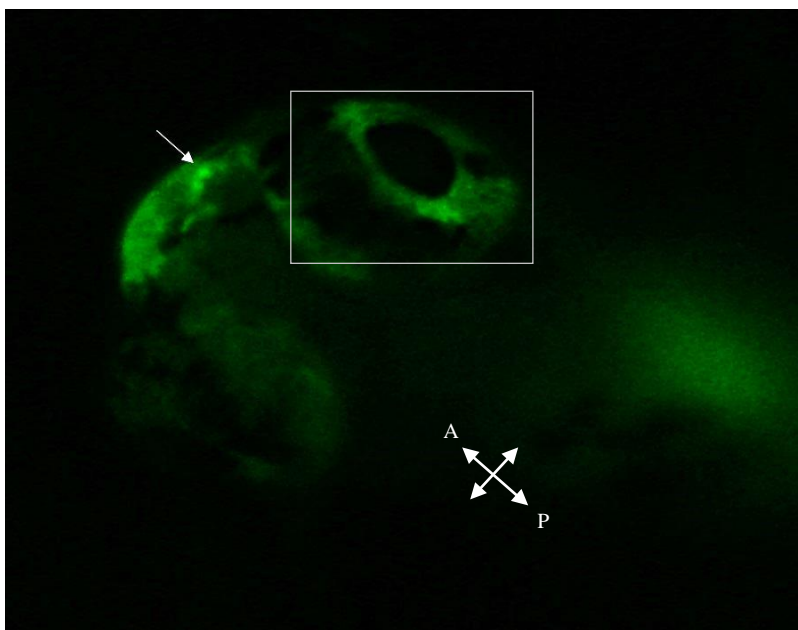


Figure 16. Whole mount Immunohistochemistry on Zebrafish larvae

TAAR13c expression is seen in 5 dpf larvae. Arrow points to labelled cells in the larval olfactory epithelium, an eye is seen highlighted by the box and the arrow axes represent the anterior to posterior orientation of the larva.

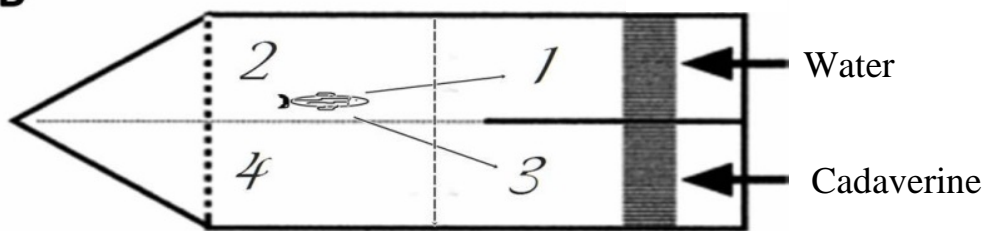
A**B**

Figure 17. The zebrafish larval behavior apparatus

A) The zebrafish larval behavior apparatus used for assessing the response of larvae to cadaverine. Methylene blue was used as a color indicator of mixing of two currents of water from the two channels. The flow is optimized using collimators and flow regulating screws attached to the connecting tubes. B) Schematic representation of the behaviour apparatus. Modifications to the Gerlach et al 2008 design include two collimators which act as dams regulating the flow.

2.9.1 Observation of behaviour upon sequential increase of cadaverine concentration from 0 mM as control until 300µM threshold

15 to 19 dpf zebrafish larvae were used in behaviour experiments to determine onset of avoidance behaviour to cadaverine since younger aged larvae were unable to swim. The aim of the experiment was to determine the lowest concentration of cadaverine at which there was a definite response which was clear and consistent. Hence the experiment was designed to test the behaviour of larvae to a sequential increase of cadaverine concentration in the water channels. The concentrations tested were 0 (water control), 10, 60, 100, 150 and 300µM respectively. 300µM was the highest concentration used, because it is expected to be already much higher than the cadaverine levels zebrafish might encounter in natural conditions. Each experiment was carried out at least three times with two larvae introduced into the mixing zone together. Zebrafish larvae are known to swim more in the presence of a second individual, opposed to freezing behaviour seen in solitary larvae (Kalueff et al., 2013). A group of 5 or more larvae bring another set of challenges as group behaviour might interfere with the specific response to cadaverine exposure which we are trying to achieve. Hence it was decided to have 2 animals together for each experiment. Each experiment consisted of 3 phases. A prephase where clean water runs through both the channels, a Cadaverine test phase where cadaverine is introduced in one of the channels at a fixed concentration followed by the post or recovery phase where water is released again through the cadaverine channel. The whole experiment runs for 15 minutes and the larvae are allowed to get acclimatised to the flow and experimental conditions for 5 minutes. Video Recording of the entire experiment was set up where the frame would include the inlet ports of the two channels up until the mixing zone of the apparatus from a non-interfering distance (30 cm above the water surface).

Visual observation of the experimental recordings showed no distinct avoidance below 60 μ M, as the larvae were seen to roam freely without any apparent distinction between the channels. At 60 μ M the larvae appeared to spend maximum time in the mixing zone. Aversion to cadaverine seemed present at concentrations of 100 μ M and higher (see appendix for videos). At 100 μ M cadaverine concentration, the larvae were seen to investigate the cadaverine channel by swimming up to the inlet source and choose the water channel side of the mixing zone with occasional forays into the inlet port of the water channel. At 150 μ M and 300 μ M there were fewer forays into the cadaverine channel showing clear aversion. The larvae were seen mainly in the water channel but were seen to swim back to the mixing zone in the recovery phase.

2.9.2 Method development and optimization for behaviour experiments

Behaviour experiments on adult zebrafish were quantified using motion tracking software like WinAnalyze and LoligoTrack. Both these softwares use an algorithm which is somewhat similar with each other. The software detects a moving object against a still background and tracks the movement by plotting the x and y coordinates of the moving object within a fixed and stipulated arena. The moving object is detected by its contrast against its background. This could either be a dark object against a bright background or *vice versa*. Adult Zebrafish could provide sufficient contrast to be detected as a moving object and be tracked very reliably. Larvae on the other hand do not provide a sufficient contrast against background, and therefore could not be detected properly by either of the tracking softwares. I tried to optimise the method by increasing the contrast produced by the larvae. The floor of the transparent larval behaviour apparatus was turned white to provide a good contrast against the larvae. Lighting of the experiment was also adjusted so that it is not reflective and is not recognised as movement by the software. Despite the measures taken to improve the setup and software upgrades from

Loligo track 3 to 4, the larvae were not registered as distinct trackable moving objects by the motion tracking software; therefore the behaviour experiments with Zebrafish larvae remain untracked for quantitative analysis. Therefore, time spent in different quadrants (water inflow, mixing zone 1, cadaverine inflow, mixing zone 2) was measured manually. Results are shown as raw values in a tabular form (Figure 18). While the variability is rather large, a trend towards aversion especially at the higher concentrations can be seen.

0 μ M Cadaverine							
Larva 1				Larva 2			
quadrant no.	Pre Phase	Cad Phase	Post Phase	quadrant no.	Pre Phase	Cad Phase	Post Phase
Q1	0	0	0	Q1	0.12	0	0.04
Q2	0	0.5	3.55	Q2	0.08	0.1	2.1
Q3	0.3	1.21	0.19	Q3	4.22	3.54	0.25
Q4	4.2	4.1	0	Q4	1	1.48	0.5
60 μ M Cadaverine							
Larva 1				Larva 2			
quadrant no.	Pre Phase	Cad Phase	Post Phase	quadrant no.	Pre Phase	Cad Phase	Post Phase
Q1	0.04	0.43	0.49	Q1	0.48	0	1.35
Q2	2.36	0.11	0.28	Q2	4.01	1.4	0
Q3	1.23	2.4	0.59	Q3	0.33	2.16	0.54
Q4	1.07	2.22	1.25	Q4	0	0.24	0.42
100 μ M Cadaverine							
Larva 1				Larva 2			
quadrant no.	Pre Phase	Cad Phase	Post Phase	quadrant no.	Pre Phase	Cad Phase	Post Phase
Q1	2.01	1.1	0	Q1	4.53	1.3	1.58
Q2	0.5	1.23	1.1	Q2	0	1.36	4.11
Q3	0.31	1.09	1.12	Q3	0	0.27	0.21
Q4	1.56	0.43	1.43	Q4	0	0.55	0.29
150 μ M Cadaverine							
Larva 1				Larva 2			
quadrant no.	Pre Phase	Cad Phase	Post Phase	quadrant no.	Pre Phase	Cad Phase	Post Phase
Q1	1.51	4.1	4.22	Q1	2.05	4.1	1.3
Q2	0.4	0	0	Q2	0.45	0	1.18
Q3	1.35	0	0	Q3	1.31	0	0.3
Q4	0.51	0	0	Q4	1.19	0	0.3
300 μ M Cadaverine							
Larva 1				Larva 2			
quadrant no.	Pre Phase	Cad Phase	Post Phase	quadrant no.	Pre Phase	Cad Phase	Post Phase
Q1	2.55	2.05	0.28	Q1	1.09	2.2	0.28
Q2	3.33	0.14	1.24	Q2	3.51	0.41	0.26
Q3	0.19	0.3	0.5	Q3	0.03	0.25	0.55
Q4	0.45	0.3	0.35	Q4	0.33	1.33	2.3

Figure 18. Larval behavior dose response with increasing concentration of Cadaverine stimulus

Each color code represents a particular concentration of cadaverine stimulus. Data is shown as time spent (in minutes) by single larva in each quadrant (Figure 17B) in three experimental phases. A trend towards avoidance of quadrant 3 (cadaverine channel) in higher concentration is seen from the data. More reliable and precise analysis methods are needed for quantitative representation of the data.

2.10 Attempted knockout of TAAR13c gene using the TALEN method

Cadaverine has been shown as a ligand for TAAR13c in a heterologous system with a very high degree of specificity. This was supported *in vivo* by neuronal activation in TAAR13c-expressing ciliated neurons upon cadaverine exposure suggesting that TAAR13c might be a major receptor underlying the observed avoidance behaviour towards cadaverine. However, to comprehensively establish the ligand receptor binding as causative for the avoidance behaviour to death-associated odour cadaverine, a knockout of the receptor gene TAAR13c would be required. In case the aversive behaviour towards cadaverine is impaired or even eliminated, TAAR13c will be shown as mediating the aversive behaviour in Zebrafish. Hence the attempts to create a knockout of TAAR13c were initiated by me. TAL effector Nucleases had been widely being used to generate knockouts in zebrafish when I started my knockout experiments and I chose to use this method to attempt a knockout of TAAR13c. TALEN-mediated genome editing has been shown to create frameshift mutations via NHEJ. In order to maximise chances of gene disruption, I chose a highly conserved 389 base pair Transmembrane 3 region spanning from base pair position 301 to 690 of the TAAR13c exon to minimize SNPs due to allelic differences. This region contains the G-protein binding site and interference with this region should thus damage protein function severely.

The exact target site, i.e. the intervening region between the two recognition sites for the TALENs, was chosen to contain a 6 bp BSR1/BME1 restriction site which would get disrupted upon NHEJ at the target site (the target site is the region of FOK1 dimerization which introduces double stranded breaks that get repaired by NHEJ). For details of the selection see Materials and Methods.

The Custom TALEN assembly for TAAR13c was procured as Plasmids from the Core Facility of the University of Utah. mRNAs synthesized from the two

TALEN plasmids (see materials and methods) were microinjected into about 500 fertilized eggs with varying mRNA concentrations (from 50ng/uL to 200ng/uL). The resulting embryos were screened at 24hpf for mutations. Primers spanning the target site were made and the PCR amplicon was restricted with BSR1 to check for mutations (Figure 19). PCR products which contained an undigested band were considered as putative knock out bands and sent for sequencing. Although several PCR products gave an undigested band, further sequencing revealed no mutation in the target site. Possibly, the undigested band resulted from incomplete digestion. In order to simplify the screening procedure, another pair of primers were used which contained the BSR1 recognition sequence. Hence, if there is any disruption of the BSR1 restriction site, no PCR product would be amplified. This screening method too failed to reveal any mutation in the target site since the PCR amplicons were obtained in each case (data not shown).

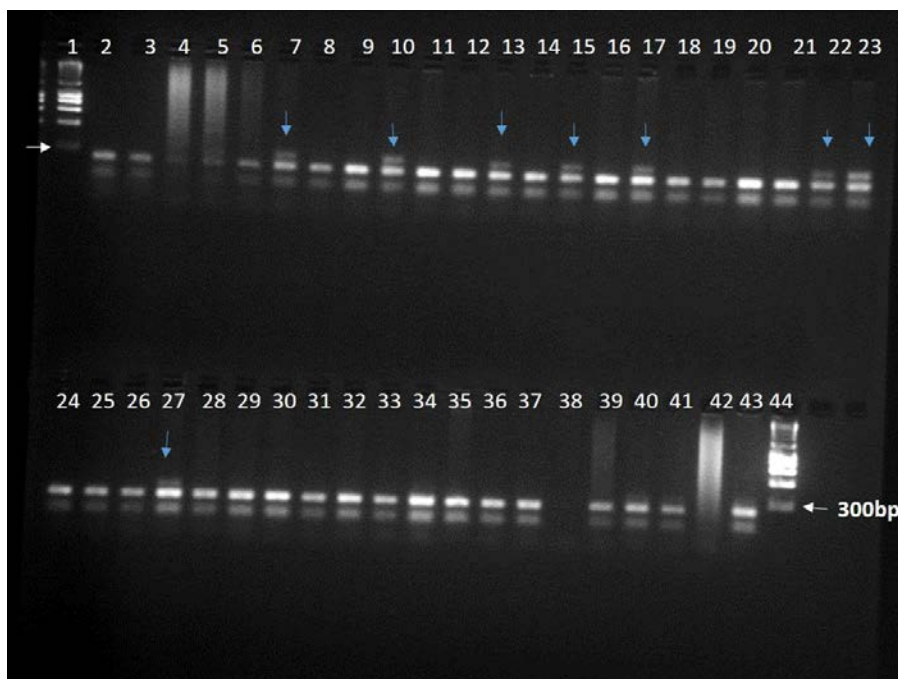


Figure 19. Screening of putative mutant larvae at 24hpf after TALEN injections in fertilized oocytes

Restriction enzyme digest of PCR amplicon with endonuclease BSR1 gives digested bands in all samples. Some lanes show undigested bands suggesting a loss of the BSR1 recognition site and thus a putative mutation. Lane 2 and 3 are uninjected controls, lanes 4 to 6 are from injected embryos not surviving until 24hpf and lane 7 to 43 are injected viable embryos. 1 kb marker is present in lane 1 and 44. Arrows indicate undigested bands in some samples.

2.11 Attempted knockout of TAAR13c gene using the CRISPR/Cas method

2.11.1 Generation of CRISPR gRNAs and CAS9 capped mRNA

Since the attempts to create a knock out using TALEN were not successful, an alternative method was searched. In the meantime, a more recent method of targeted mutagenesis, CRISPR/CAS9 had rapidly gained widespread acceptance and so I decided to use this method. CRISPR/CAS9 has been reported to have fewer off-target effects and offers a more flexible choice for target regions (Carroll, 2014; Gaj et al., 2013). Three different guidance RNA's targeting the TAAR13c exon were designed using the ZiFiT targeter design tool (see materials and methods). For each guide RNA the corresponding sense and antisense Oligos which additionally have overhangs corresponding to a Bsa1 cut site were annealed and cloned into the guidance RNA scaffold in the Bsa1 restricted linearized pDr274 plasmid obtained from Addgene (Addgene plasmid #42250). The insertion of the target site into the plasmid was confirmed by sequencing. gRNA was synthesised from this plasmid by *in vitro* transcription of Dra1-digested gRNA expression vector. Cas9 mRNA was synthesised from another plasmid from Addgene called the pMLM3619. This plasmid was restricted by Pme1 and *in vitro* transcribed to synthesize Cas9 capped mRNA which was co-injected with the guidance RNA into single cell staged embryos at a concentration of 15ng/uL of gRNA and 300ng/uL of Cas9 mRNA(see materials and methods). Genomic DNA from the Injected embryos was extracted 24 hrs post fertilization for mutations analysis. PCR primers spanning at least 200bp upstream and downstream of the target site were used and the PCR amplicon was used for screening for mutation events.

Surveyor assay was performed by T7 endonuclease digestion of the heteroduplex PCR amplicon. The T7 endonuclease cuts the heteroduplexes which contain mismatches. Multiple bands were obtained for several

amplicons indicating putative mutations (Figure 20). These amplicons were sequenced and analysed.

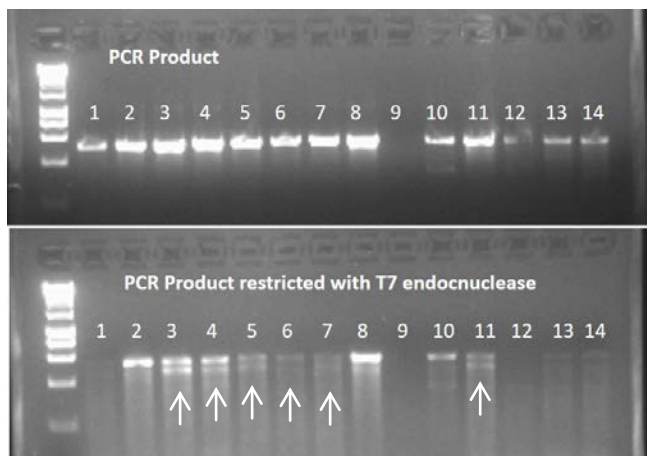


Figure 20. Initial Screening for putative mutants using Surveyor assay

TAAR13c primers which include the target site were used to amplify genomic DNA purified from individual 24hpf embryos. The PCR products were separated on a 2% agarose gel. Multiple bands were seen in many samples suggesting potential mutants (see arrows). The corresponding PCR products were sequenced, but turned out to be false positives (see Figure 22).

2.11.2 Sequencing revealed high number of background SNP's resulting from the amplification of different TAAR13 subfamily genes

The sequence analysis revealed several SNPs in the sequence; however, all the SNPs were detected outside the target site. TAAR13 is a multigene family which contains TAAR13A, TAAR13B, TAAR13c, TAAR13D, TAAR13E located on the same chromosome side by side. These genes share a high level of similarity (Figure 21). The sequences obtained were therefore aligned with all the TAAR13 genes to check if the resulting SNPs are due to amplification of different genes within this family. Indeed, when sequences were carefully aligned, it was evident that the amplicons are from different genes (Figure 22). Due to high levels of background SNPs, it was difficult to distinguish the actual mismatches from the background. Since the TAAR13 gene family has very high sequence similarity, it was difficult to choose a primer pair which only binds TAAR13c and no other TAAR13 gene. The

primers were probably binding different genes leading to several false positives in surveyor assay.

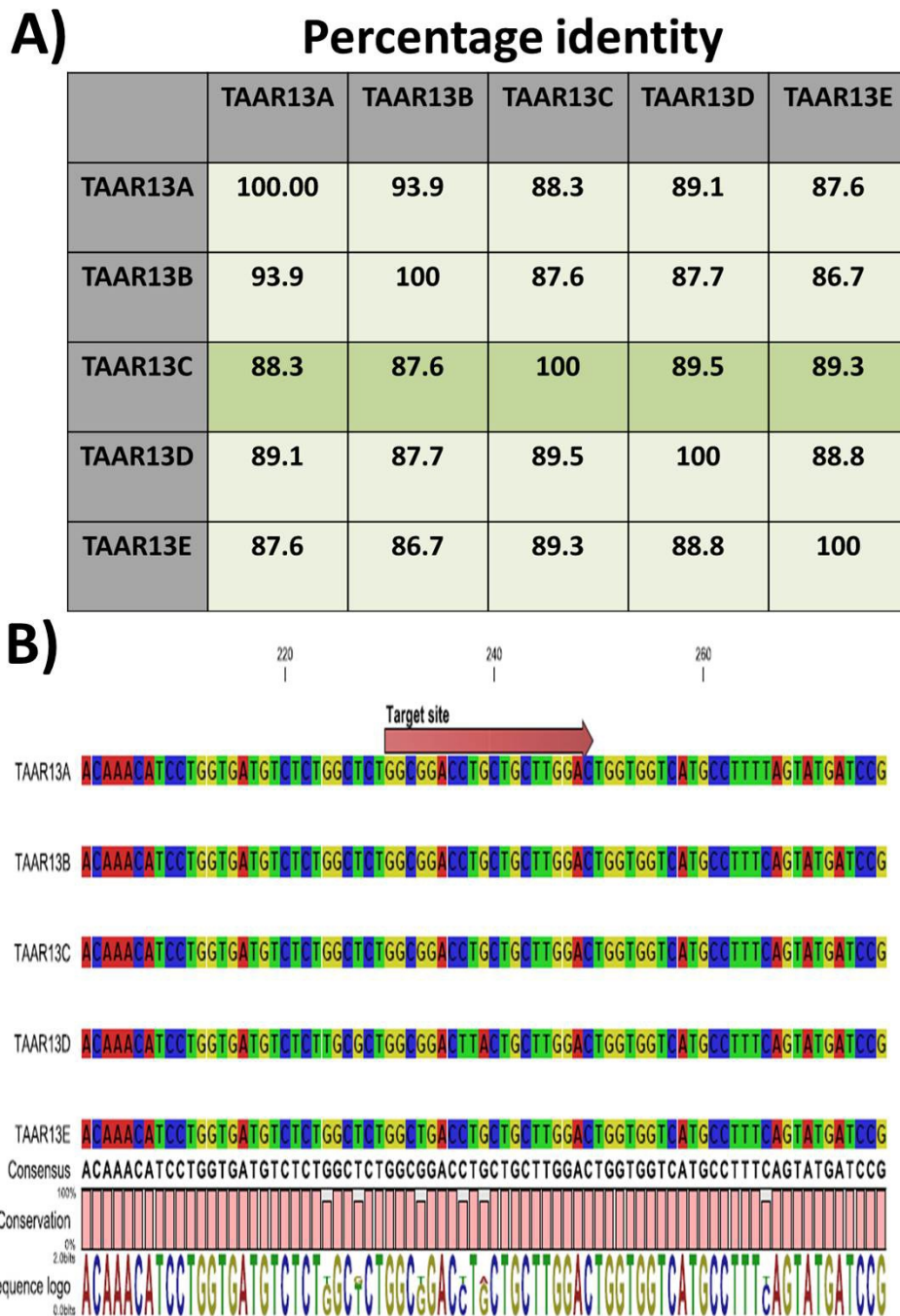


Figure 21. The high sequence identity within TAAR13 gene family

A) Percentage nucleotide sequence similarity between different TAAR13 genes. TAAR13c shares close to 90% similarity with other members of the family B) The sequence alignment between the TAAR 13 gene family spanning the target site. The sequence within and around the target site optimized for TAAR13c is nearly identical for all subfamily members. This results in high chances of other TAAR genes being targeted by the CAS9 mRNA. Unfortunately, the choice of target site is highly limited due to the AT-rich regions and lack of PAM sequences in the exon (see Methods for a more detailed discussion).

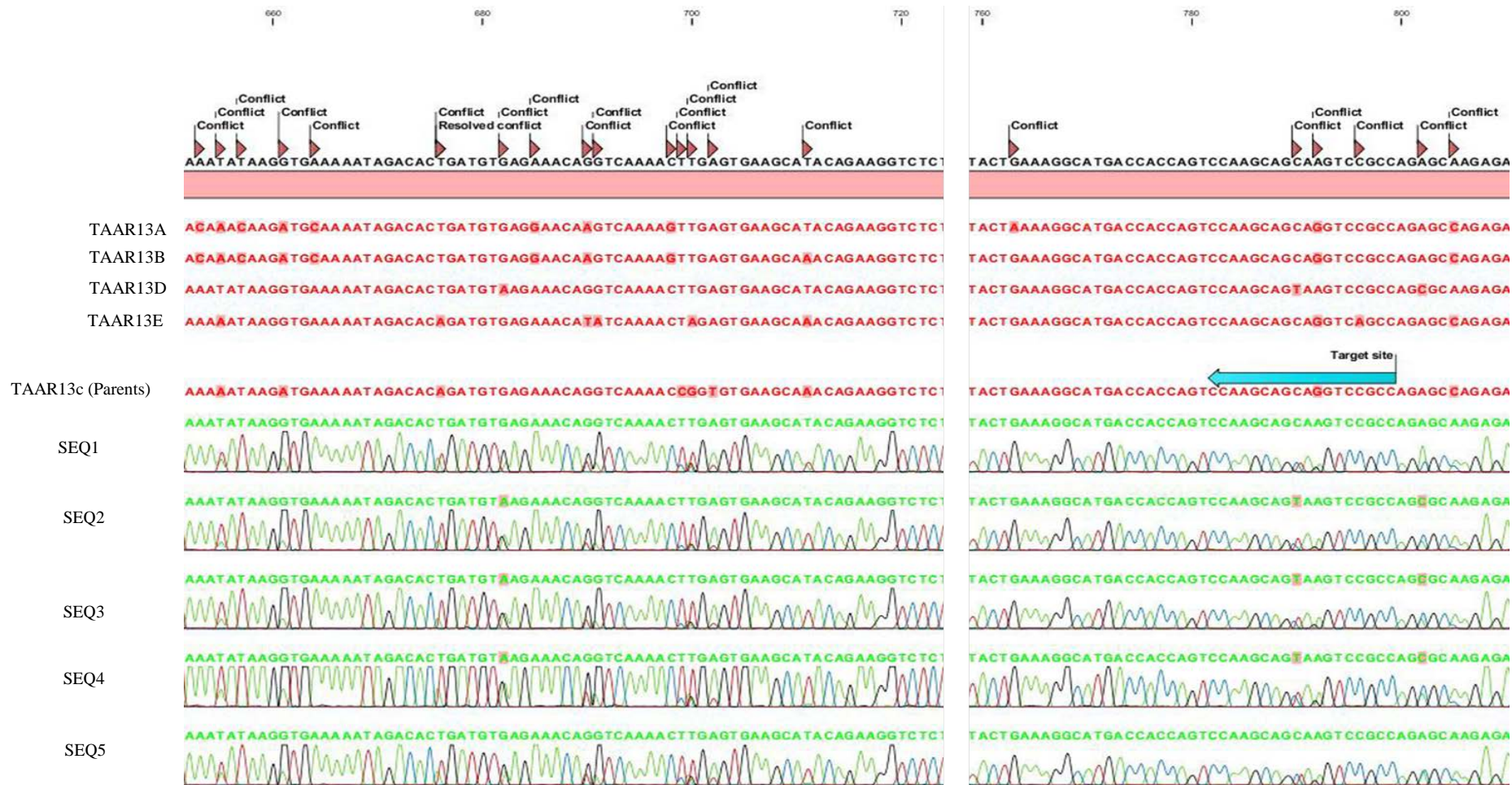


Figure 22. Alignment of sequenced amplicons with TAAR13 subfamily

Amplicons giving multiple bands in surveyor assay with the primer pair TAAR 1F and 1R were sequenced and aligned with all the TAAR13 genes in the region preceding the PAM sequence, where mutations would be expected. The TAAR13c sequence shown is from uninjected parents to rule out any individual SNPs. Although several SNP deviations from the TAAR13c sequences were observed in sequence 1 to 5, the majority could be due to amplification of other subfamily members by the TAAR13c primers, since it was difficult to select TAAR13c-specific primers. Thus, the deviations from TAAR13c sequence are unlikely to constitute Crispr/Cas-induced mutations.

In order to lessen the false positives and improve the specificity of PCRs, a primer pair was carefully designed which is most specific to TAAR13c and has lesser chances of binding other TAAR genes (see materials and methods). Moreover, a new guide RNA was chosen via an improved targeting algorithm (<http://crispr.mit.edu>) Injections were then performed with the new guide RNA, and the screening was repeated using the specific primers. Surveyor assay gave lesser multiple bands indicating that the primers were more specific. An amplicon which gave multiple bands using the more specific primers was sequenced and analysed for mismatches (Figure 23).

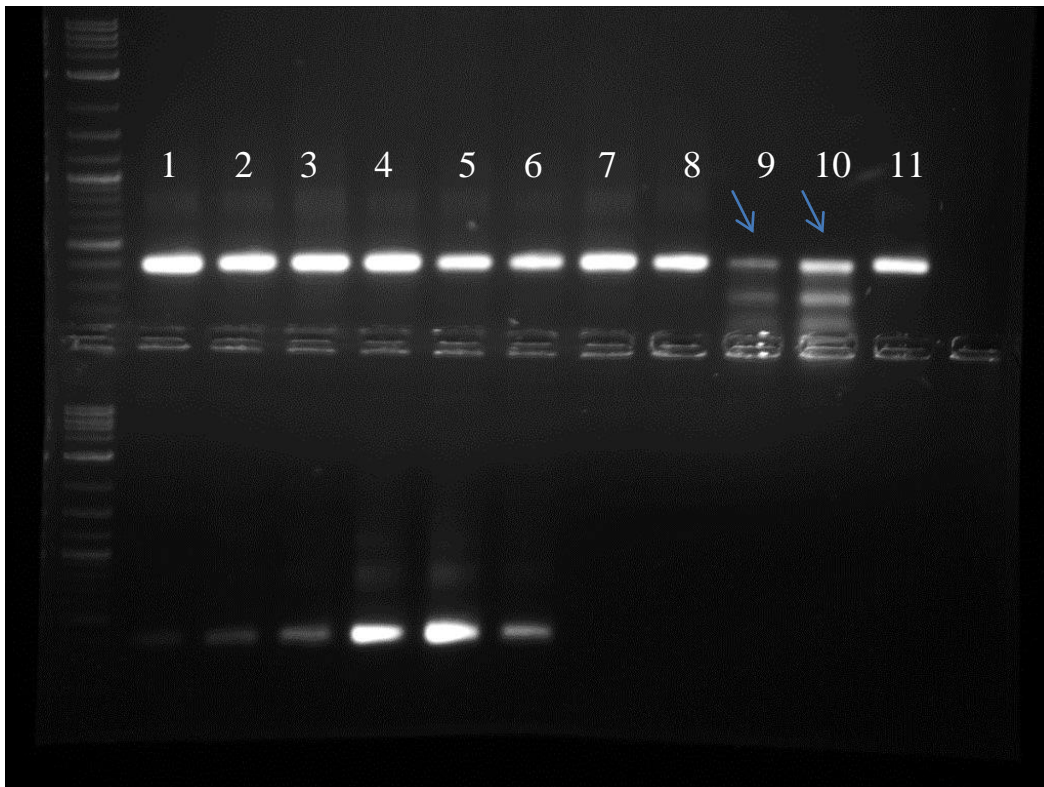


Figure 23. Screening for putative mutants using the most specific TAAR13c primers possible that also enclose the target site

(A) Primers were used to amplify genomic DNA purified from individual 24hpf embryos. The PCR products were separated on a 2.5% agarose gel. Surveyor Assay of PCR product showed multiple bands in lanes 9 and 10. Another aliquot of the PCR product from lanes 9 and 10 was subcloned and sequenced.

Sequence analysis revealed mutations in two independent subclones which were absent in all the members of gene family (Figure 24, Figure 25). The first subclone labelled colpcrt13c15-M13 had a single base deletion resulting in a frameshift mutation and introduction of premature stop codon at amino acid position 144. It also had three amino acids changes, two of which resulted from a frame shift (F60→L, T142→K and R143→E). The second subclone labelled p3s1-M13 had three base substitutions. These mutations resulted in V35→A, C135→R and T142→K substitutions. The mutations were seen in two independent subclones from the same PCR amplicon, suggesting they do not result from any sequencing or PCR-induced error.

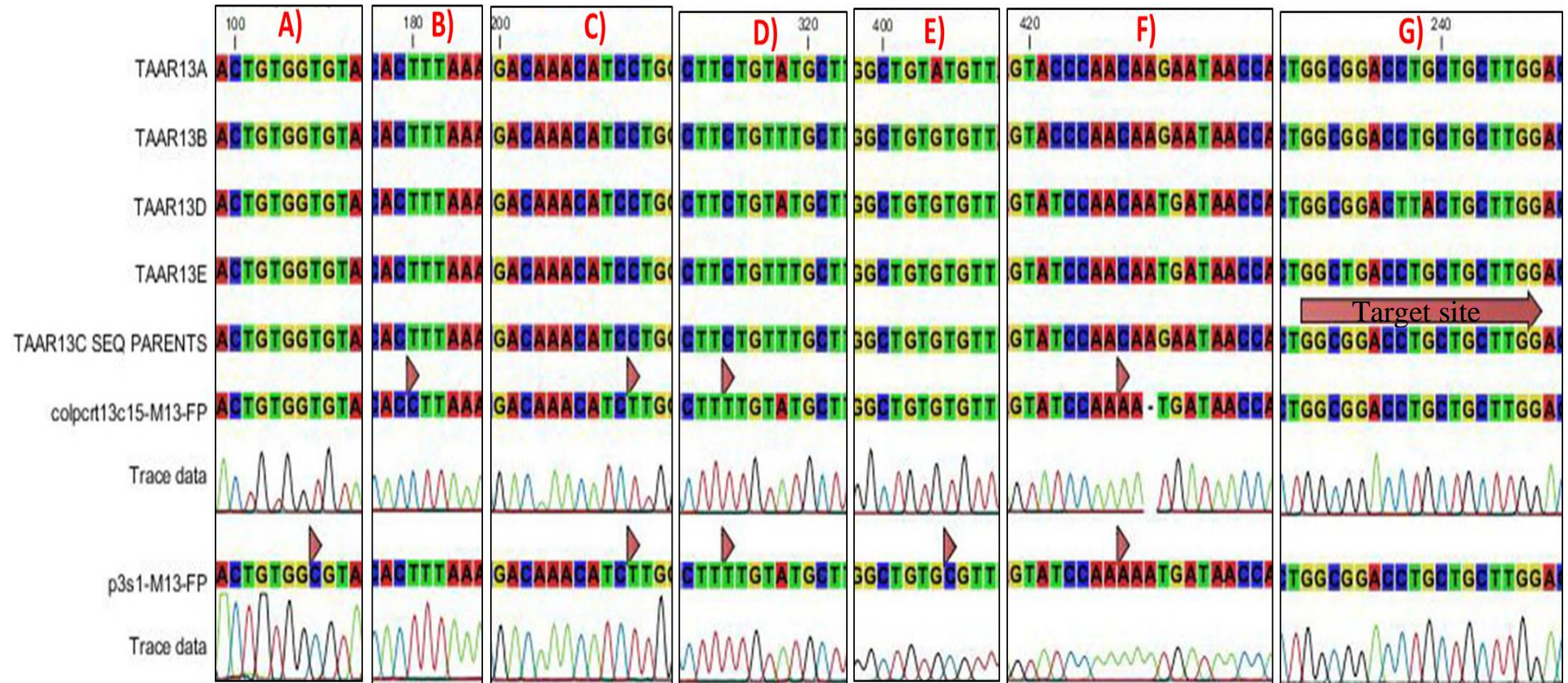


Figure 24. Sequence analysis of putative knock outs

Two potential functional knockouts were obtained after sequencing and analysis which contained SNPs absent in any of the TAAR genes. The one labelled colpcrt13c15-M13 had three base substitutions (two from frame shift mutation) and one base deletion mutation resulting in frameshift and premature stop codon while the one labelled p3s1-M13 had three base substitutions. A)-F) shows position of mismatches and indel mutation. G) Shows the position of the target site which is present on approximately 230-247 base pair position in TAAR13c. The mismatches and indel were hence approximately 40-200 base pairs away from the target site depending on the mutation. The corresponding changes at amino acid level are depicted in Figure 25.

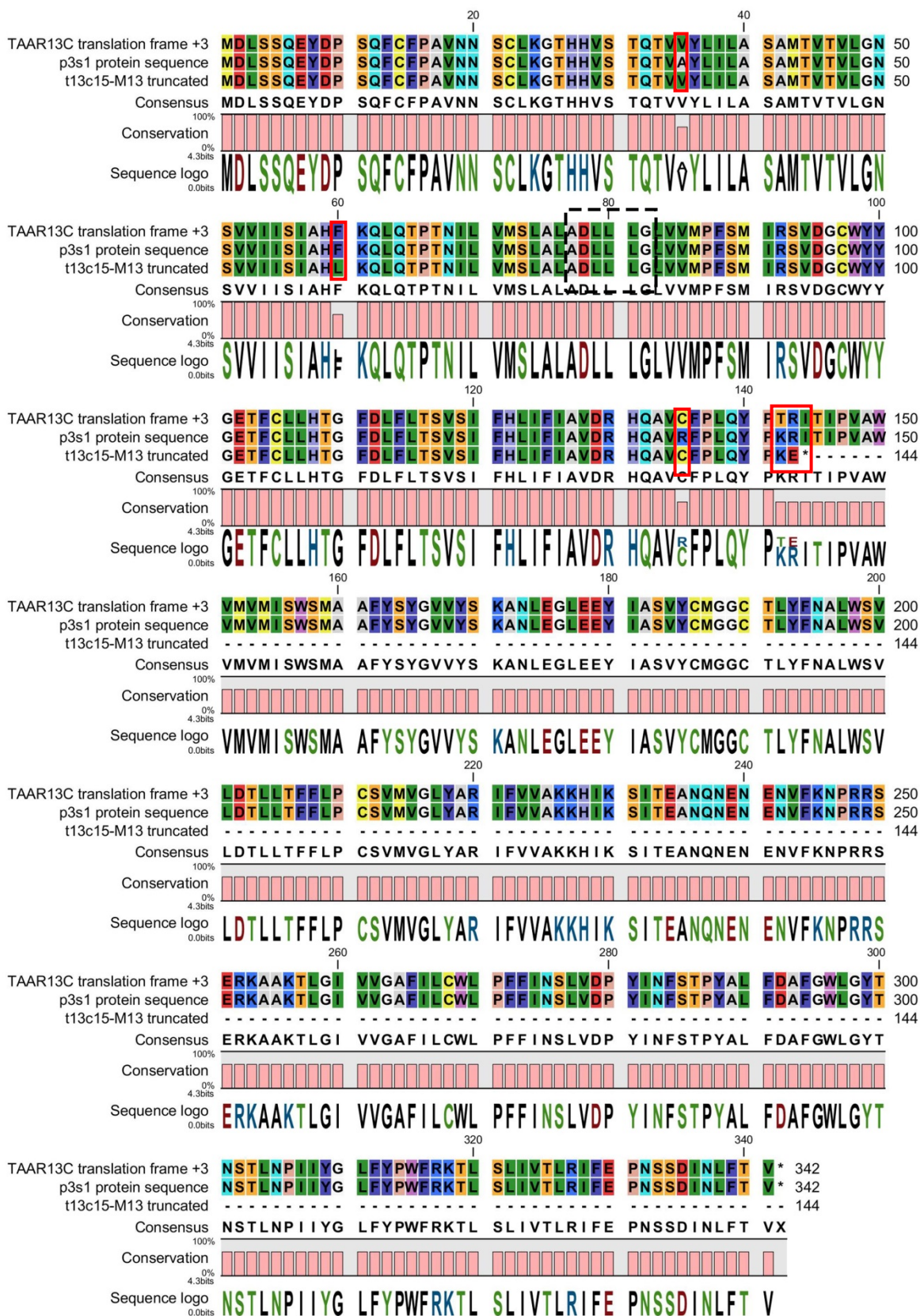


Figure 25. Amino acid sequences of putative knock out within TAAR13 subfamily

PCR amplicons from lanes 9 and 10 in Figure 23 were subcloned and sequenced. Sequence analysis shows that colpert13c15-M13 has 3 amino acid substitutions (F60→L, T142→K and R143→E) and a premature stop codon at position 144 (red boxes) resulting from a single base deletion. p3s1-M13 had 3 amino acid exchanges (V35→A, C135→R and T142→K) (red boxes) as compared to TAAR13c which are close to the PAM site (the approximate target site is in dashed black box) and thus might result from CRISPR/Cas-induced mutation. However, it was tricky to map the mutated sequence to a specific gene within TAAR13 subfamily.

This indicated a potential knock out in the TAAR13 subfamily. It is however not clear, in which gene it may have happened, since the mutant sequence was similar to both TAAR13a and TAAR13d. The embryos from this batch of injections showed high mortality, and could unfortunately not be raised until finclip analysis would have been possible. A high rate of mortality of zebrafish embryos was also observed in multiple rounds of injections using this guide RNA. As a result, very few live eggs were obtained in each round of injection which hampered the further analysis procedures. Hence, the mutation could not be confirmed in live zebrafish. However, the putative knock out obtained indicated that the more specific screening procedures such as the one described above can help in getting a potential knock out of TAAR13c in future.

2.11.3 Initiation of TAAR13 gene family cluster knock out

Since the homology within TAAR13 gene family is very high, it was difficult to design guidance RNA which was highly specific for a target site within TAAR13c. The guide RNA had high chances of targeting other TAAR13 genes. The flexibility of choosing a specific target site was also hindered due to presence of an AT rich region in the exon. In order to address this issue, I initiated an experiment for generation of a cluster knock out of all five TAAR13 subfamily members by targeting the 5' UTR of the leftmost gene (TAAR13c) and the 3' UTR of the rightmost gene (TAAR13e), in effect flanking the entire Taar13 family cassette. Two guidance RNAs were designed for each side of the cluster and the corresponding oligos were cloned into the Dr274 plasmid (see material and methods for details). Coinjection of a 'left' guide RNA together with a 'right' guide RNA would then knock out the entire TAAR13 gene family cluster. For the success of this procedure it was essential to strategize the screening of potential mutants. Hence two sequencing based screening strategies were designed.

In the first case primers were designed spanning the target site from the 5'UTR region to the TAAR13c exon and the Second strategy was to design a primer pair with the forward primer in the 5'UTR and the reverse primer in the 3' UTR. In the first case a homozygous knockout would be indicated by no PCR product since the reverse primer binding site would be disrupted by the deletion of the TAAR13 exons, a wild type or heterozygous mutation would still result in a PCR product and this would be analysed by subcloning and sequencing of the PCR product.

In the second case Primers are designed in such a way that a PCR product is seen only in the event of a homozygous or heterozygous mutation event while no PCR product would be amplified in wildtype since the PCR amplicon expected is more than 6kb. Hence the two knockout screening strategies described above should prove substantial in identifying a putative knockout.

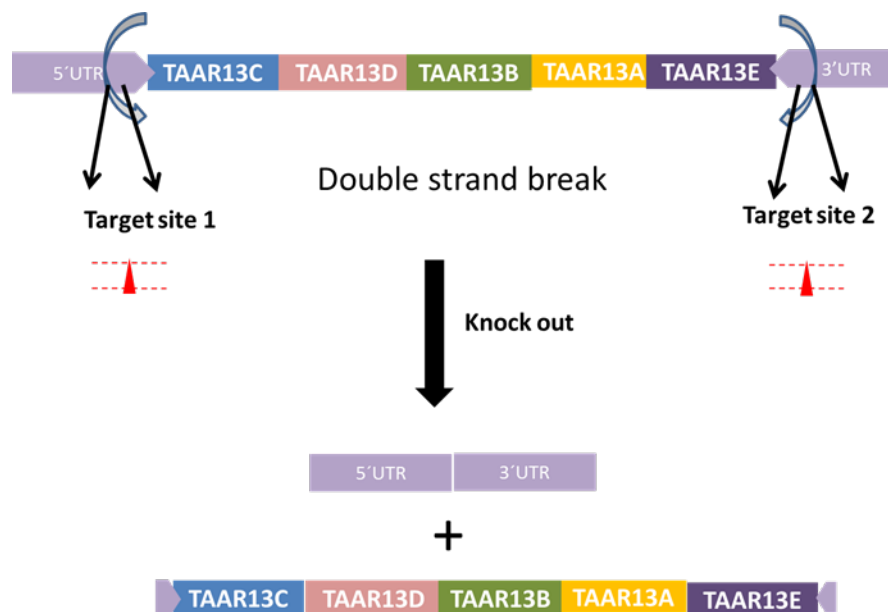


Figure 26. Strategy for creating a TAAR13 subfamily knockout

Two target sites are chosen, one from 5' and another from 3' UTR. The CAS9 mediated double strand break should knock out the entire gene family located between 5'UTR and 3'UTR. 8 different target sites, four on each side of the cluster, were chosen and cloned into pDR274.

DISCUSSION

Molecular characterization of TAAR13c as an olfactory receptor

The characterization of ligand/receptor interactions in the field of olfactory receptors is still very much in flux, and even new classes of OSNs continue to be found (Ahuja et al., 2014; Omura and Mombaerts, 2015). The TAAR family of olfactory receptors gained importance due to its function in recognizing a particular group of odours, amines, and the roles many of them play as social signals (Hussain et al., 2013; Liberles, 2015). The family is expressed widely in vertebrates, from fishes to mammals. Recently the first fish TAAR receptor was deorphanized and shown to be a highly sensitive and specific receptor for cadaverine, a molecule emanating from decayed flesh (Hussain et al., 2013).

In this context it became important to develop an *in vivo* approach to localise TAAR13c protein expression, characterize the cell type expressing TAAR13c and to examine the extent to which TAAR13c-expressing cells carry the neuronal response to cadaverine. The successful purification and characterization of TAAR13c antibody (Figure 6) allowed to show TAAR13c expression at the protein level in cells with neuronal morphology (Figure 7). The comparison of TAAR13c mRNA expression by *in situ* hybridisation (Hussain et al., 2009) to the results of immune staining with the newly purified antibody was encouraging (Figure 27).

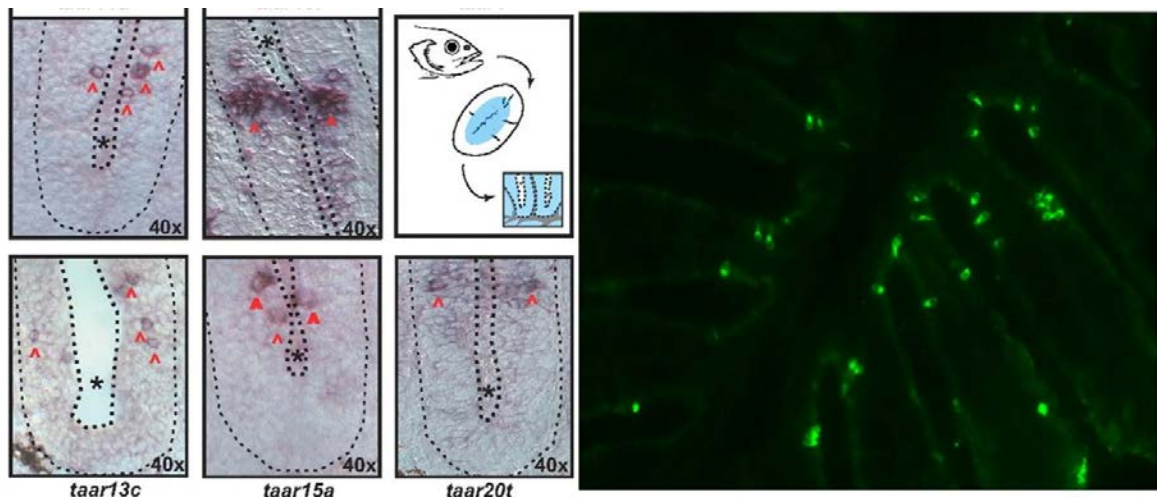


Figure 27. In situ hybridisation and TAAR13c IHC (Right)

In situ hybridisation (left), panel modified from (Hussain et al., 2009) and IHC (Right) using the purified TAAR13c antibody showing comparative labelling index and localisation in the sensory regions of fish olfactory epithelia.

The purity and specificity of this antibody was shown by western blotting (Figure 6) and an olfactory epithelium-specific band at an appropriate size was detected. Thus, the purified and specific TAAR13c antibody generated in this study provides a valuable tool to monitor the subcellular localization of TAAR13c by immunofluorescence (Hussain et al., 2013). This antibody is the first antibody against TAAR13c in absence of any commercial antibody recognising specifically the TAAR13c isoform of the protein. The antibody may also a good tool to be used in future for testing interactions of TAAR13c with other proteins, eliminating the necessity to express TAAR13c with a fusion tag.

In situ hybridization labeled several fold more cells compared to the immunohistochemical staining with anti-TAAR13c antibody (Figure 7, Figure 27). The localization of labelling was in the olfactory sensory region in both in situ and the antibody staining. Presumably cross-hybridization of the *in situ* probe to the four other TAAR13c family members is responsible

for the higher numbers in the *in situ* hybridization, see also (Hussain et al., 2009).

It is generally believed that OSNs express specific olfactory receptors in a very restricted manner. Different types of Neurons express different families of receptors and an individual neuron selects a particular member within the respective gene family, a phenomenon commonly referred to as “one neuron one receptor” (Buck and Axel, 1991). The co-expression of TAAR13c antibody staining with acetylated tubulin and G_{olf} staining showed the specificity of TAAR13c expression in ciliated Neurons (Figure 8, Figure 9). The suitability of acetylated tubulin as marker for ciliated neurons has been shown in several publications (Bazaes et al., 2013; Kang et al., 2010; Kishimoto et al., 2011; Lee et al., 2014; Pathak et al., 2007; Vina et al., 2015), likewise for Golf (Ahuja et al., 2014; Hansen et al., 2003; Liberles and Buck, 2006; Oka and Korsching, 2011; Oka et al., 2009).

The cells which show expression of TAAR13c could also be confirmed as Ciliated cells based on the morphological appearance of these neurons (Hansen and Zielinski, 2005; Kermen et al., 2013). The cilia on these cells could be seen in the IHC stained pictures (Figure 7).

Taken together, this is a finding which deciphers the cell type which expresses this specific receptor, consistent with observations of *taar* gene expression in ciliated neurons in diverse species such as mice (Ferrero et al., 2012; Zhang et al., 2013).

As mentioned above, the difference between higher numbers of TAAR13c-expressing cells as observed by *in situ* hybridization compared to antibody staining is probably due to cross-reactivity of the *in situ* probe. The immunizing peptide was selected for maximal specificity to TAAR13c (19-38% difference in sequence for other TAAR13 subfamily members) and may thus be expected to be more specific for TAAR13c than the probe (about 90% difference in nucleotide sequence between subfamily members).

However, one cannot exclude that to some extent this difference could reflect a difference between RNA and protein levels, which could indicate a possible regulation at the level of translation. This is an interesting possibility, which would need to be followed up in further experiments.

After the specific labelling and localization confirmation of TAAR13c in the ciliated cells of the OE, the next question was, whether or to what extent cadaverine-responding cells *in vivo* would be TAAR13c-expressing neurons. The activation of neurons is a signalling cascade leading to an increase in several neuronal activity markers. Three of these, two marker genes and one change in phosphorylation, were analysed.

The first activity marker to be examined was *egr1*. *Egr1* is an essential part of zebrafish larval development; it is seen expressed at basal levels throughout the larval stage (Isogai et al., 2011; Kress and Wullimann, 2012). Nevertheless, *egr1* was upregulated after cadaverine exposure of the fish. However, the response was not limited to the olfactory epithelium, and also not specific to cadaverine, as similar activation with food was also observed (Figure 12), making *egr1* an unsuitable marker to study specific neuronal activation due to cadaverine and also for co-localization studies with TAAR13c. Therefore *Egr1* was not examined further.

cFOS which is a known IEG and is expressed in response to stimuli which trigger an olfactory response in animals (Isogai et al., 2011). Diamines like cadaverine and putrescine activate neurons (Rolen et al., 2003). Thus, an increase in cFOS protein levels was tested as a plausible readout of cadaverine-specific neuronal activation. Indeed several diamines and also cadaverine activated cFOS and TAAR13c expression seemingly above the background level observed with water alone (Figure 11). However, the diamine stimuli in diverse concentrations activated cFOS in far too many cells as compared to those which expressed TAAR13c leading to a speculation that from the time of cadaverine stimulus to maximal increase in

cFOS protein (which is roughly 1 hour) many other parallel factors influence the experimental setup. Factors like Non-olfactory physical stress due to forced aversion, fear response mediated faecal and urinal excretion, long physical presence in a constrained experimental setup, and also secondary signaling stemming from cells adjacent to the cadaverine-activated cells could all together lead to an increased number of cells positive for cFOS expression.

Considering these plausible factors and that the very same result was obtained several times (Figure 11, (Hussain et al., 2013) and unpublished results) a cautious decision was made to search for another marker to monitor rapid ligand-specific neuronal activation. Phosphorylation of ERK has been used as an indicator of neuronal activation (Mirich et al., 2004). Phosphorylation of ERK is also a very rapid response upon ligand stimulus compared to changes in gene expression. Five minutes of ligand exposure resulted in maximal signal compared to one hour for cFos. Thus, all the stress factors mentioned above may be assumed to contribute less to the pERK signals and pERK may be expected to result in more specific signals compared to cFos and Egr1. I have examined four different pERK antibodies and found only one to result in clearly labeled cells after ligand exposure. This antibody was used for subsequent experiments, and indeed labelled much fewer cells than the cFos antibody after cadaverine exposure. At 100 μ M cadaverine some pERK-labeled cells were found to be TAAR13c-positive in double immunohistochemistry, suggesting that TAAR13c *in vivo* responds to cadaverine with activation. However at this relatively high ligand concentration some other receptors may be also activated. For time reasons another graduate student in the lab undertook the double labeling for a tenfold lower concentration (Hussain et al., 2013). These experiments showed less pERK-labeled cells, but a higher ratio of co-staining with TAAR13c.

Hence, the conclusion is that TAAR13c-expressing ciliated neurons carry a small percentage of the cadaverine response at high concentrations, but a higher percentage at lower concentrations, suggesting TAAR13c as an essential receptor in the neuronal cadaverine response.

The different diamines with variable lengths of carbon chains (C3 to C10) were tested for activation of neurons using pERK expression as marker. Putresine, cadaverine and other diamines activated the neurons with varied efficacy, with cadaverine and diaminohexane the most effective activators of cells at three different concentrations. This experimental outcome differs somewhat from the results of the HEK cell reporter analysis which served as a primary data set in identifying TAAR13c as a target of cadaverine among other TAAR family receptors. Probably other, as yet unidentified receptors for diaminohexane, different from TAAR13c are responsible for that difference.

After confirmation of the expression of TAAR13c in ciliated neurons and its co-localization with pERK in response to cadaverine, attempts were made for the identification of TAAR13c glomerulus in the olfactory bulb as one of the first steps towards understanding olfactory signal transduction and the neuronal circuit in higher brain center. Hence the TAAR13c antibody was used to label all the cells expressing TAAR13c in a whole mount of zebrafish olfactory organ (OE and OB). The Olfactory bulb was stained with a synaptic marker protein SV2 which is known to label glomeruli (Braubach et al., 2012; Braubach et al., 2013). As previously mentioned (Figure 15) the labelling of glomeruli with SV2 was clearly visible but no TAAR13c-staining could be detected in the glomeruli, presumably because the expression levels of TAAR13c in the native bulb were below detection limits. Attempts to increase the labeling of cells using cadaverine stimuli showed very weak labeling in sub regions of the OB, but it has not been possible to detect labeled glomerular structures. TCA fixation to coagulate protein on surface

(Ramos-Vara and Miller, 2013) has been a known way to increase the detection of surface receptors but even after TCA treatment TAAR13c-staining in glomeruli was not visible.

Ontogenetic onset of avoidance behaviour towards cadaverine

Cadaverine behavioral response had been previously shown in adult Zebrafish (Hussain et al., 2013), but the ontogenetic onset of this response was not known. Therefore I attempted to delineate the ontogenetic onset of avoidance behavior to cadaverine.

Furthermore, such results would be very helpful, when testing TAAR13c knockout fish for their behavioral response, since the tests could be done much earlier, if larval testing would be available. To conclusively demonstrate TAAR13c as essential component of the cadaverine-elicited behavioral response, such a TAAR13c knock out would be essential.

Since the TAAR13c expression was evident in zebrafish larvae as early as 5dpf (Figure 16) and zebrafish larvae have been shown to elicit specific behavioral responses to other stimuli including odors at 5 dpf (Budick and O'Malley, 2000; Gerlach et al., 2008; Martineau and Mourrain, 2013; Muller and van Leeuwen, 2004), the earliest age examined for cadaverine behavioral response was 5dpf zebrafish larvae. However, when zebrafish larvae as young as 5-7dpf were being tested in two choice apparatus used by Gerlach et al. 2008 (Figure 17), the primary problem was the near absence of spontaneous larval swimming, so avoidance behavior could not be tested. Many experimental conditions such as water current, lighting, background noise and video recording set up were modified in an attempt to increase free swimming. Modifications to apparatus design like collimators and flow regulators were employed and care was taken to eliminate environmental noise and visual stimuli, which might frighten the larvae. Flow was minimized to the extent allowed to obtain minimal flowback into the

respective other channel. Despite such measures, 5-7dpf larvae did not swim freely and were often prone to freezing behavior.

Therefore, the age of zebrafish larvae used for behavior analysis was raised to 15-19 dpf. At this age the larvae were much stronger and had relatively developed fins and therefore could cope better with the flow in the channels. Once all the experimental conditions had been optimized, specific response to cadaverine was analyzed. 100 μ M cadaverine was seen to elicit a specific response in TAAR13c in a heterologous system and in adult zebrafish (Hussain et al., 2013) and hence this concentration was chosen to analyze aversive behavior in zebrafish larvae. Visual analysis by time-based tracking was performed to analyze larval response (see appendix for videos). At 100 μ M cadaverine, larvae seemed to show aversion response to cadaverine, but it was not an immediate response and larvae additionally exhibited exploratory behavior with darts into the cadaverine channel up to the source. At higher concentrations of cadaverine (150 μ M and 300 μ M), aversion was seen earlier and more extensive, while at 60 μ M and less, no aversion was seen. These experiments showed a dose-dependent response towards cadaverine and 100 μ M was established as the threshold for definitive behavior towards cadaverine. Attempts were made for quantitative analysis of this data using Winanalyze and LoligoTrack, the two softwares which are well established for tracking movement of adult zebrafish. Winanalyze could recognize zebrafish larvae against the background but the contrast generated was not sufficient enough for the software to continuously track larval movement, thereby introducing excessive amount of artifacts. Three different versions of loligoTrack (versions 2, 3 &4) were used for analysis. The first two were not successful in recognizing larvae as the target for motion tracking. The last version (LoligoTrack 4) could recognize larvae but could not distinguish between the two individual larvae and was prone to overlap and switch between the two animals whilst tracking.

Mutagenesis of TAAR13c using CRISPR-CAS9

Current results from injections (Figure 24, Figure 25) suggest that CRISPR-Cas 9 can be successfully used to create functional knock out of TAAR13c albeit with some considerations. Furthermore, the novel strategy for creation of cluster knock out of TAAR13 subfamily (Figure 26) may be able to overcome these limitations.

The attempts to create a functional knockout of TAAR13c were hampered by several problems. In choosing the sequences as target site and screening primers, we at first did not take into account the high identity that exists within the TAAR13 subfamily. Five TAAR13 genes are arranged tandemly in the chromosome with nucleotide identities around 90% (Figure 21). As a result, the gRNAs used in the beginning had extremely high chances of targeting other family members. Also the primers used for amplifying the putative mutated regions showed unspecific binding and amplification (Figure 22). This resulted in high number of false positives in surveyor assay as the PCR product obtained mostly consisted of amplicons from more than one gene within family (Figure 20, Figure 22), which would generate many SNPs due to formation of heteroduplexes.

Subsequently, attempts were made to improve the specificity of gRNA and primers chosen for amplification of targeted site. However, given the high identity within family, no completely specific solution was possible. Another major limitation was the high AT content of the coding region, and correspondingly infrequent occurrence of PAM sites, which are required for mutagenesis. This further limits the flexibility in choice of more specific target sites. The lack of highly specific primers makes it necessary to avoid the T7 endonuclease assay which gives several false positives and rather screen for putative mutants by sub-cloning of PCR amplicon and sequencing. Two putative functional knockouts within TAAR13 were obtained after several attempts (Figure 24, Figure 25). One of them had a single base

deletion which resulted in a frame shift mutation leading to introduction of a premature stop codon. Single base indels have been reported as a common form of CRISPR-induced mutations in some cases (Hyun et al., 2015; Lin et al., 2014; Ronda et al., 2014). Another had three amino acid substitutions at position 35, 135, 142, which were absent in all of the potentially parental TAAR13 genes. TAAR13c sequence used in this study was not from annotated sequence, but obtained from the un-injected parents and hence, SNP's observed could not be due to possible deviations between parental TAAR13c sequence and the annotated sequence from the database. However, due to background introduced by the presence of several SNPs between the different subfamily members, it was not possible to map the two mutations mentioned above to a particular gene within the TAAR13 subfamily.

The high mortality rate of injected eggs was also an interesting and uncommon observation. Very few larvae survived for Fin-Clip analysis. Fin-Clip analysis of surviving fishes did not show any mutation. One reason for low survival rates could be impure RNA used for injections. Although RNA used for injections in this study was extensively purified using standard protocols and its integrity was also confirmed on gel prior to injections, it cannot be excluded that some impurities might remain. However, another possibility is that the Mutation or knockout of the TAAR13c gene might have a detrimental effect on the survival of the injected eggs which made it difficult to obtain live mutant larvae. There is no known report of the plausible role of the TAAR family of protein in embryonic development and there are knockouts of other related TAARs in mice which are not embryonically lethal (Dewan et al., 2013; Li et al., 2013). So a survival effect of a TAAR13c knockout appears unlikely, although it cannot be completely excluded.

Taken together, the construction of a TAAR13c knockout turned out to be more complex than initially assumed. The primary problem was the high

sequence identity among TAAR13 subfamily members leading to many false-positive results in the screening assay as well as cross-over between templates in the analytical PCRs required. Among several approaches tested, the most promising is the cluster knockout of the whole TAAR13 subfamily (Figure 26), which was begun in this study with designing of constructs, but could not be carried through for time reasons. Such a cluster knockout is expected to generate in future a useful tool to analyze the physiological function of the TAAR13 subfamily.

KEY FINDINGS AND CONCLUSIONS

The successful purification and characterization of TAAR13c antibody allowed monitoring TAAR13c expression at the protein level in cells with neuronal morphology. Thus, the purified and specific TAAR13c antibody generated in this study provides a valuable tool to monitor the subcellular localization of TAAR13c by immunofluorescence. The co-expression of TAAR13c antibody staining with acetylated tubulin and G_{olf} staining showed the specificity of TAAR13c expression in ciliated Neurons. The cells which show expression of TAAR13c could also be confirmed as ciliated cells based on the morphological appearance of these neurons. This is a finding which deciphers the cell type which expresses this specific receptor, consistent with observations of *taar* gene expression in ciliated neurons in diverse species such as mice.

Search for a neuronal activity marker upon Cadaverine stimulation was sought for and two well-known immediate early genes *cFos* and *egr1* were tested and found unsuitable for TAAR13c specific neuronal activity. pERK which does not rely on gene expression was chosen for its relatively rapid activation by phosphorylation of ERK and sparse activation of cells after stimulus with cadaverine and other diamines of different chain length. Double labelling of pERK antibody and TAAR13c antibody showed co-label in pERK and TAAR13c signaling cells.

Search for TAAR13c glomerulus using the TAAR13c Antibody was unsuccessful presumably because the expression levels of TAAR13c in the native bulb were below detection limits. Attempts to improve detection of TAAR13c signal using cadaverine stimulus and TCA fixation also did not help in labelling the glomeruli.

Ontogenetic onset of avoidance behavior was studied using a two channel choice apparatus in Zebrafish larvae. A trend towards avoidance of

cadaverine was observed from the larval behavior experiments after several optimizations. More reliable and precise analysis methods are needed for quantitative representation of the data.

The construction of a TAAR13c knockout turned out to be more complex than initially assumed. The primary problem was the high sequence identity among TAAR13 subfamily members leading to many false-positive results in the screening assay as well as cross-over between templates in the analytical PCRs required. Two putative knockout mutations were obtained with optimized screening methods. Among several approaches tested, the most promising is the cluster knockout of the whole TAAR13 subfamily, which was begun in this study with designing of constructs, but could not be carried through for time reasons. Such a cluster knockout is expected to generate in future a useful tool to analyze the physiological function of the TAAR13 subfamily.

MATERIALS AND METHODS

Animal Strains, Breeding and Maintenance

In vivo work carried out in this doctoral work is using the *Danio rerio* (Zebrafish) of the Ab/Tü strain (mix between the Oregon and Tubingen strains). Adult zebrafish (*Danio rerio*) were maintained in water (one-to-one mixture of desalted water and tap water) in an aquaria with constant temperature of 28 degrees, a day/night rhythm of 14/10 hours and were fed daily with dry flake foods and brine shrimp (artemia; Brustmann, Oestrich-Winkel). Single or sparse colonies were avoided for good animal behaviour.

Breeding of stock colonies was done by putting selected female and male fishes into the same tank separated by a transparent wall, a day before mating. At the time of onset of light cycle to day; the plastic separator was removed to allow free mating. Fertilized eggs were collected and used as per the requirement of the experiment or for further maintenance.

Zebrafish embryos and larvae were kept in petri dishes at a density of about 50 embryos/petri dish in embryo medium (E3: 5 mM NaCl, 0.17 mM KCl, 0.33 mM CaCl₂, 0.33 MgSO₄, Methyleneblue 5-10%) at 28°C without feeding for the first five days of post fertilization (dpf).

The embryos were then raised and collected at 24h intervals for histological and immunohistochemical analysis. Embryos fixed at a stage older than 24 h postfertilization (hpf) were raised in 2 mM 1-phenyl-2-thiourea (PTU) in embryo medium after the epiboly stage (about 12 h) to prevent pigmentation.

Plastic ware

All disposable plastic ware like 15 ml and 50 ml Falcon tubes, 6-, 24-, 48-, 96-well plates, Petri dishes in various sizes were from BD or Castor, 0.2 ml

PCR tubes and sterile pipette tips and Special filter tips used for all work involving DNA and RNA were from VWR.

Chemicals, Enzymes, oligos and Kits

Chemicals used in this study were from Ambion (Austin, USA), Amersham Pharmacia Biotech (Freiburg), Applichem (Darmstadt), JTBaker supplied by Fisher Scientific (Schwerte), Biozym (Hessisch Oldendorf), Calbiochem (Darmstadt), Difco (Detroit, USA), Fluka (Neu-Ulm), Merck (Darmstadt), Molecular Probes (Leiden, NL), Roth (Karlsruhe), Serva (Heidelberg), or Sigma (Deisenhofen) , Life technologies (USA).

Reagents and Solutions

All buffers and solutions were prepared with autoclaved distilled or Milli-Q water. Solutions were autoclaved for 20 min at 121 bar or filter sterilized (0.2 µm sterile filters). Glassware was autoclaved and oven baked for 2 h at 180°C. DEPC treated water was prepared by shaking 0.1% diethylpyrocarbonate in Milli-Q for 30 minutes followed by autoclaving. Buffers for molecular biology / RNA work were subsequently prepared in DEPC treated water. Most of the standard stock solutions like EDTA, Tris, TAE, TBE, TE, PBS, SDS, SSC, NaOAc, and culture media like LB and SOC were prepared as per standard protocol described in (Sambrook J 1989).

Primary Antibodies

1:200 c-Fos (E-8) rabbit polyclonal (Santa Cruz), G_{olf} (E-7) Mouse monoclonal (Santa Cruz) 1:200, Acetylated tubulin(Santa Cruz) mouse monoclonal 1:200, 1:500 Anti-DIG sheep Fab fragment coupled with alkaline phosphatase, Roche, 1:500-1000 Anti-Flu sheep Fab fragment coupled with alkaline phosphatase, Roche, 1:500-1000 phospho specific p44/42 (ERK1/2) 9106 (Cell Signaling) mouse monoclonal; p44/42 (ERK1/2) (3A7) mouse monoclonal; p44/42 (ERK1/2) (LL34F12) mouse monoclonal (Cell Signaling) 1:100.

Secondary antibodies

Donkey Y-rabbit, Alexa Fluor 488 coupled, Molecular Probes, 1:200 Donkey Y-rabbit, Alexa Fluor 594 coupled, Molecular Probes, 1:200, Goat Y-Mouse Alexa fluor 488 coupled, Goat Y-Mouse Alexa Fluor 594 Coupled, 1:200(Molecular Probes)

Laboratory equipment

General lab equipments were used for the molecular and cell biology techniques, including – balances, centrifuges, electrophoresis equipment, electroporation pulser, heating blocks and plates, hybridization and incubation ovens, micropipettes, PCR and gradient thermocyclers, pH meter, shakers, sterile hood, UV transilluminator, vortexes and water baths. Fresh frozen and PFA fixed tissue (in Tissue-Tek) cryosections were obtained using the Cryostat CM 1900, Leica. Non-fluorescent and Fluorescent images were documented with a BZ-X700 Fluorescent/ Phase contrast microscope from Keyence Corporation, Japan with Nikon CF160 series objectives from Nikon Corporation, Japan.

Bacterial Strains

Escherichia coli DH5 α strain was used for cloning and transformations.

Dissection

Adult Zebrafish heads were decapitated and fixed in 4% PFA for 7 minutes and then dissected to harvest 5 major organs. The scalp was removed to expose the brain, telencephalon and the olfactory system. The first to be removed were the eyes followed by the brain with the olfactory system attached and the olfactory bulb and olfactory epithelium were removed separately from the brain tissue. After the removal of the brain, the heart and gills were also removed and snap frozen in liquid nitrogen.

Tissue Lysis and protein estimation

The harvested organs were lysed in 1X RIPA buffer at 4°C with protease inhibitor PMSF added just before the lysis at 1mM concentration. The organs were placed in microcentrifuge tubes and 100µl of cold RIPA buffer was added and incubated in ice for 30 minutes followed by homogenisation by sonication. The sonication cycle was repeated twice to ensure complete homogenisation. The tubes were then centrifuged for 10 minutes at 10000 rpm. The supernatant was frozen at -20°C for further analysis and the pellet was discarded.

Concentration of total protein in lysate was determined by Bradford assay. Briefly, 5 microlitres of the lysate was taken in 145 microlitres of commercial `Bradford's reagent and incubated for 5 minutes at RT. The absorbance was measured at 595 nM. For determination of absolute protein quantity, a standard curve with 100 mg/ml to 0.01 mg/ml BSA dissolved in the same RIPA buffer was used. The O.D. values of the lysate was extrapolated on a standard curve and absolute protein amounts determined. Equal amounts of protein from each lysate was taken in Laemmili buffer, boiled at 95 degrees for 5 minutes and loaded onto a SDS PAGE gel.

Western Blotting

After running the SDS-PAGE gel, the proteins were transferred to a PVDF membrane with an area slightly exceeding that of the gel on a semi-dry transfer apparatus. Blocking was done with 5% milk in PBST with the membrane immersed and kept on a gentle rocker for 2 hours. The primary antibody- Rabbit Anti-TAAR13c antibody was added at a concentration of 1:1000 to the blocking solution of 5% milk in PBST for a total volume of 30 ml. The membrane was carefully pushed into a 50ml falcon tube containing the primary antibody mix and the tube was placed on gentle rollers for overnight incubation at 4°C.

Signal detection

The membrane was washed 3 times for 10 minutes each in 1X PBST and incubated in 5% milk in PBST containing the secondary antibody. The Secondary antibody was conjugated to HRP and was used at a concentration of 1:5000. HRP substrate was used for detection and the chemiluminescent reaction was detected on a photographic film.

Immunohistochemistry

Adult Zebrafish heads were decapitated and fixed by immersing in 4% paraformaldehyde for 7 minutes. After the fixation procedure, the scalp was dissected to expose the brain and olfactory system and careful removal of the olfactory epithelium was performed. The olfactory epithelia were then instantly immersed in OCT medium and frozen for Cryosectioning. The frozen blocks of OCT medium (Tissue Tek) were mounted on a Cryostat with optimized cutting temperature and angle of sectioning platform. 10 micron thick sections were made and embedded on frosted slides (Thermo superfrost). The slides were dried at 55°C for 20 minutes. The frosted slides were immersed in cold Acetone for 10 minutes to remove the OCT medium and fix the tissue permanently to the slides. The Slides were allowed to dry and excess acetone was absorbed onto an absorbent paper wipe. The slides were then washed in 1xPBS thrice followed by blocking for 2 hours in 5% normal goat serum in 1XPBS. The slides were incubated with primary antibody at 4°C overnight and next day washed thrice in 1XPBST containing 0.1% tween20. The slides were incubated with secondary antibody solution containing the animal specific antibody conjugated with a fluorophore against the primary antibody in 1XPBST. In case of co-labelling secondary antibodies with different fluorescent dyes were used to distinguish and recognize the two primary antibodies. After the incubation, the secondary antibody solution was drained off each slide and mounted with 35µL

Vectashield mounting media containing DAPI. All images were taken on a BZ8100 fluorescent microscope (Keyence).

Preparation of the whole mount zebrafish larvae for in-situ hybridization

Zebrafish whole mount larvae which were used for the in-situ experiments were raised in E3 media at 28°C until 10hpf, the E3 was supplemented with 0.0045% (w/v) Phenylthiourea to block pigmentation, the E3/PTU solution was changed regularly. The larvae were raised until 5dpf, sacrificed and fixed in 4% Paraformaldehyde O/N at 4°C. Subsequently washed with PBS and dehydrated gradually in Meth OH, then stored in 100% MetOH at -20°C until use. In Situ Hybridization for zebrafish larvae was performed according to Thisse et. al (Thisse and Thisse, 2014) with minor modifications. Rehydration was only performed if larvae were stored in methanol. Digestion with Proteinase K was performed for 30 min. (10µg/mL). Anti-DIG antibody solution was adsorbed to 5 dpf larvae. Prehybridization was done for 1 hour and the Hybridization was done at 65°C o/n. The staining (NBT/BCIP as substrate for digoxigenin coupled alkaline phosphatase, 1:1000 (Roche) was stopped when enough signal was obtained usually not less than 10 hours at 4°C. All photographs of whole mounts were taken with a digital camera (Nikon) attached to the stereo microscope (Nikon). Microtome sections were processed as explained in the IHC part, except here using 35 µL Vecta Mount as mounting media.

Zebrafish larval behavior Analysis.

The larval behavior apparatus consists of two separated channels and a convergence chamber. The channel heads are blocked by two collimators which smoothens the flow. The flow-out has two screws which allow adjusting the height and the outflow of water. Wired gauze prevents the larvae from being flown out. Base of ZLBA was colored with white tape

which provides contrast. The experimental setup included the left and right channels of the apparatus connected with 3 pumps in three tanks (two pumps connected to one channel via switch). One tank was filled with X- μ M cadaverine solution, and the other two with fish water. An overhead camera was set up to record the experiment. Experiment was divided into three phases:

Pre-phase, cadaverine phase and post-phase. The larvae were introduced by a cut pasteur pipet into the convergence chamber. The larvae were primed for 1-2 minutes in fishwater. Every phase is about 5 minutes. The cadaverine channel was switched from left to right channels from time to time. Same no. of trials was made with both the channels. A flow regulating switch was used to direct cadaverine containing water and freshwater through the channels between phases. No external sound or physical disturbances are made during the course of the experiment. One of the two channels was dyed with minute quantity of methylene blue to give a slight tinge of blue colour to observe mixture from the two currents in the four chambers. The flow was adjusted until each current flows with minimal mixture (via screws at the tubes). By collecting the outflow of water of the apparatus per minute we found out the flowrate and optimized it two 200mL/min at which the ideal condition of minimal mixing and free swimming larvae was achieved. Flowrate was not changed in all the experiments hereafter.

Genome editing using TALEN

The TALENs designed to bind the TAAR13c coding sequence were provided by the core facility of the University of Utah in pCS2+ backbones with the following DNA binding domains:

pCS2TAL3-taar-TALEN-DDD- TGTACTCAAARRRGCTAACTT

Spacer: ggaaggactggaggaat

pCS2TAL3-taar-TALEN-RRR: ACATTGCATCAGTGTACTGT A

mRNA transcription in vitro

Supercoiled DNA of the pCS2+ plasmid was subjected to restriction digest with NotI and the linearized DNA template was purified using the innuPREP PCRpure kit (Analytik Jena) according to the manufacturer's protocol. TALEN DDD and TALEN RRR mRNA transcription in vitro from the SP6 promoter was performed using the mMessage machine (Ambion) according to the manufacturer's protocol. The mRNA was purified using the RNeasy RNA purification kit (Qiagen) according to the manufacturers protocol and stored at -80°C . 50pg/nL was microinjected into single cell stage embryos

Genome editing using CRISP-CAS9

Vectors

The MLM3616 Plasmid (Addgene plasmid #42251) was used as Cas9 expression vector. It harbours the T7 promoter sequence enabling the in vitro transcription (IVT) of the Cas9 cDNA from *Streptococcus pyogenes*. The DR274 Plasmid (Addgene plasmid #42250) was used as guide RNA expression vector. The DR274 Vector also has a T7 promoter sequence used for in vitro transcription, which is followed by a guideRNA (crRNA:tracrRNA chimera). The customized target site (see table 2) were cloned in this vector

Production of Cas9 mRNA

Five μg of the purified MLM3616 vector were linearized with 5U of PmeI restriction enzyme o/n at 37°C , the product was subsequently purified by standard Phenol-Chloroform extraction (Liu and Harada, 2013) and precipitated with 1 volume of Isopropanol. mMESSAGING mMACHINE® Kit (Life Technologies) was used to in vitro transcribe $1\mu\text{g}$ of linearized MLM3616 vector according to the manufacturer's instructions. The whole mRNA product was digested with $1\mu\text{L}$ DNase I for 15 min. at 37°C and subsequently purified with the RNeasy Kit (Qiagen) according to Kit

instructions. The product was polyadenylated with 1U of Poly-A-Polymerase (NEB) and 1 μ L of 10mM ATPs. This product was purified with the Qiagen RNAeasy kit. The polyadenylated and 5' capped Cas9 mRNA was used for microinjection in the concentration of 300pg/nL.

Production of TAAR13c specific guide RNA

The CRISPR ZiFit targeter from the ZiFit webpage was used to design specific gRNAs for targeting the ORF of TAAR13c gene. The target sites were crosschecked in <http://crispr.mit.edu/> for off-targets in the zebrafish genome. The website used for cross checking potential off-target sites utilizes a published algorithm (Cong et al., 2013) and displays the off-targets in form of scores showing intronic and exonic regions. Scores higher than 1 were considered potential off-targets and were checked with the T7 Endonuclease I assay (see Results). Each target site was produced by annealing equal molar and volume ratio of two complementary oligos resulting in one double stranded oligo bearing the respective target site. The oligos were annealed by heating at 95°C for 5 minutes and gradually cooling down to RT. The resulting double stranded oligonucleotides had sticky overhangs compatible to BsaI digested DR274 (5`TAGG and complementary 5`AAA) enabling the ligation to DR274. Target sites and oligos used are listed in Table 1 and Table 2.

After annealing of target site oligos, 5 μ g of DR274 Plasmid were digested with 5U of BsaI restriction enzyme (NEB) o/n at 37°C, subsequently the linearized vector backbone band was purified using plasmid purification kit (Qiagen). The annealed oligonucleotides were ligated to the linearized vector (3:1 ratio in 10 μ L) with 1U of T4 ligase in appropriate buffer o/n at 16°C at the position. Five μ L of the ligation product was transformed in electro competent DH5 α cells and plated on agar plates containing 25 μ g Kanamycin. After 16hrs at 37°C single clones were picked and standard colony PCR (M13 Fw-primer and Oligo2 as Rev-Primer) was performed to screen for

clones which carry the plasmid of DR274 with the desired target site. The positive clones were inoculated in selective LB-Media containing 25µg/mL Kanamycin and sequenced (GATC Biotech.) after plasmid isolation by using the M13 Fw Primer (GTAAAACGACGGCCAGT). For creating the TAAR13c specific single guide RNA, 2µg of the DR274 (A) and DR274 (B) plasmid (i.e. DR274 plasmid bearing the TAAR13c specific target site), were purified using the Plasmid purification Kit (Qiagen) and digested with 5U of DraI restriction enzyme o/n at 37°C, purified again and used for in vitro transcription (IVT) with the mMachine T7 Transcription Kit (Life Technologies).

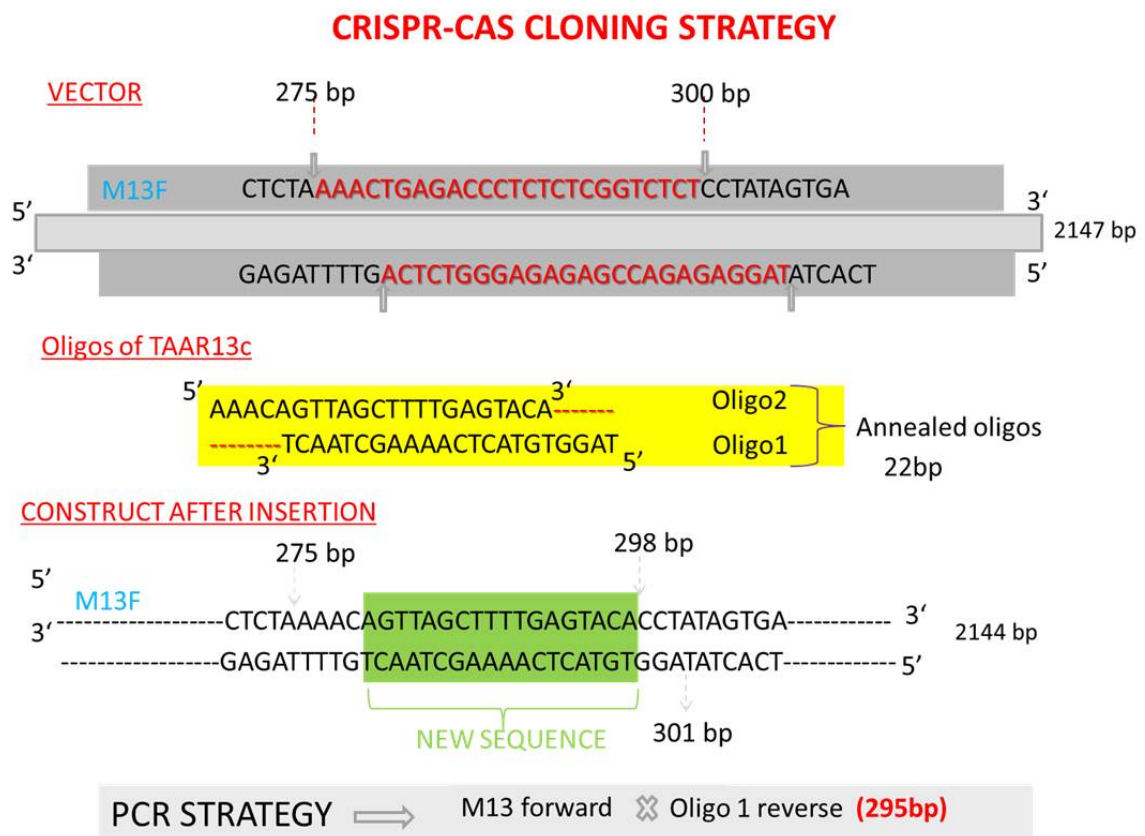


Figure 28. CRISPR-CAS cloning strategy

The Crispr target site was cloned into the Dr274 plasmid vector and screened for positive insertion after restriction with BSA1. The primers used for screening were M13 forward and oligo 1 as reverse.

Microinjection of CRISPR/Cas9 vectors and screening for genomic alterations

Biopsies of all adult WT/KS zebrafish which were used as P0 to produce eggs for the microinjection were sequenced (GATC Biotech) several times before mating, to make sure no single nucleotide polymorphism (SNP) is present in the genomic region, which is chosen for targeting. After mating, one cell stage zebrafish embryos (WT/KS) were collected in agarose microinjection moulds, oriented and injected with the Pneumatic Pico Pump PV 830 (World Precision Instruments), which was calibrated to an eject pressure of ~40 psi. The hold-pressure was adjusted as such that no unwanted in- or outflow occurred. Borosilicate glass capillaries (1.0 mm O.D. x 0.58 mm I.D, Harvard Apparatus), pulled with a Flaming/Brown micropipette puller (Sutter Instruments), have been used. The drop volume was adjusted to 0.8-1 nL by using an object micrometer, and the embryos were injected with ca. 300pg of Cas9 and ca. 15pg of one single guide RNA. All embryos were injected in the cell mass or in the yolk sac immediately after fertilization. After injection, the embryos were raised in E3 medium supplemented with 0.002% (w/v) Methylene Blue. After 4 hpf, dead or grossly deformed embryos were discarded, the rest was raised in E3-media o/n at 28°C. Embryos were collected separately or in pools and incubated in genomic DNA lysis buffer (10mM Tris pH8, 2mM EDTA, 0.2% Triton X-100) for 30 min. at 53°C containing 200µg of Proteinase K. After the incubation the lysates were precipitated with 1 Vol. of Isopropanol and used for the T7 endonuclease I assay.

T7 Endonuclease I assay

Twenty ng gDNA of previously microinjected 24hpf embryos was supplied to a standard PCR reaction (20µL, Tab. 3) using the Green Go-Taq 2x Mix (Promega) along with primers (5µM each) enclosing approx. 200bp downstream and upstream of the targeted genomic region. After the PCR

reaction the product was purified with the PCR extraction Kit (Qiagen), a 3 μ L aliquot was checked on a 2% agarose gel. If the PCR reaction result was showing the desired band of approx. 400 bp, an 10 μ L aliquot of the PCR Sample were applied to the annealing procedure, by setting the PCR cycler with the following program: 95°C for 10 min, 95° to 85°C in increments of -2°C/s, 85° to 25°C in increments of -0.1°C/s, and a 4°C hold (Qiu et al., 2004). After this the annealed amplicons were digested with 2U of T7 Endonuclease I (NEB) in recommended buffer at 37°C for 30 min. Three ml aliquots of each sample were not digested to serve as a control. The samples which showed multiple bands after the T7 Endonuclease I assay, were further subjected for subcloning and sequencing.

Subcloning and Sequencing of T7 Endonuclease I assay-samples

Residual sample volume was ligated to a TA cloning vector (pGEMT, Promega) in 3:1 (insert: vector) ratio by using 1 U of T4 ligase o/n at 16°C. This ligation product was transformed to DH5a electro competent cells and then plated on agar plates cont. 50 μ g Ampicillin, single clones were sequenced (GATC Biotech.) by using the M13 Fw- Primer (GTAAAACGACGGCCAGT).

Primers and target sites used in TALEN and Crispr-Cas mediated mutations

List of primers used in shown in table 1. Some Primers designed for TALEN were also used in Crispr analysis. The target sites used in this study are shown in table2.

Table 1. List of primers used in this study

DRTAAR13c fw	GGTCATCAGGTGTGTGAGGTC
DRTAAR13c REV	CGCGTTCAGTCTCTACACAAC
DRTAAR13c TALEN1FW	CTGCTTGGACTGGTGGTCAT
DRTAAR13c TALEN1REV	CTTTCAGACCGTCGAGGGTT
TAAR13c TALEN LA	TCGACATCAGGCTGTGTGTT
TAAR13c TALEN RA	CTGACCACAAGGCATTGAAA
TALEN BSR1	TGACTACGTTACATAAGGAGGT
TAAR13c FW FLANKING	AAGCACAACAACAGTAAATAAA
TAAR13c REV FLANKING	ACTAGCACACTATGTTTGGCAAT
TAAR13c primer FW	ATGTCTCCACTCAGACTGTGG
TAAR13c primer REV	GCAGCCATGCTCCA ACTTAT
TAAR13c SITE1 FW	ATGTCTCCACTCAGACTGTGG
TAAR13c SITE1 REV	GATCAACAGCAATACAAACAAGATG
CLUSTER_1_Primer_F	AGCACTGAAAAGACATGGACA
CLUSTER_1_Primer_R	GCCAAAGTAGCTGGTGGTTC
TAAR13E UTR-FW PRIMER	TCCTGCCACATGTAGTGTATTG
TAAR13E UTR-REV PRIMER	ACTTCCACGCTCAGTTGATG
TAAR13c FWD PRIMER UNIQUE	CTGGCGGACCTGCTGCTTGGACTGGTGGTCAT
TAAR13c REV PRIMER UNIQUE	AACCCTCGACGGTCTGAAAG
CRISPR FWD	ATGGATTTATCATCACAAG
CRISPR REV	AACTGACCACAAGGCATTGAA
CRISPR REV 2	TGGAGGAATACATTGCATCAGT

Table 2. List of target sites used in this study

CRISPR NEW SITE-1 OLIGO1	TAGGCGGACCTGCTGCTTGGAC
CRISPR NEW SITE-1 OLIGO2	AAACGTCCAAGCAGCAGGTCCG
CRISPR NEW SITE-2 OLIGO1	TAGGTGATGTCTCTGGCTCTGG
CRISPR NEW SITE-2 OLIGO2	AAACCCAGAGCCAGAGACATCA
CLSTR CRISPR OLIGO1	TAGGTGGATAATAATTAAGTAA
CLSTR CRISPR OLIGO2	AAACTTACTTAATTATTATCCA
CLSTR CRISPR OLIGOA1	TAGGAGATTTCTTTCAAATGA
CLSTR CRISPR OLIGOA2	AAACTCATTTGAAAGGAAATCT
CLSTR CRISPR OLIGOR1	TAGGGTCAGTTAGCATTTTCAGT
CLSTR CRISPR OLIGOR2	AAACTGAAATGCTAACTGAC
CLSTR CRISPR OLIGOS1	TAGGTCAGTTGTCATTTCTGTG
CLSTR CRISPR OLIGOS2	AAACCACAGAAATGACAACTGA
TAAR13E UTR-OLIGO1	TAGGTAATCATCAACTGTAAGT
TAAR13E UTR-OLIGO2	AAACTTACAGTTGATGATTA
Crispcas target oligo 1	TAGGTGTACTCAAAGCTAACT
Crispcas target oligo2	AAACAGTTAGCTTTTGAGTACA

REFERENCES

- Ahuja, G., I. Ivandic, M. Salturk, Y. Oka, W. Nadler, and S.I. Korsching. 2013. Zebrafish crypt neurons project to a single, identified mediodorsal glomerulus. *Sci Rep.* 3:2063.
- Ahuja, G., S.B. Nia, V. Zapilko, V. Shiriagin, D. Kowatschew, Y. Oka, and S.I. Korsching. 2014. Kappe neurons, a novel population of olfactory sensory neurons. *Sci Rep.* 4:4037.
- Bazaes, A., J. Olivares, and O. Schmachtenberg. 2013. Properties, projections, and tuning of teleost olfactory receptor neurons. *J Chem Ecol.* 39:451-464.
- Behrens, M., O. Frank, H. Rawel, G. Ahuja, C. Potting, T. Hofmann, W. Meyerhof, and S. Korsching. 2014. ORA1, a zebrafish olfactory receptor ancestral to all mammalian VIR genes, recognizes 4-hydroxyphenylacetic acid, a putative reproductive pheromone. *J Biol Chem.* 289:19778-19788.
- Borowsky, B., N. Adham, K.A. Jones, R. Raddatz, R. Artymyshyn, K.L. Ogozalek, M.M. Durkin, P.P. Lakhani, J.A. Bonini, S. Pathirana, N. Boyle, X. Pu, E. Kouranova, H. Lichtblau, F.Y. Ochoa, T.A. Branchek, and C. Gerald. 2001. Trace amines: Identification of a family of mammalian G protein-coupled receptors. *Proceedings of the National Academy of Sciences.* 98:8966-8971.
- Bozza, T., P. Feinstein, C. Zheng, and P. Mombaerts. 2002. Odorant receptor expression defines functional units in the mouse olfactory system. *The Journal of neuroscience : the official journal of the Society for Neuroscience.* 22:3033-3043.
- Bozza, T.C., and J.S. Kauer. 1998. Odorant Response Properties of Convergent Olfactory Receptor Neurons. *The Journal of Neuroscience.* 18:4560-4569.

- Braubach, O.R., A. Fine, and R.P. Croll. 2012. Distribution and functional organization of glomeruli in the olfactory bulbs of zebrafish (*Danio rerio*). *The Journal of comparative neurology*. 520:2317-2339, Spc2311.
- Braubach, O.R., N. Miyasaka, T. Koide, Y. Yoshihara, R.P. Croll, and A. Fine. 2013. Experience-dependent versus experience-independent postembryonic development of distinct groups of zebrafish olfactory glomeruli. *The Journal of neuroscience : the official journal of the Society for Neuroscience*. 33:6905-6916.
- Braubach, O.R., H.D. Wood, S. Gadbois, A. Fine, and R.P. Croll. 2009. Olfactory conditioning in the zebrafish (*Danio rerio*). *Behav Brain Res*. 198:190-198.
- Buck, L., and R. Axel. 1991. A novel multigene family may encode odorant receptors: a molecular basis for odor recognition. *Cell*. 65:175-187.
- Budick, S.A., and D.M. O'Malley. 2000. Locomotor repertoire of the larval zebrafish: swimming, turning and prey capture. *The Journal of experimental biology*. 203:2565-2579.
- Bunzow, J.R., M.S. Sonders, S. Arttamangkul, L.M. Harrison, G. Zhang, D.I. Quigley, T. Darland, K.L. Suchland, S. Pasumamula, J.L. Kennedy, S.B. Olson, R.E. Magenis, S.G. Amara, and D.K. Grandy. 2001. Amphetamine, 3,4-methylenedioxymethamphetamine, lysergic acid diethylamide, and metabolites of the catecholamine neurotransmitters are agonists of a rat trace amine receptor. *Molecular pharmacology*. 60:1181-1188.
- Campbell, J.M., K.A. Hartjes, T.J. Nelson, X. Xu, and S.C. Ekker. 2013. New and TALEnted genome engineering toolbox. *Circ Res*. 113:571-587.
- Carroll, D. 2011. Genome engineering with zinc-finger nucleases. *Genetics*. 188:773-782.

- Carroll, D. 2014. Genome engineering with targetable nucleases. *Annu Rev Biochem.* 83:409-439.
- Catania, S., A. Germana, R. Laura, T. Gonzalez-Martinez, E. Ciriaco, and J.A. Vega. 2003. The crypt neurons in the olfactory epithelium of the adult zebrafish express TrkA-like immunoreactivity. *Neurosci Lett.* 350:5-8.
- Chess, A., I. Simon, H. Cedar, and R. Axel. 1994. Allelic inactivation regulates olfactory receptor gene expression. *Cell.* 78:823-834.
- Cong, L., F.A. Ran, D. Cox, S. Lin, R. Barretto, N. Habib, P.D. Hsu, X. Wu, W. Jiang, L.A. Marraffini, and F. Zhang. 2013. Multiplex genome engineering using CRISPR/Cas systems. *Science.* 339:819-823.
- DeMaria, S., A.P. Berke, E. Van Name, A. Heravian, T. Ferreira, and J. Ngai. 2013. Role of a ubiquitously expressed receptor in the vertebrate olfactory system. *The Journal of neuroscience : the official journal of the Society for Neuroscience.* 33:15235-15247.
- DeMaria, S., and J. Ngai. 2010. The cell biology of smell. *J Cell Biol.* 191:443-452.
- Dewan, A., R. Pacifico, R. Zhan, D. Rinberg, and T. Bozza. 2013. Non-redundant coding of aversive odours in the main olfactory pathway. *Nature.* 497:486-489.
- Doudna, J.A., and E. Charpentier. 2014. Genome editing. The new frontier of genome engineering with CRISPR-Cas9. *Science.* 346:1258096.
- Dulac, C. 2000. Sensory coding of pheromone signals in mammals. *Curr Opin Neurobiol.* 10:511-518.
- Eisen, J.S., and J.C. Smith. 2008. Controlling morpholino experiments: don't stop making antisense. *Development.* 135:1735-1743.
- Ferrero, D.M., and S.D. Liberles. 2010. The secret codes of mammalian scents. *Wiley Interdiscip Rev Syst Biol Med.* 2:23-33.
- Ferrero, D.M., D. Wacker, M.A. Roque, M.W. Baldwin, R.C. Stevens, and S.D. Liberles. 2012. Agonists for 13 trace amine-associated receptors

- provide insight into the molecular basis of odor selectivity. *ACS Chem Biol.* 7:1184-1189.
- Fishman, M.C. 2001. Genomics. Zebrafish--the canonical vertebrate. *Science.* 294:1290-1291.
- Fleischer, J., H. Breer, and J. Strotmann. 2009. Mammalian olfactory receptors. *Front Cell Neurosci.* 3:9.
- Gaillard, I., S. Rouquier, and D. Giorgi. 2004. Olfactory receptors. *Cell Mol Life Sci.* 61:456-469.
- Gaj, T., C.A. Gersbach, and C.F. Barbas, 3rd. 2013. ZFN, TALEN, and CRISPR/Cas-based methods for genome engineering. *Trends Biotechnol.* 31:397-405.
- Gayoso, J., A. Castro, R. Anadon, and M.J. Manso. 2012. Crypt cells of the zebrafish *Danio rerio* mainly project to the dorsomedial glomerular field of the olfactory bulb. *Chemical senses.* 37:357-369.
- Gerlach, G., A. Hodgins-Davis, C. Avolio, and C. Schunter. 2008. Kin recognition in zebrafish: a 24-hour window for olfactory imprinting. *Proc Biol Sci.* 275:2165-2170.
- Germana, A., G. Montalbano, R. Laura, E. Ciriaco, M.E. del Valle, and J.A. Vega. 2004. S100 protein-like immunoreactivity in the crypt olfactory neurons of the adult zebrafish. *Neurosci Lett.* 371:196-198.
- Hansen, A., S.H. Rolen, K. Anderson, Y. Morita, J. Caprio, and T.E. Finger. 2003. Correlation between olfactory receptor cell type and function in the channel catfish. *The Journal of neuroscience : the official journal of the Society for Neuroscience.* 23:9328-9339.
- Hansen, A., and B.S. Zielinski. 2005. Diversity in the olfactory epithelium of bony fishes: development, lamellar arrangement, sensory neuron cell types and transduction components. *J Neurocytol.* 34:183-208.
- Hansen, A., H.P. Zippel, P.W. Sorensen, and J. Caprio. 1999. Ultrastructure of the olfactory epithelium in intact, axotomized, and bulbectomized goldfish, *Carassius auratus*. *Microsc Res Tech.* 45:325-338.

- Hayden, S., and E.C. Teeling. 2014. The molecular biology of vertebrate olfaction. *Anat Rec (Hoboken)*. 297:2216-2226.
- Heale, V.R., K. Petersen, and C.H. Vanderwolf. 1996. Effect of colchicine-induced cell loss in the dentate gyrus and Ammon's horn on the olfactory control of feeding in rats. *Brain research*. 712:213-220.
- Hubbard, B.P., A.H. Badran, J.A. Zuris, J.P. Guilinger, K.M. Davis, L. Chen, S.Q. Tsai, J.D. Sander, J.K. Joung, and D.R. Liu. 2015. Continuous directed evolution of DNA-binding proteins to improve TALEN specificity. *Nature methods*.
- Hussain , A. 2010. The teleost taar family of olfactory receptors: From rapidly evolving receptor genes to ligand-induced behavior (PhD dissertation). University of Köln.
- Hussain, A., L.R. Saraiva, D.M. Ferrero, G. Ahuja, V.S. Krishna, S.D. Liberles, and S.I. Korsching. 2013. High-affinity olfactory receptor for the death-associated odor cadaverine. *Proc Natl Acad Sci U S A*. 110:19579-19584.
- Hussain, A., L.R. Saraiva, and S.I. Korsching. 2009. Positive Darwinian selection and the birth of an olfactory receptor clade in teleosts. *Proc Natl Acad Sci U S A*. 106:4313-4318.
- Hyun, Y., J. Kim, S.W. Cho, Y. Choi, J.S. Kim, and G. Coupland. 2015. Site-directed mutagenesis in *Arabidopsis thaliana* using dividing tissue-targeted RGEN of the CRISPR/Cas system to generate heritable null alleles. *Planta*. 241:271-284.
- Isogai, Y., S. Si, L. Pont-Lezica, T. Tan, V. Kapoor, V.N. Murthy, and C. Dulac. 2011. Molecular organization of vomeronasal chemoreception. *Nature*. 478:241-245.
- Jinek, M., K. Chylinski, I. Fonfara, M. Hauer, J.A. Doudna, and E. Charpentier. 2012. A programmable dual-RNA-guided DNA endonuclease in adaptive bacterial immunity. *Science*. 337:816-821.

- Kalueff, A.V., M. Gebhardt, A.M. Stewart, J.M. Cachat, M. Brimmer, J.S. Chawla, C. Craddock, E.J. Kyzar, A. Roth, S. Landsman, S. Gaikwad, K. Robinson, E. Baatrup, K. Tierney, A. Shamchuk, W. Norton, N. Miller, T. Nicolson, O. Braubach, C.P. Gilman, J. Pittman, D.B. Roseberg, R. Gerlai, D. Echevarria, E. Lamb, S.C. Neuhaus, W. Weng, L. Bally-Cuif, H. Schneider, and C. Zebrafish Neuroscience Research. 2013. Towards a comprehensive catalog of zebrafish behavior 1.0 and beyond. *Zebrafish*. 10:70-86.
- Kang, N., H. Ro, Y. Park, H.T. Kim, T.L. Huh, and M. Rhee. 2010. Seson, a novel zinc finger protein, controls cilia integrity for the LR patterning during zebrafish embryogenesis. *Biochem Biophys Res Commun*. 401:169-174.
- Kermen, F., L.M. Franco, C. Wyatt, and E. Yaksi. 2013. Neural circuits mediating olfactory-driven behavior in fish. *Front Neural Circuits*. 7:62.
- Kim, H., and J.S. Kim. 2014. A guide to genome engineering with programmable nucleases. *Nat Rev Genet*. 15:321-334.
- Kishimoto, N., C. Alfaro-Cervello, K. Shimizu, K. Asakawa, A. Urasaki, S. Nonaka, K. Kawakami, J.M. Garcia-Verdugo, and K. Sawamoto. 2011. Migration of neuronal precursors from the telencephalic ventricular zone into the olfactory bulb in adult zebrafish. *The Journal of comparative neurology*. 519:3549-3565.
- Koide, T., N. Miyasaka, K. Morimoto, K. Asakawa, A. Urasaki, K. Kawakami, and Y. Yoshihara. 2009. Olfactory neural circuitry for attraction to amino acids revealed by transposon-mediated gene trap approach in zebrafish. *Proc Natl Acad Sci U S A*. 106:9884-9889.
- Korsching, S. 2009. The molecular evolution of teleost olfactory receptor gene families. *Results Probl Cell Differ*. 47:37-55.

- Korsching, S.I., S. Argo, H. Campenhausen, R.W. Friedrich, A. Rummrich, and F. Weth. 1997. Olfaction in zebrafish: what does a tiny teleost tell us? *Semin Cell Dev Biol.* 8:181-187.
- Kress, S., and M.F. Wullimann. 2012. Correlated basal expression of immediate early gene *egr1* and tyrosine hydroxylase in zebrafish brain and downregulation in olfactory bulb after transitory olfactory deprivation. *J Chem Neuroanat.* 46:51-66.
- Lee, C., J.B. Wallingford, and J.M. Gross. 2014. *Cluap1* is essential for ciliogenesis and photoreceptor maintenance in the vertebrate eye. *Invest Ophthalmol Vis Sci.* 55:4585-4592.
- Leinders-Zufall, T., P. Brennan, P. Widmayer, P.C. S, A. Maul-Pavicic, M. Jager, X.H. Li, H. Breer, F. Zufall, and T. Boehm. 2004. MHC class I peptides as chemosensory signals in the vomeronasal organ. *Science.* 306:1033-1037.
- Leinders-Zufall, T., T. Ishii, P. Chamero, P. Hendrix, L. Oboti, A. Schmid, S. Kircher, M. Pyrski, S. Akiyoshi, M. Khan, E. Vaes, F. Zufall, and P. Mombaerts. 2014. A family of nonclassical class I MHC genes contributes to ultrasensitive chemodetection by mouse vomeronasal sensory neurons. *The Journal of neuroscience : the official journal of the Society for Neuroscience.* 34:5121-5133.
- Li, L., L.P. Wu, and S. Chandrasegaran. 1992. Functional domains in Fok I restriction endonuclease. *Proceedings of the National Academy of Sciences of the United States of America.* 89:4275-4279.
- Li, Q., W.J. Korzan, D.M. Ferrero, R.B. Chang, D.S. Roy, M. Buchi, J.K. Lemon, A.W. Kaur, L. Stowers, M. Fendt, and S.D. Liberles. 2013. Synchronous evolution of an odor biosynthesis pathway and behavioral response. *Current biology : CB.* 23:11-20.
- Li, Q., Y. Tachie-Baffour, Z. Liu, M.W. Baldwin, A.C. Kruse, and S.D. Liberles. 2015. Non-classical amine recognition evolved in a large clade of olfactory receptors. *Elife.* 4:e10441.

- Liberles, S.D. 2015. Trace amine-associated receptors: ligands, neural circuits, and behaviors. *Curr Opin Neurobiol.* 34:1-7.
- Liberles, S.D., and L.B. Buck. 2006. A second class of chemosensory receptors in the olfactory epithelium. *Nature.* 442:645-650.
- Lin, Y., T.J. Cradick, M.T. Brown, H. Deshmukh, P. Ranjan, N. Sarode, B.M. Wile, P.M. Vertino, F.J. Stewart, and G. Bao. 2014. CRISPR/Cas9 systems have off-target activity with insertions or deletions between target DNA and guide RNA sequences. *Nucleic Acids Res.* 42:7473-7485.
- Liu, X., and S. Harada. 2013. DNA isolation from mammalian samples. *Current protocols in molecular biology / edited by Frederick M. Ausubel ... [et al.]*. Chapter 2:Unit2 14.
- Luu, P., F. Acher, H.O. Bertrand, J. Fan, and J. Ngai. 2004. Molecular determinants of ligand selectivity in a vertebrate odorant receptor. *The Journal of neuroscience : the official journal of the Society for Neuroscience.* 24:10128-10137.
- Mahfouz, M.M., A. Piatek, and C.N. Stewart, Jr. 2014. Genome engineering via TALENs and CRISPR/Cas9 systems: challenges and perspectives. *Plant Biotechnol J.* 12:1006-1014.
- Mansour, S.L., K.R. Thomas, and M.R. Capecchi. 1988. Disruption of the proto-oncogene int-2 in mouse embryo-derived stem cells: a general strategy for targeting mutations to non-selectable genes. *Nature.* 336:348-352.
- Martineau, P.R., and P. Mourrain. 2013. Tracking zebrafish larvae in group – Status and perspectives(). *Methods (San Diego, Calif.)*. 62:292-303.
- Mirich, J.M., K.R. Illig, and P.C. Brunjes. 2004. Experience-dependent activation of extracellular signal-related kinase (ERK) in the olfactory bulb. *The Journal of comparative neurology.* 479:234-241.

- Miyasaka, N., A.A. Wanner, J. Li, J. Mack-Bucher, C. Genoud, Y. Yoshihara, and R.W. Friedrich. 2013. Functional development of the olfactory system in zebrafish. *Mech Dev.* 130:336-346.
- Mombaerts, P. 2004. Odorant receptor gene choice in olfactory sensory neurons: the one receptor–one neuron hypothesis revisited. *Current Opinion in Neurobiology.* 14:31-36.
- Muller, U.K., and J.L. van Leeuwen. 2004. Swimming of larval zebrafish: ontogeny of body waves and implications for locomotory development. *The Journal of experimental biology.* 207:853-868.
- Munger, S.D., T. Leinders-Zufall, and F. Zufall. 2009. Subsystem organization of the mammalian sense of smell. *Annual review of physiology.* 71:115-140.
- Oka, Y., and S.I. Korsching. 2011. Shared and unique G alpha proteins in the zebrafish versus mammalian senses of taste and smell. *Chemical senses.* 36:357-365.
- Oka, Y., L.R. Saraiva, and S.I. Korsching. 2012. Crypt neurons express a single V1R-related ora gene. *Chemical senses.* 37:219-227.
- Oka, Y., L.R. Saraiva, Y.Y. Kwan, and S.I. Korsching. 2009. The fifth class of Galpha proteins. *Proc Natl Acad Sci U S A.* 106:1484-1489.
- Omura, M., and P. Mombaerts. 2015. Trpc2-expressing sensory neurons in the mouse main olfactory epithelium of type B express the soluble guanylate cyclase Gucy1b2. *Mol Cell Neurosci.* 65:114-124.
- Pacifico, R., A. Dewan, D. Cawley, C. Guo, and T. Bozza. 2012. An olfactory subsystem that mediates high-sensitivity detection of volatile amines. *Cell Rep.* 2:76-88.
- Pathak, N., T. Obara, S. Mangos, Y. Liu, and I.A. Drummond. 2007. The zebrafish fleer gene encodes an essential regulator of cilia tubulin polyglutamylolation. *Mol Biol Cell.* 18:4353-4364.

- Pfister, P., J. Randall, J.I. Montoya-Burgos, and I. Rodriguez. 2007. Divergent evolution among teleost V1r receptor genes. *PLoS One*. 2:e379.
- Pfister, P., and I. Rodriguez. 2005. Olfactory expression of a single and highly variable V1r pheromone receptor-like gene in fish species. *Proc Natl Acad Sci U S A*. 102:5489-5494.
- Pin, J.P., T. Galvez, and L. Prezeau. 2003. Evolution, structure, and activation mechanism of family 3/C G-protein-coupled receptors. *Pharmacol Ther*. 98:325-354.
- Ramirez, C.L., J.E. Foley, D.A. Wright, F. Muller-Lerch, S.H. Rahman, T.I. Cornu, R.J. Winfrey, J.D. Sander, F. Fu, J.A. Townsend, T. Cathomen, D.F. Voytas, and J.K. Joung. 2008. Unexpected failure rates for modular assembly of engineered zinc fingers. *Nat Meth*. 5:374-375.
- Ramos-Vara, J.A., and M.A. Miller. 2013. When Tissue Antigens and Antibodies Get Along: Revisiting the Technical Aspects of Immunohistochemistry—The Red, Brown, and Blue Technique. *Veterinary Pathology Online*.
- Rolen, S.H., P.W. Sorensen, D. Mattson, and J. Caprio. 2003. Polyamines as olfactory stimuli in the goldfish *Carassius auratus*. *The Journal of experimental biology*. 206:1683-1696.
- Ronda, C., L.E. Pedersen, H.G. Hansen, T.B. Kallehauge, M.J. Betenbaugh, A.T. Nielsen, and H.F. Kildegaard. 2014. Accelerating genome editing in CHO cells using CRISPR Cas9 and CRISPy, a web-based target finding tool. *Biotechnol Bioeng*. 111:1604-1616.
- Saraiva, L.R., and S.I. Korsching. 2007. A novel olfactory receptor gene family in teleost fish. *Genome Res*. 17:1448-1457.
- Sato, K., and N. Suzuki. 2001. Whole-cell response characteristics of ciliated and microvillous olfactory receptor neurons to amino acids, pheromone candidates and urine in rainbow trout. *Chemical senses*. 26:1145-1156.

- Sato, Y., N. Miyasaka, and Y. Yoshihara. 2005. Mutually exclusive glomerular innervation by two distinct types of olfactory sensory neurons revealed in transgenic zebrafish. *The Journal of neuroscience : the official journal of the Society for Neuroscience*. 25:4889-4897.
- Sato, Y., N. Miyasaka, and Y. Yoshihara. 2007. Hierarchical regulation of odorant receptor gene choice and subsequent axonal projection of olfactory sensory neurons in zebrafish. *The Journal of neuroscience : the official journal of the Society for Neuroscience*. 27:1606-1615.
- Scanlan, T.S., K.L. Suchland, M.E. Hart, G. Chiellini, Y. Huang, P.J. Kruzich, S. Frascarelli, D.A. Crossley, J.R. Bunzow, S. Ronca-Testoni, E.T. Lin, D. Hatton, R. Zucchi, and D.K. Grandy. 2004. 3-Iodothyronamine is an endogenous and rapid-acting derivative of thyroid hormone. *Nat Med*. 10:638-642.
- Schmid, B., and C. Haass. 2013. Genomic editing opens new avenues for zebrafish as a model for neurodegeneration. *J Neurochem*. 127:461-470.
- Serizawa, S., K. Miyamichi, H. Nakatani, M. Suzuki, M. Saito, Y. Yoshihara, and H. Sakano. 2003. Negative feedback regulation ensures the one receptor-one olfactory neuron rule in mouse. *Science*. 302:2088-2094.
- Shi, L., and J.A. Javitch. 2002. The binding site of aminergic G protein-coupled receptors: the transmembrane segments and second extracellular loop. *Annual review of pharmacology and toxicology*. 42:437-467.
- Shi, P., and J. Zhang. 2009. Extraordinary diversity of chemosensory receptor gene repertoires among vertebrates. *Results Probl Cell Differ*. 47:1-23.
- Smithies, O., R.G. Gregg, S.S. Boggs, M.A. Koralewski, and R.S. Kucherlapati. 1985. Insertion of DNA sequences into the human chromosomal [beta]-globin locus by homologous recombination. *Nature*. 317:230-234.

- Sullivan, R.M., and M. Leon. 1986. Early olfactory learning induces an enhanced olfactory bulb response in young rats. *Brain research*. 392:278-282.
- Thisse, B., and C. Thisse. 2014. In situ hybridization on whole-mount zebrafish embryos and young larvae. *Methods in molecular biology (Clifton, N.J.)*. 1211:53-67.
- Van Regenmortel, M.H. 2001. Antigenicity and immunogenicity of synthetic peptides. *Biologicals : journal of the International Association of Biological Standardization*. 29:209-213.
- Venkatesh, B., A.P. Lee, V. Ravi, A.K. Maurya, M.M. Lian, J.B. Swann, Y. Ohta, M.F. Flajnik, Y. Sutoh, M. Kasahara, S. Hoon, V. Gangu, S.W. Roy, M. Irimia, V. Korzh, I. Kondrychyn, Z.W. Lim, B.-H. Tay, S. Tohari, K.W. Kong, S. Ho, B. Lorente-Galdos, J. Quilez, T. Marques-Bonet, B.J. Raney, P.W. Ingham, A. Tay, L.W. Hillier, P. Minx, T. Boehm, R.K. Wilson, S. Brenner, and W.C. Warren. 2014. Elephant shark genome provides unique insights into gnathostome evolution. *Nature*. 505:174-179.
- Vina, E., V. Parisi, F. Abbate, R. Cabo, M.C. Guerrero, R. Laura, L.M. Quiros, J.C. Perez-Varela, T. Cobo, A. Germana, J.A. Vega, and O. Garcia-Suarez. 2015. Acid-sensing ion channel 2 (ASIC2) is selectively localized in the cilia of the non-sensory olfactory epithelium of adult zebrafish. *Histochem Cell Biol*. 143:59-68.
- Wang, H.W., C.J. Wysocki, and G.H. Gold. 1993. Induction of olfactory receptor sensitivity in mice. *Science*. 260:998-1000.
- Wyman, C., and R. Kanaar. 2006. DNA Double-Strand Break Repair: All's Well that Ends Well. *Annual Review of Genetics*. 40:363-383.
- Yang, X. 2015. Applications of CRISPR-Cas9 mediated genome engineering. *Mil Med Res*. 2:11.
- Yoshihara, Y. 2009. Molecular genetic dissection of the zebrafish olfactory system. *Results Probl Cell Differ*. 47:97-120.

- Youngentob, S.L., and P.F. Kent. 1995. Enhancement of odorant-induced mucosal activity patterns in rats trained on an odorant identification task. *Brain research*. 670:82-88.
- Zapilko, V., and S.I. Korsching. 2016. Tetrapod V1R-like ora genes in an early-diverging ray-finned fish species: the canonical six ora gene repertoire of teleost fish resulted from gene loss in a larger ancestral repertoire. *BMC Genomics*. 17:83.
- Zhang, J., R. Pacifico, D. Cawley, P. Feinstein, and T. Bozza. 2013. Ultrasensitive detection of amines by a trace amine-associated receptor. *The Journal of neuroscience : the official journal of the Society for Neuroscience*. 33:3228-3239.
- Zucchi, R., G. Chiellini, T.S. Scanlan, and D.K. Grandy. 2006. Trace amine-associated receptors and their ligands. *Br J Pharmacol*. 149:967-978.

APPENDIX

The videos for larval behaviour, sequences from CRISPR and Talen mutagenesis attempts are provided in the appendix section in the form of DVD.

ERKLÄRUNG

Ich versichere, dass ich die von mir vorgelegte Dissertation selbstständig angefertigt, die benutzten Quellen und Hilfsmittel vollständig angegeben und die Stellen in der Arbeit -einschließlich Tabellen, Karten und Abbildungen -, die anderen Werken im Wortlaut oder dem Sinn nach entnommen sind, in jedem Einzelfall als Entlehnung kenntlich gemacht habe; dass diese Dissertation noch keiner anderen Fakultät oder Universität zur Prüfung vorgelegen hat; dass sie - abgesehen von den unten angegebenen Teilpublikationen – noch nicht veröffentlicht worden ist, sowie dass ich eine solche Veröffentlichung vor Abschluss des Promotionsverfahrens nicht vornehmen werde. Die Bestimmungen dieser Promotionsordnung sind mir bekannt. Die von mir vorgelegte Dissertation ist von Prof. Dr. S. I. Korsching betreut worden.

Köln, 7.03.16

Venkatesh S. Krishna

Teilpublikationen:

Ashiq Hussain, Luis R. Saraiva, David M. Ferrero, Gaurav Ahuja, Venkatesh S. Krishna, Stephen D. Liberles, and Sigrun I. Korsching. High-affinity olfactory receptor for the death-associated odor cadaverine; PNAS, doi/10.1073/pnas.1318596110 (2013).

LEBENS LAUF

Angaben zur Person

Name: Venkatesh Krishna Subramanian

Anschrift: Nikolaus Str.124, Köln, De-50937

Geburtsdatum/-ort: 27th April, 1987 in Modinagar, India

Familienstand: Ledig

Staatsangehörigkeit: Indisch

Ausbildung

seit 03/2012 **Promotions-Studium** an der Universität zu Köln, Köln, Deutschland

Institute für genetik, AG Prof. Dr. Sigrun Korsching

09/2009-12/2011 **Wissenschaftlicher Mitarbeiter**

Wockhardt Genomics and Biotechnology, India

07/2007– 08/2009 **Master-Studium** an der Bharathiar University, Coimbatore, India

Abschluss: MS Biotechnology

06/2004 – 06/2007 **Bachelor-Studium** an der University of Madras, Chennai, India

Abschluss: Bachelor of Science in Biochemistry